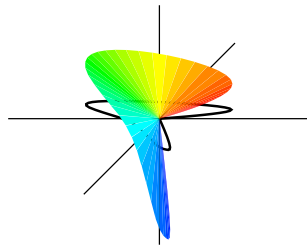


# Colore, visione a colori e colori elementari nella tecnologia dell'informazione a colori



Autore:

Prof. Dr. Klaus Richter

Edizione speciale per la esposizione

**Colore e visione a colori (Farbe und Farbsehen)**

al

“Das Sekretariat des Fachgebiete Lichttechnik der TU” di Berlino

Einsteinufer 19

10587 Berlin, Germany

see: <http://www.li.tu-berlin.de>

Questa pubblicazione (IS15.PDF) esce in diverse versioni:

per monitor (S) e stampa (S),

francese (F), italiano (I), ed norvegese (N) vedi

<http://farbe.li.tu-berlin.de/color> o

<http://130.149.60.45/~farbmetrik/color>

**Indice**

01 Metrica del colore	4
02 Colore e visione a colori	4
03 Molteplicità dei colori	5
04 Solido dei colori	9
05 Colori elementari	10
06 Cerchio delle tinte simmetrico	13
07 Colori a croma massima	16
08 Attributi dei colori: croma e chiarezza	17
09 Attributi dei colori: Brillanza e bianchezza	18
10 Spettro dei colori e colori elementari	20
11 Dispositivo per miscelare i colori spettrali e riflettanza	25
12 Fluorescenza	27
13 Retroriflessione	29
14 Miscela di colori	30
15 Radiazione spettrale	40
16 Contrasto	44
17 Specificazione standard del colore e misurazione standard del colore	49
18 Proprietà speciali della visione a colori	56
19 Colori elementari e tecnologia dell'informazione a colori	64
20 Output dei Colori elementari indipendente dal dispositivo per la riproduzione del colore	67
21 Riproduzione del colore affine	68
22 Riferimenti	69
23 Rigraziamenti	70
24 Test charts and technical remarks	72

## Osservazioni sulle cartelle test.

Le **cartelle test n. 1 - 3 per la resa del colore** (PI13, PI23, PI33) sono utilizzate nell'illuminazione e nella tecnologia dell'immagine. Le valutazioni visive e le specificazioni colorimetriche seguenti sono possibili tra la sorgente reale di luce e quella di riferimento (D65, D50, P4000, A) o tra la riproduzione reale e quella voluta:

**Fedeltà del colore:** differenza di colore nella riproduzione (CIELAB  $\Delta E^*_{ab}$ )

**Posizione delle tinte elementari:** Posizione delle quattro tinte elementari (CIE-LAB  $\Delta h_{ab}$ ) della realtà e della riproduzione voluta.

**Scala delle tinte:** spostamento delle tinte (CIELAB  $\Delta h_{ab}$ ) all'interno di ogni settore di tinte

**Colori metamerici:** Differenza di colore (CIELAB  $\Delta E^*_{ab}$ ) tra una sorgente di luce reale e quella di riferimento (D65, D50, P4000, A), o tra uno scanner reale e quello ideale (i.e. colorimetrico).

**Preferenza del colore:** Differenza di colore (CIELAB  $\Delta E^*_{ab}$ ) con voluto aumento della chiarezza  $L^*$  e / o della croma  $C^*_{ab}$ .

Gli **standard internazionali** ISO/IEC 15775 e ISO 9241-306 e la serie standard DIN 33866-15, e DIN 33872-16 usano per l'input e l'output serie di colori visivamente equispaziati in 5 e 16 passi. Solitamente le differenze uguali sono valutate visivamente. La specificazione colorimetrica considera le differenze di colore tra il colore reale e il colore voluto in output secondo CIELAB (ISO 11644-4).

Una tabella nella pagina interna della seconda copertina fornisce una descrizione tecnica per ottenere i colori voluti in output.

## 1 Metrica del colore

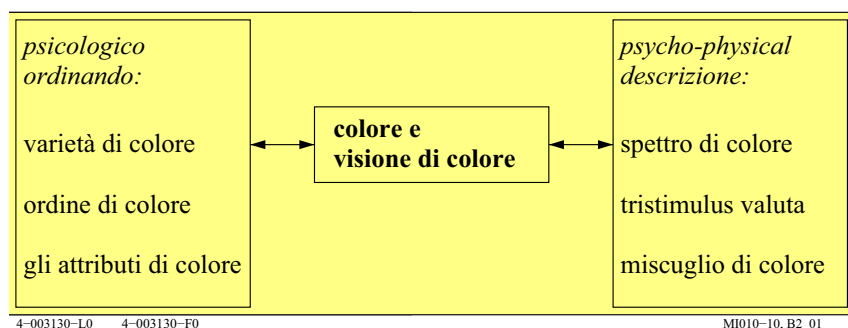
La metrica del colore riguarda la definizione e la misurazione dei colori e delle differenze di colore. La metrica del colore si basa sulla pubblicazione CIE 15 *Colorimetry della Commissione internazionale per l'illuminazione (CIE)*.

## 2 Colore e visione a colori

Una descrizione della qualità della resa del colore è possibile solo sulla base di una buona conoscenza delle proprietà visive nella visione umana a colori. Pertanto è essenziale approfondire le conoscenze con una ricerca sulla visione. Col supporto del “Deutsche Forschungsgemeinschaft” tedesco (DFG) K. Richter (1979, 1985) ha curato due rapporti di ricerca del BAM. Ci sono molte altre pubblicazioni nel campo delle scale dei colori, delle soglie di discriminazione dei colori e delle tinte elementari.

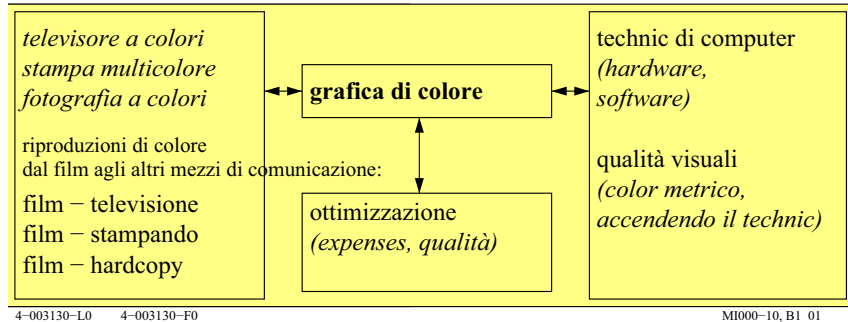
Importanti capitoli di *colore e visione a colori* sono dedicati all'ordine psicologico dei colori prodotto dalla percezione umana. La descrizione psicofisica del sistema visivo è basata sulla misurazione fisica e sulla percezione.

Le proprietà di base nel campo *colore e visione a colori* sono esposte nelle sezioni seguenti.



**Fig. 1: Suddivisione in capitoli di colore e visione a colori**

La figura 1 mostra gli importanti capitoli di colore e visione a colori, descritti qui di seguito con molte figure a colori.



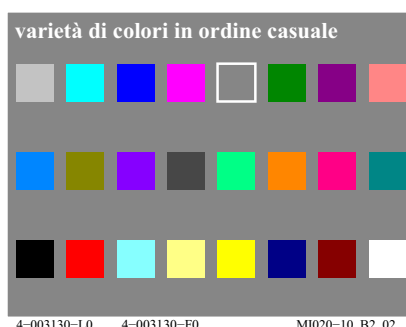
**Fig. 2: Grafica a colori come applicazione delle proprietà della visione a colori**

Fig. 2 mostra il campo della grafica a colori, che si fonda principalmente sulle proprietà visive della visione a colori. Inoltre, per l'ottimizzazione delle varie applicazioni, si devono considerare le potenzialità della riproduzione del colore e della tecnica di calcolo.

### 3 Molteplicità dei Colori

Tutto ciò che vediamo è colorato. I colori sono elementi delle nostre sensazioni visive. I materiali e i processi che producono i colori sono fenomeni differenti dalle sensazioni visive. Le molteplicità dei colori sono organizzate in seguito. Ciò ci porta a colori con uguali attributi di colore.

Secondo Judd e Wyszecki (1975) le persone con visione a colori normale sono in grado di distinguere circa 10 milioni di colori diversi. È quindi necessario classificare questa molteplicità di colori usando attributi convenzionali.



**Fig. 3: Colour multiplicity**

Fig. 3 mostra una disposizione casuale di campioni di colore, i quali possono essere separati nel gruppo dei colori acromatici e in quello dei colori cromatici.

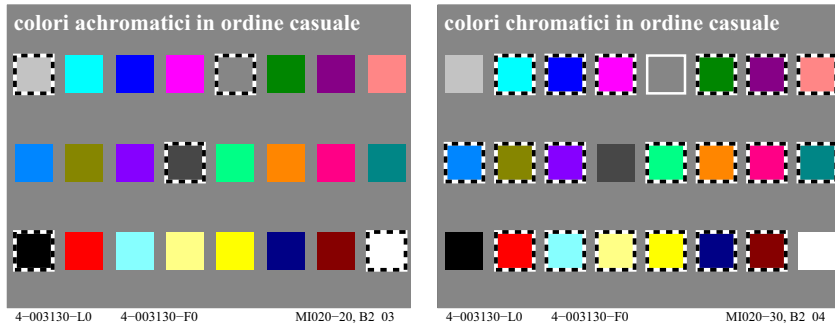


Fig. 4: Colori cromatici e colori acromatici

In Fig. 4 a sinistra sono evidenziati i colori acromatici e a destra i colori cromatici, selezionati da un insieme di colori disposti in modo casuale.

Colori acromatici	colori cromatici	colori cromatici, colori del dispositivo
<b>colori intermedi</b>	<b>colori elementari</b>	
<b>5 colori acromatici:</b>	<b>colori "né-né"</b>	<b>TV, stampa PR, fotografia PH</b>
$N$ nero (noir francese)	<i>quattro colori elementari (e):</i>	<i>sei colori del dispositivo (d):</i>
$D$ grigio scuro	$R = R_e$ rosso	$C = C_d$ blu ciano (cyan)
$Z$ grigio medio	<i>né giallo né blu</i>	$M = M_d$ rosso magenta (magenta)
$H$ grigio chiaro	$G = G_e$ verde	$Y = Y_d$ giallo (yellow)
$W$ bianco	<i>né verde né rosso</i>	$O = R_d$ rosso arangio (red)
<i>due colori intermedi:</i>	$B = B_e$ blu	$L = G_d$ verde foglia (green)
$C_e = G50B_e$ blu-verde	<i>né verde né rosso</i>	$V = B_d$ blu violetto (blue)
$M_e = B50R_e$ blu-rosso	$J = Y_e$ giallo (jaune francese)	

4-003130-L0 4-003130-F0 MI080-10

Tabella 1: Colori elementari e colori generati da dispositivi della tecnologia dell'informazione

La tabella 1 mostra la definizione dei colori elementari (pedice e) ed i colori prodotti da un mezzo della tecnologia informatica (pedice d). Ci sono quattro colori elementari RGBYe e sei colori del dispositivo per la riproduzione  $RGB-CMY_d$ . Per alcune applicazioni, ai quattro colori elementari si aggiungono i colori visivamente intermedi,  $C_e$  (blu-verde) e  $M_e$  (blu-rosso), producendo in tutto sei colori (in basso a sinistra). La Tabella 1 comprende 5 colori acromatici  $NDZHW$ , dal nero  $N$  (= nero francese), al grigio medio  $Z$  e al bianco  $W$ . Tutti gli altri sono colori cromatici.

I nomi  $O$ ,  $L$  e  $V$  sono utilizzati in molti testi standard (per esempio ISO/IEC 15.775, ISO/IEC 24.705, ISO 9241-306, DIN 33.866-1 5, e DIN 33.872-1 6). I nomi  $O$ ,  $L$  e  $V$  hanno il vantaggio di sintetizzare in una sola lettera l'apparenza.



In Fig. 5 (a sinistra) i colori acromatici del dispositivo di riproduzione (“device” = pedice d) sono specificati da tre numeri esadecimali uguali. Per i colori cromatici almeno due numeri dei tre sono differenti. Il colori  $rgb_d$  e  $cmyd$  del dispositivo di riproduzione a colori sono trasformati dai valori  $rgb_d$  a quelli  $cmy_d$  secondo la “1-minus-relation”. Ad esempio per il colore blu i dati  $rgb_d$  00F<sub>d</sub> sono trasformati nei dati  $cmyd$  FF0<sub>d</sub>. Se nel file dei colori sono utilizzate queste due definizioni colorimetriche, i colori in output possono essere prodotti uguali o diversi. Con un file secondo DIN 33872-4, l’uguaglianza dell’output è testata considerando entrambe le definizioni, vedi  
<http://www.ps.bam.de/De14/10L/L14e00NP.PDF>

Fig. 5 (a destra) mostra i valori  $rgbde$  e  $cmyde$  per la stampa dei colori elementari (pedice de = “device to elementary data”) specificati da tre cifre esadecimali. Anche in questo caso i dati  $rgbde$  sono trasformati in dati  $cmyde$  in base alla “1-minus-relation”. Tuttavia, per esempio in Fig. 5 a pagina 7 il blu (prima fila, terzo colore) è definito dal numero esadecimale 06Fde invece di 00Fd. Il blu di fig. 5 (a destra) è il blu  $B_d$  del mezzo di riproduzione e il blu in fig. 5 (a sinistra) è il blu elementare  $B_e$ . Entrambi appaiono differenti,  $B_d$  appare rossastro e  $B_e$  né verde né rosso. Negli standard *sRGB* dei monitor e della stampa offset, i numeri esadecimali per la riproduzione del blu  $B_e$  sono diversi.

Nel caso di scale di colore visivamente equidistanti, le coordinate colorimetriche sono distinte dal simbolo \* (asterisco), come per esempio nella scala dei 16 valori di grigio equispaziati. Ad esempio, l’attributo visivo chiarezza  $L^*$  utilizza il simbolo \* (asterisco) mentre la luminanza  $L$  no. In modo simile si può aggiungere ai dati  $rgb$  il simbolo \* (asterisco), e chiamarlo  $rgb^*$ . Questo codice simbolico comporta per esempio che la serie esadecimale di dati  $rgb^*e = 000, 111, 222, \dots, EEE, FFF$  produca una serie di grigi visivamente equidistanti.

Invece dei numeri esadecimalesi possono usare numeri compresi tra 0.0 e 1.0. Ad esempio, il numero decimale corrispondente all’esadecimale 5 è 0,3333 (= 5 / F = 5/15). La tecnologia informatica usa i 256 numeri tra 00 e 9F e da A0 a FF, invece dei 16 numeri tra 0 e 9 e da A a F. Questi numeri esadecimalesi sono trasformabili in numeri decimali. Per esempio il numero esadecimale 55 è uguale al numero decimale 0,3333 (= 55/FF = 85/255).

Molti problemi si verificano nell’output di programmi dovuti al passaggio tra dati di colori equivalenti rapt e cmy0. Per esempio, colori equivalenti  $rgb$  e  $cmy0$  trattati dal software *Acrobat di Adobe* (tutte le versioni superiori a 3 in *Mac* e *Windows*) risultano differenti in output su display, mentre se trattati da *FrameMaker di Adobe* (versione 8, *Windows*, 2011) risultano uguali. Altro esempio, le stampanti a colori PostScript producono spesso risultati diversi mentre stampanti *PostScript-blackwhite* risultati uguali. Per i file di prova,

seguendo la norma DIN 33872-4 e -2, l'uguaglianza del risultato è testata, vedi <http://www.ps.bam.de/33872E>

## 4 Solido dei colori

*Leonardo da Vinci* (morto nel 1519) ha disposto la moltitudine di colori selezionando sei colori "elementari": una coppia di colori neutri o acromatici, bianco-nero, e due coppie cromatiche, rosso-verde e giallo-blu. Il doppio cono di Fig.6 è un modello semplificato per illustrare le sue idee. L'asse verticale è la linea di colori neutri (dal bianco al nero) e il cerchio la linea dei colori cromatici puri.

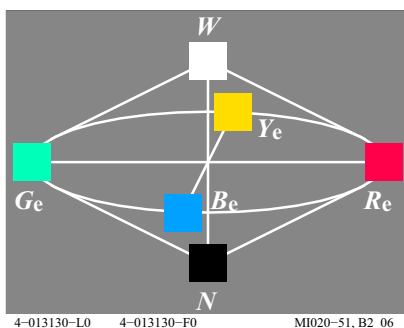


Fig. 6: Colour double cone

Fig. 6 mostra il doppio cono con i sei colori "semplici". In Fig. 6 le lettere stanno per:

$W$  bianco

$N$  nero

$Y_e$  giallo

$B_e$  blu

$R_e$  rosso

$G_e$  verde

Qui i sei colori "semplici" sono i sei colori "elementari" (pedice e).

Il Comitato Tecnico ISO TC 159/WG2/SC4 *Ergonomics, Visual Display Requirements* ha raccomandato, per produrre i quattro colori elementari  $RYGB_e$ , con le seguenti quattro dati d'ingresso  $rgb^*_e$  di 100, 110, 010, e 001 (vedi CIE R1-47). Ci sono almeno tre metodi per calcolare i dati  $rgbde$  (il pedice de significa "colori elementari del dispositivo") in output del dispositivo: un metodo posto nel dal produttore del dispositivo e l'altro proprio del file d'immagine. Il metodo del file d'immagine è stato utilizzato per modificare in questa pubblicazione tutti i dati  $rgb$  delle figure a seconda del dispositivo scelto per l'output ( $sRGB$  o stampa offset). Il file d'immagine consta di 729 (= 9x9x9) dati,  $RGB$  o  $CIELAB$ , a seconda del dispositivo per l'output (dati ottenuti da misurazione del colore).

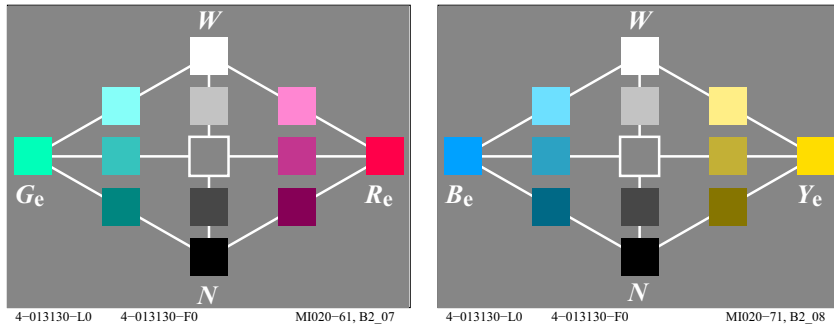


Fig. 7: sezione del piano delle tinte  $RG_e$ - $e$ - $YB_e$

La Fig. 7 mostra due sezioni del doppio cono dei colori con colori intermedi: a sinistra c'è la sezione verticale con i colori dal rosso al verde e a destra i colori dal giallo al blu. L'asse acromatico, dal bianco al nero, si trova al centro in entrambe le figure.

## 5 Colori elementari

Nel cerchio delle tinte ci sono quattro colori cromatici, che sono percettivamente semplici (confronta Tabella 1 a pagina 6). Questi colori, detti "elementari", sono il rosso elementare, il giallo elementare, verde elementare e il blu elementare.

In pratica il giallo elementare è individuabile se inserito ordinatamente nel cerchio delle tinte. Il giallo elementare è chiamato colore "unico" e, in questo caso, è un colore né rosso né verde, differente dal giallo-verde che, inserito nel cerchio delle tinte, si trova tra il giallo e il verde ed è così detto colore "binario".

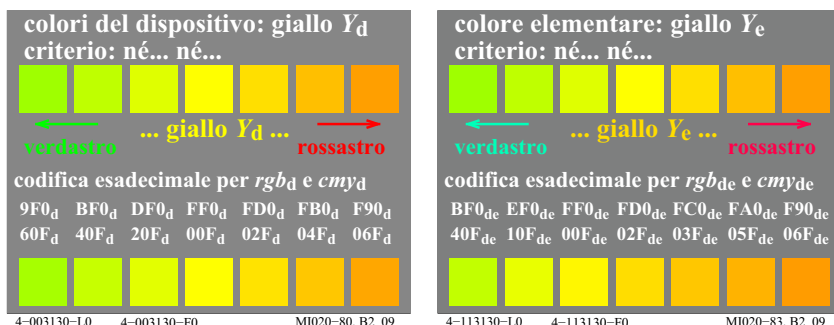


**Fig. 8: Colore del dispositivo e colore elementare ordinati seguendo il criterio per individuare il giallo elementare  $Y_e$**

Fig. 8 presenta il criterio per determinare nella regione dei colori gialli il colore giallo elementare  $Y_e$  senza usare il cerchio delle tinte. Solitamente, il dispositivo produce il colore giallo  $Y_d$  in corrispondenza ai dati d'ingresso  $rgb_d(1, 1, 0)$  o FF0. Il criterio per individuare il giallo elementare come colore né verde né rosso è qui soddisfatta in modo solo approssimato (a sinistra). Il dato d'ingresso  $(1, 0, 86, 0) = FD0$  produrre il previsto giallo elementare  $Y_e$  che gode della proprietà visiva “né verde né rosso”. L'esempio proposto a destra riguarda la stampa offset standard (a destra). In stampa offset la differenza tra il giallo elementare  $Y_e$  e il giallo del dispositivo  $Y_d$  è piccolo. Tuttavia per il blu è grande..

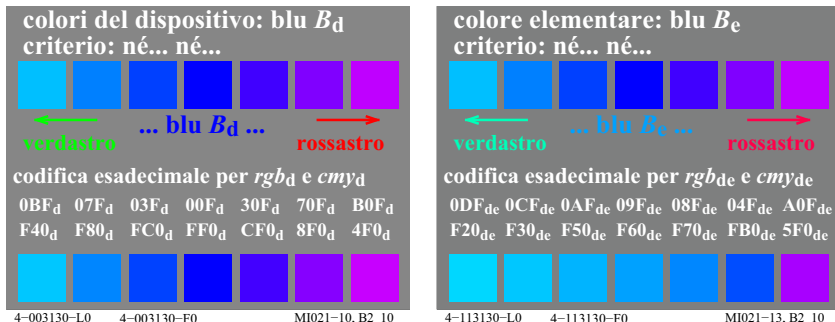


**Fig. 9: Colore del dispositivo e colore elementare ordinati seguendo il criterio per individuare il blu elementare  $B_e$**

Fig. 9 presenta il criterio per determinare nella regione dei colori blu il colore blu elementare  $B_e$  senza usare il cerchio delle tinte. Solitamente, il dispositivo produce il colore giallo  $Y_d$  in corrispondenza ai dati d'ingresso  $rgb_d(0, 0, 1)$  o 00F. Il criterio per individuare il blu elementare come colore né verde né rosso non è qui soddisfatta (a sinistra). Il dato d'ingresso  $(1, 0, 40, 0) = 06F$  produce il previsto blu elementare  $B_e$  che gode della proprietà visiva di essere *né verde né rosso*. L'esempio proposto a destra riguarda la stampa offset standard.

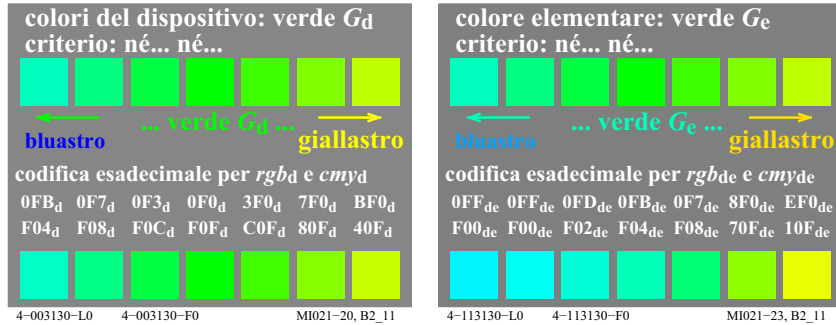


Fig. 10: Colore del dispositivo e colore elementare ordinati seguendo il criterio per individuare il verde elementare  $G_e$

Fig. 10 presenta il criterio per determinare nella regione dei colori verdi il colore verde elementare  $G_e$  senza usare il cerchio delle tinte. Solitamente, il dispositivo produce il colore giallo  $Y_d$  in corrispondenza ai dati d'ingresso  $rgb_d$  (0, 1, 0) o 0F0. Il criterio per individuare il verde elementare come colore né blu né giallo non è qui soddisfatta (a sinistra). Il dato d'ingresso (0, 1, 0,06) = OF1 produce il previsto verde elementare  $G_e$  che gode della proprietà visiva di essere né blu né giallo. L'esempio proposto a destra riguarda la stampa offset standard. La differenza tra il verde del dispositivo  $G_d$  e il verde elementare  $G_e$  è più piccola rispetto a quella del blu in stampa offset.

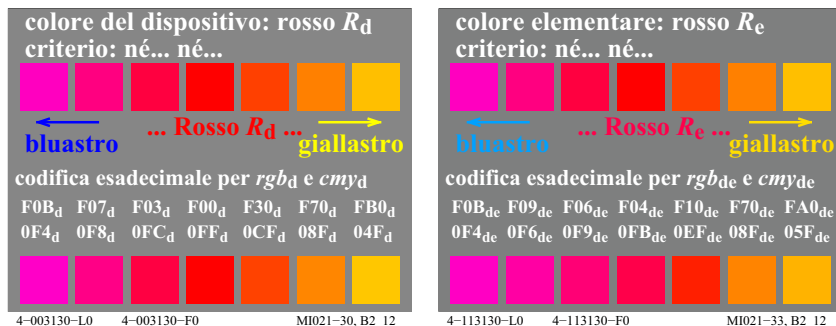


Fig. 11: Colore del dispositivo e colore elementare ordinati seguendo il criterio per individuare il rosso elementare  $R_e$

Fig. 11 presenta il criterio per determinare nella regione dei colori rossi il colore rosso elementare  $R_e$  senza usare il cerchio delle tinte. Solitamente, il dispositivo produce il colore rosso  $R_d$  in corrispondenza ai dati d'ingresso  $rgb_d$

(1, 0, 0) o F00. Il criterio per individuare il rosso elementare come colore *né blu né giallo* non è qui soddisfatta (a sinistra). Il dato d'ingresso (1, 0, 0,20) = F03 produce il voluto rosso elementare  $R_e$  che gode della proprietà visiva di essere *né blu né giallo.* ”. L'esempio proposto a destra riguarda la stampa offset standard.

*K. Miescher* (1948) ha determinato sperimentalmente i colori elementari su un cerchio delle tinte suddiviso in 400 passi impiegando 28 osservatori con sistema visivo adattato alla luce del giorno. I colori furono determinati con una deviazione standard di 4 passi per  $R_e$ , e  $Y_e$ , e  $G_e$  (1% = 4 passi su 400) e 8 passi per  $B_e$  (2%) (vedi CIE R1-47). I colori del cerchio delle tinte usato avevano alta croma rispetto ai colori dal n. 9 al 12 del CIetest (vedi fig. 52 a pagina 51).

## 6 Cerchio delle tinte simmetrico

I colori su entrambi i lati dei due assi perpendicolari, aventi tinte elementari  $R_e$ - $G_e$  e  $Y_e$ - $B_e$ , partendo dal centro acromatico diventano rispettivamente sempre più blu e gialli, rossi e verdi.

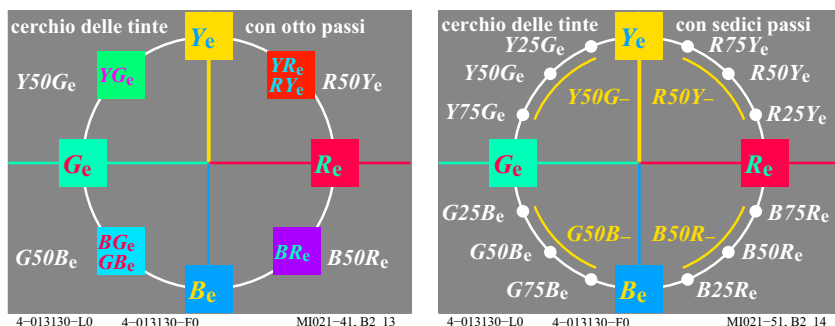


Fig. 12: cerchio delle tinte simmetrico e nomi dei colori intermedi

Fig. 12 mostra il cerchio delle tinte simmetrico con i colori elementari opposti, rosso - verde e giallo – blu, e i colori intermedi.

Nella maggior parte delle lingue (ad esempio tedesco, inglese, francese), i nomi “giallo” e “blu” sono usati come primo nome per chiamare colori composti, per esempio il colore giallo-rosso  $YR$ , il giallo-verde  $YG$ , il blu-verde  $BG$  e il blu-rosso  $BR$ . Questa denominazione scelta in queste lingue è seguita in Fig. 12 (a sinistra). In Fig. 12 (a destra) si usa l'angolo e la segale denominazione ordinata,  $RY_e$ ,  $YG_e$ ,  $GB_e$  e  $BR_e$ .

Inoltre, il sistema CIELAB colori (ISO 11664-4/CIE S 014-4) utilizza per la tinta hab l'angolo, detto *angolo di tinta*. L'angolo parte da 0 gradi, per il rosso elementare  $R_e$ , e cresce a 90 gradi, per  $Y_e$ , a 180 gradi per  $G_e$  e 270 gradi per  $B_e$ .

Il sistema dei colori CIELAB definisce 100 passi tra il bianco e il nero. Si possono usare 100 passi di tinta tra due tinte elementari contigue. Ciò porta a definire i nomi delle tinte intermedie (Fig. 12). La tecnologia dell'informazione raccomanda di usare quattro passi tra tinte contigue: per es. dal rosso  $R_e$  al giallo  $Y_e$  i contenuti di  $Y_e$  sono 0%, 25%, 50% e 75% e 100%. Molti dispositivi producono sfumature di tinta indefinite che fanno parte di una vasta gamma tra il  $Y_e$  e il  $Y_e$ .

Una tecnologia colorimetrica dell'informazione raccomanda di ottenere il colore visivo intermedio con la tinta  $R50Y_e$ . Per molti dei dispositivi di output le tinte prodotte per  $R50Y_e$  appartengono ad una vasta gamma  $R50Y_$  (gamma gialla) e similmente per le altre tinte intermedie  $Y50G_e$ ,  $G50B_e$  e  $B50R_e$ .

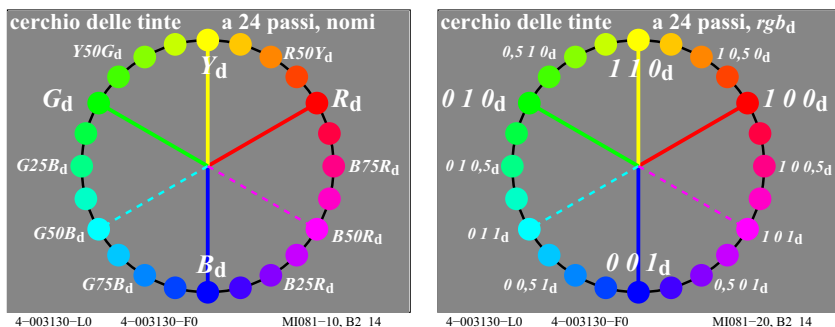
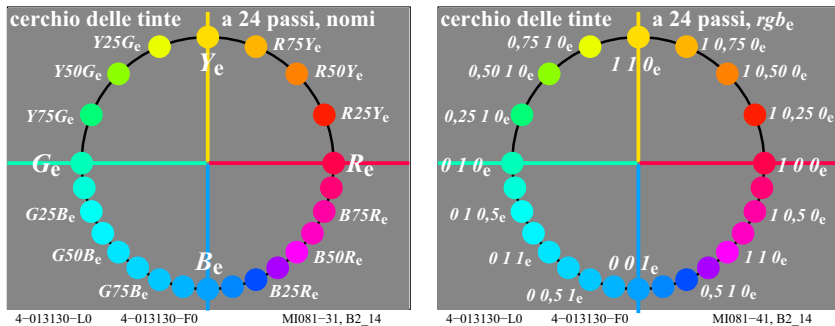


Fig. 13: Cerchio delle tinte prodotte dal dispositivo a 24 passi nella tecnologia dell'informazione

Fig. 13 mostra cerchio delle tinte prodotte dal dispositivo a 24 passi nella tecnologia dell'informazione. Per esempio si danno i colori  $RGB_d$  del dispositivo (*a sinistra*) e i corrispondenti dati d'ingresso  $rgb$   $(1\ 0\ 0)_d$ ,  $(0\ 1\ 0)_d$ , e  $(0\ 0\ 1)_d$  (*a destra*). Le tinte intermedie  $Y_d$ ,  $G50B_d$  e  $B50R_d$  sono prodotte dal dispositivo dai corrispondenti dati d'ingresso  $rgb$   $(1\ 1\ 0)_d$ ,  $(0\ 1\ 1)_d$  e  $(1\ 0\ 1)_d$ .

Per le applicazioni nella tecnologia, il design e l'arte la gamma dei colori più chiari tra il rosso al giallo al verde è più importante rispetto alla gamma di colori più scuri tra il verde verso il blu al rosso. Inoltre nel campo giallo del croma CIELAB  $C_{ab}^*$  di colori di superficie è due volte più grande rispetto alla gamma del blu, vedere la tabella con  $C_{ab}^*$  per 48 tinta sul retro della copertina interna.

Quindi per differenza angolo uguale differenze di tinta visive è due volte più grande nell'intervallo giallo rispetto alla gamma blu. Entrambi i motivi sono utilizzati per aumentare l'intervallo tra rosso al giallo al verde da 120 gradi a 180 gradi, e per ridurre il campo tra verde al blu al rosso da 240 gradi a 180 gradi.



**Fig. 14: Cerchio delle tinte elementari a 24 passi nella tecnologia dell'informazione**

Fig. 14 mostra la relazione tra le tinte elementari  $RYGB_e$  (a sinistra) e i dati d'ingresso  $rgb^*_e$  (a destra) nella tecnologia dell'informazione per un cerchio delle tinte a 24 passi. Fig. 14 mostra le tinte elementari  $RYGB_e$  relative ai dati d'ingresso  $rgb^*_e (1\ 0\ 0)_e, (1,\ 1\ 0)_e, (0\ 1\ 0)_e$  e  $(0\ 0\ 1)_e$ . Il flusso di lavoro del file in uscita deve produrre i dati  $rgbde$  per il voluto output di tinte elementari. Nel caso più semplice il produttore del dispositivo può produrre la trasformazione per il suo dispositivo. La norma DIN 33872-5 contiene una cartella di prova nei formati *PDF* e *PS (PostScript)*. Di solito le tinte elementari in output sono verificate visivamente, ma possono essere specificate anche colorimetricamente.

La discriminazione minore delle tinte dei colori di superficie si trova nella gamma dei colori più scuri, dal verde al blu fino al rosso. Perciò, in questa zona di colori più scuri, si raccomanda di usare soltanto i colori associati a passi pari.

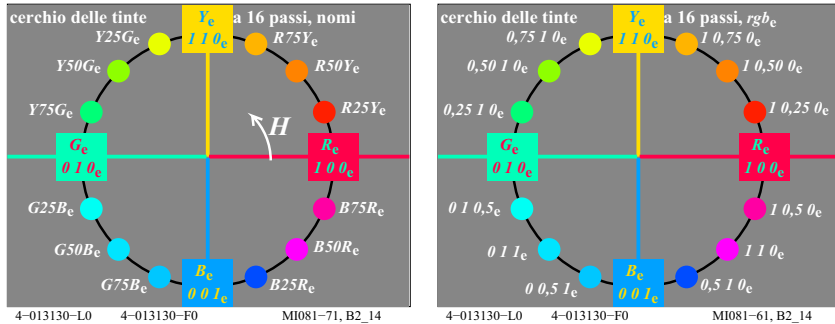


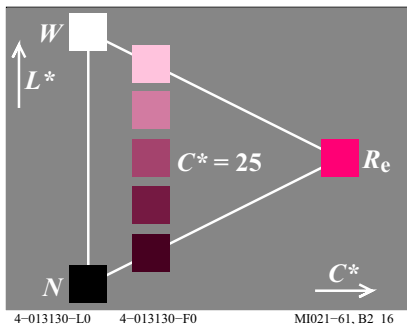
Fig. 15: Cerchio delle tinte elementari a 16 passi nella tecnologia dell'informazione

Fig. 15 mostra la relazione tra le tinte elementari  $RYGB_e$  (a sinistra) e i dati d'ingresso  $rgb^*$  (a destra) su un cerchio delle tinte a 16 passi nel campo della tecnologia dell'informazione. Le tinte elementari  $RYGB_e$  sono prodotte per i dati d'ingresso  $rgbe$  ( $1\ 0\ 0_e$ ,  $(1\ 1\ 0)_e$ ,  $(0\ 1\ 0)_e$  e  $(0\ 0\ 1)_e$ ). La tinta cambia col crescere dell'angolo di tinta in modo simile a quello dell'angolo di tinta  $hab$  del sistema dei colori CIELAB (ISO 11564-4). Secondo la norma CIE R1-47 gli angoli delle tinte elementari hanno nel sistema di ordinamento dei colori CIELAB gli angoli di tinta  $h_{ab}$  di  $26^\circ$ ,  $92^\circ$ ,  $162^\circ$  e  $272^\circ$ . In particolare il rossoelementare  $R_e$  e il verde elementare  $G_e$  non si trovano sull'asse orizzontale del sistema dei colori CIELAB.

## 7 Colori con croma massima

In una successione ordinata di colori con diverse quantità di colore, che parte dal bianco e giunge al nero attraverso colori cromatici, prima biancastri e poi nerastri, vi è un colore che viene percepito possedere il massimo contenuto di colore, ossia la massima croma.

La successione ordinata dei colori (*Bracketing*) consente di individuare il rosso più rosso. Questa individuazione si ottiene ordinando i colori in successione seguendo il criterio per cui un colore diventa più acromatico o più cromatico e contemporaneamente diventa più bianco o più nero.

**Fig. 16: Maximum chroma**

In Fig. 16, si può facilmente individuare il colore cromatico più rosso. Si danno i criteri per determinare il colore di chroma massima in una successione di colori con diverse quantità di materia colorante. Le denominazioni stanno per:

$R_e$ rosso	$W$ bianco	$N$ nero
$c$ più cromatico	$w$ più bianco	$n$ più nero
$C^*$ croma	$L^*$ chiarezza	

Generalmente, nella tecnologia dell'informazione, il colore di qualsiasi tinta più cromatico (colore specificato da maggiore croma  $C^*_{ab}$  nel sistema CIELAB) viene mescolato col bianco  $W$  e col nero  $N$ . Per la miscela del colore più cromatico  $R_e$  e il più bianco  $W$  a partire dal più cromatico la differenza di cromaticità CIE decresce con continuità, mentre per la miscela del colore più cromatico  $R_e$  col nero  $N$  la cromaticità è approssimativamente costante. La sintesi additiva dei colori su monitor a colori (display) e la sintesi sottrattiva dei colori sottrattiva in stampa offset verranno discusse nella sezione 20 a pagina 64.

In Fig. 16, i colori visualmente intermedi  $RW_e$  e  $RN_e$  sono compresi rispettivamente tra  $R_e$  e  $W$  e tra  $R_e$  e  $N$ . Analogamente a quanto mostrato in fig. 10 di pagina 11, i colori in output appartengono ad una grande gamma dipendente dal dispositivo (*gamma dei colori gialli*).

## 8 Attributi colore: croma e chiarezza

Tre attributi del colore specificano un colore percettivamente. La maggior parte dei sistemi di colori scelgono la tinta come primo attributo: per esempio il sistema dei colori di *Munsell*, il sistema dei colori DIN 6164 e il sistema dei colori *NCS*. Questi sistemi di colore differiscono nella scelta degli altri due attributi del colore. Sistemi di colore diversi sono confrontabili se i loro sistemi di coordinate sono simili a questo. In colorimetria si considera una sezione del

solido dei colori contenenti i colori a tinta costante. Si usa la croma  $C^*$  in ascissa e la chiarezza  $L^*$  in ordinata.

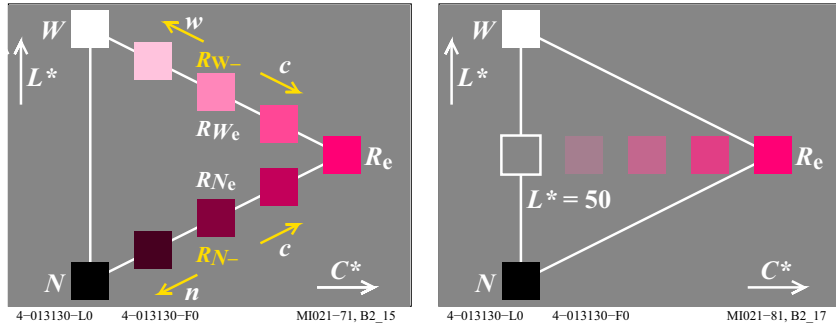


**Fig. 17: Colori ad uguale croma  $C^*_e$  colori ad uguale chiarezza  $L^*$**

Fig. 17 (*a sinistra*) mostra colori a tinta costante e croma  $C^* = 25$ . I colori ad uguale croma sono situati su colonne parallele all'asse acromatico. In colorimetria si può utilizzare croma  $C^* = 100$  per il rosso più cromatico  $R_e$ . In Fig. 17 (*a sinistra*) si considerano i colori con croma  $C^* = 25$ .

Fig. 17 (*a destra*) mostra colori di tinta costante e luminosità  $L^* = 50$ . I colori di uguale chiarezza si trovano su righe orizzontali, perpendicolari all'asse acromatico. In colorimetria associa la chiarezza  $L^* = 100$  al bianco  $W$ . In fig. 17 (*a destra*) si considerano i colori con chiarezza  $L^* = 50$ .

Le scale di colori a tinta costante, a croma costante e a chiarezza costante furono definite per la prima volta nel sistema *Munsell-colore*. Questo sistema consta di campioni di colore di 40 tinte diverse. Oggi la metrica del colore negli spazi dei colori (ISO 11564-4 e -5) definisce le coordinate croma  $C^*$  (designata con  $C^*_{ab}$  nel CIELAB e con  $C^*_{uv}$  nel CIELUV) e chiarezza  $L^*$ .

Nel sistema ordinato dei colori *RAL-Design* i campioni di colore di 36 tinte CIELAB  $h_{ab} = 0, 10, a 350$  costituiscono una rete, i cui passi sono in croma con  $\Delta C^*_{ab} = 10$  e in chiarezza con  $\Delta L^* = 10$ .

## 9 Attributi del colore: brillantezza e bianchezza

. Ci sono più attributi del colore, oltre ai tre attributi di tinta, di croma e di chiarezza. In un piano a tinta costante gli ulteriori attributi del colore, la nerezza (attributo opposto di brillantezza) e la bianchezza (attributo opposto di profondità di colore) hanno una relazione lineare con la croma e la chiarezza.

Gli attributi del colore nerezza e brillantezza descrivono la stessa proprietà. Tuttavia, i valori di questi attributi cambiano secondo direzioni opposte, in modo simile a quelli di chiarezza e scurezza. Inoltre la bianchezza e la profondità colore corrono in direzioni opposte. La nerezza (*Blackness*) è un attributo di colore importante nel *Natural Color System (NCS)* svedese. Il sistema dei colori *NCS* sceglie come attributi del colore la tinta, la nerezza e la croma (*chiarezza* "chromaticness"). La attributo del colore chiarezza non è utilizzato nel sistema dei colori di *Munsell*.

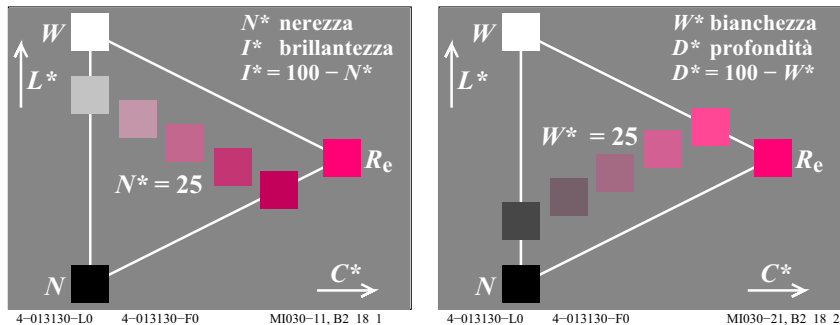


Fig. 18: Nerezza  $N^* = 25$  e bianchezza  $W^* = 25$ .

Fig. 18 colori spettacoli di nero uguale a  $N^*$  (*a sinistra*) con il nero  $N^* = 25$  e del candore pari  $W^*$  (*a destra*) con il bianco  $W^* = 25$ . Invece del nero  $N^*$  la brillantezza attributo di colore  $I^* = 100 - N^*$  può essere scelto. Invece di bianco  $W^*$  l'attributo di profondità colore  $D^* = 100 - W^*$  può essere scelto.

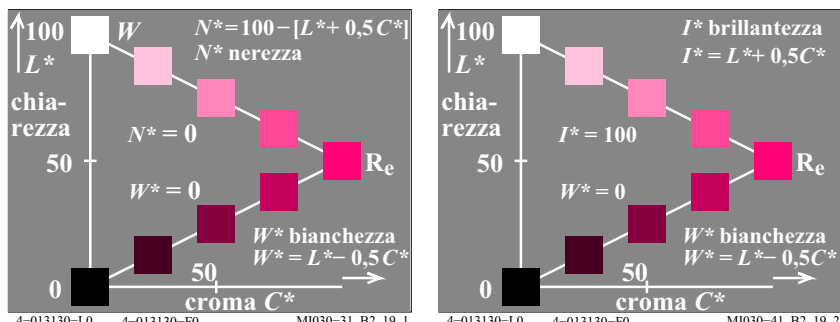


Fig. 19: Nerezza  $N^*$ , bianchezza  $W^*$  e brillantezza  $I^*$

Fig. 19 mostra la relazione dei tre attributi del colore, nerezza  $N^*$ , bianchezza  $W^*$  e brillantezza  $I^*$ , con i due attributi dei colori chiarezza  $L^*$  e croma  $C^*$ . Fig. 19 mostra le relazioni mediante equazioni lineari.

Ci si aspetta che le relazioni lineari siano connesse con i segnali fisiologici acromatici e cromatici di Fig. 54 a pagina 54 ed i valori cromatici della Fig. 58 a pagina 61 (*in basso a sinistra*).

## 10 Spettro dei colori e colori elementari

### 10.1 Valenza luminosa e chiarezza

Lo spettro dei colori della luce diurna, che può essere prodotto da un prisma e che fu studiato da *Newton* (morto 1727), contiene la radiazione luminosa dalle corte lunghezze d'onda del violetto-blu (circa R60B<sub>c</sub>) e le lunghe lunghezze d'onda del rosso giallastro (circa J90R<sub>c</sub>). Le radiazioni luminose di luci colorate differiscono nella loro distribuzione spettrale. La distribuzione spettrale della radiazione luminosa che giunge all'occhio è stata modificata dalle riflessioni su superfici, che appaiono colorate. Per esempio tale modifica in riflessione è dovuta ai pigmenti, solitamente prodotti nell'industria chimica.

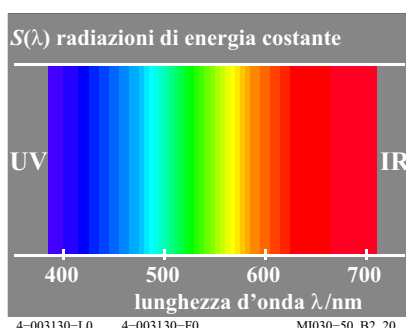


**Fig. 20: Visible spectral region**

Fig. 20 mostra schematicamente la regione della radiazione luminosa con tutte le lunghezze d'onda nello spettro visibile compresa tra circa  $\lambda = 380\text{nm}$  e  $\lambda = 720\text{nm}$  ( $1\text{ nm} = 10^{-9}\text{m}$ ). La radiazione al di fuori di questo intervallo è detta *ultravioletta* (UV) e *infrarossa* (IR). Fig. 20 mostra uno spettro, che può essere prodotto da un filtro linearmente variabile posto sul piano portadiapositiva di un proiettore. Il filtro linearmente variabile ha la proprietà di farsi attraversare dalla radiazione luminosa visibile tra circa 380nm e 720nm selezionata dal filtro in lunghezza d'onda secondo linee contigue mutuamente parallele.

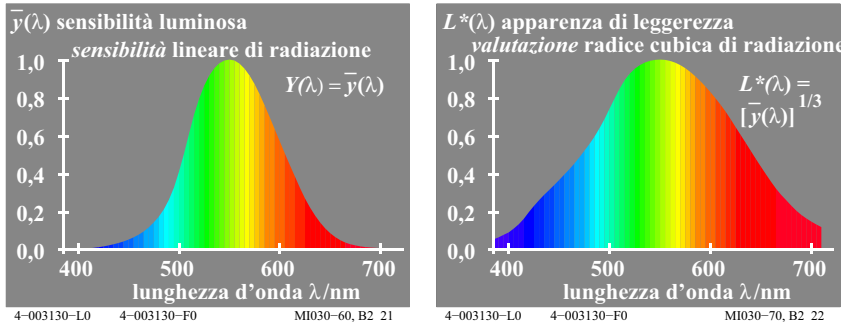


**Fig. 21: Sensibilità luminosa spettrale e apparenza della chiarezza**

In Fig. 21 (a sinistra) la sensibilità luminosa spettrale  $Y(\lambda)$  ha il massimo al centro della regione giallo-verde. Questa proprietà è una conseguenza della efficienza luminosa spettrale  $Y(\lambda) = V(\lambda) = y_q(\lambda)$  dell'occhio. Questa efficienza ha un massimo vicino 555nm e scende a meno di 1% vicino 400nm e 700nm. La funzione di efficienza luminosa spettrale relativa  $y_q(\lambda)$  rappresenta la valenza luminosa del colore ottenuto dalla miscela di colori spettrali, per esempio di 10 nm e una banda di larghezza uguale energia della radiazione luminosa. Pertanto il valore che è descritto dalla funzione di efficienza luminosa  $y_q(\lambda)$  può essere chiamato anche valore luminoso o valenza luminosa.

Nel CIE 15 Colorimetria tristimolo il valore  $Y$  con la normalizzazione  $Y_W = 100$  per il bianco  $W$ , è definito, confrontare sezione 17 a pagina 47

Diverso dalla funzione lineare  $Y(\lambda)$  è una funzione non lineare  $L^*(\lambda)$  che descrive l'aspetto leggerezza dei colori spettrali di uguale radiazione luminosa. Questa funzione non lineare diminuisce dal centro dello spettro a entrambe le estremità da una relazione non lineare che è approssimativamente cubica per grigio e quadratica per il bianco circonda, confronta sezione 16 a pagina 42.

Fig. 21 (a destra) mostra la luminosità  $L^*$  aspetto ( $\lambda$ ). La funzione  $L^*(\lambda)$  diminuisce molto meno rispetto alla funzione  $Y(\lambda)$  (a sinistra).

Nota: CIE 15 definisce la seguente relazione tra  $L^*$  leggerezza e il valore di tristimolo  $Y$ :

$$L^* = 116 [Y/100]^{1/3} - 16 \quad (Y > 0,8)$$

Approssimazioni sono le relazioni:

$$L^* = 100 [Y/100]^{1/3} \text{ e } L^* = Y^{1/3}$$

che viene utilizzato per i colori spettrali in Fig. 21..

## 10.2 Chromatic Value (Valence) and Chroma

Nella miscela dei colori dello spettro viene valutato da *valori luminosi* e in aggiunta da *valori cromatici*.

Lo spettro visibile include una serie continua di colori, e si può riconoscere in esso tre colori spettrali elementari. I colori spettrali elementari si trovano vicino al 475nm per il blu elementare  $B_e$ , 503nm per il verde elementare  $G_e$ , e 575nm per le elementari  $Y_e$  giallo.

Elementare rosso si trova fuori dello spettro visibile e può essere prodotta per esempio da una adatta miscela di colori 400nm e 700nm. I colori porpora prodotti in questo modo sono specificati da lunghezze d'onda di compensazione rispetto a E illuminante (uguale energia della radiazione luminosa). Per elementare  $R_e$  rosso questo risultato è la lunghezza d'onda dominante  $\lambda_{d,E} = 494c$  nm, vedi fig. 50 a pagina 47.

Alle due estremità spettrali dello spettro dei valori di rosso, verde e giallo-blu cromatiche cambiare il segno da negativo a positivo o in senso opposto.

*The following text is only mainly in English. We hope that we can translate the text soon into Italian.*

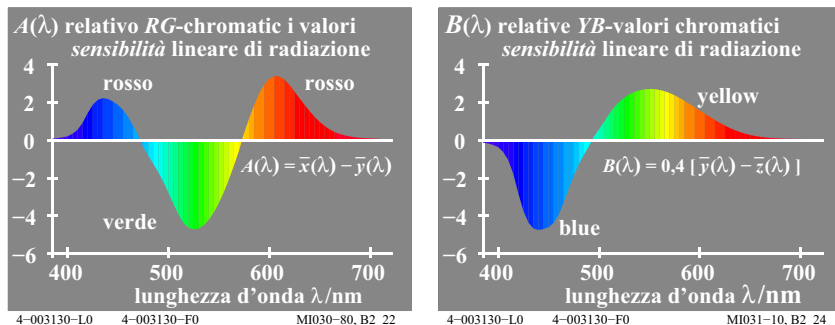


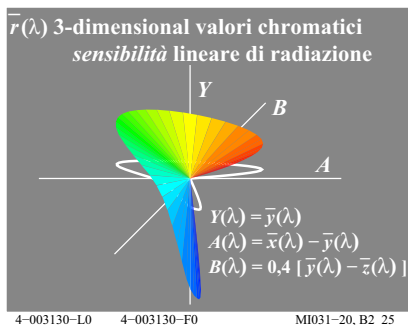
Fig. 22: **RG-chromatic values and YB-chromatic values**

Fig. 22 (*left*) shows the red-green-chromatic values  $A(\lambda)$ , which are the red-green-valences (values) in the colour mixture, as function of wavelength. The zero points are near 475nm and 575nm and specify the spectral elementary colours blue  $B_e$  and yellow  $Y_e$ .

Fig. 22 (*right*) shows the yellow-blue-chromatic values  $B(\lambda)$ , which are the yellow-blue-valences (values) in the colour mixture, as function of wavelength.

The cero point is near 503nm and specifies the spectral elementary colour green  $G_e$ .

For the spectral colours of equal energy the luminous values and the red-green- and yellow-blue-chromatic values produce three numbers (a vector) for any wavelength  $\lambda$ , for example of the band width 10nm between 380nm and 720nm. In the 3-dimensional space a point is created for the coordinates red-green-chromatic value  $A$ , yellow-blue-chromatic value  $B$  and luminous value or tristimulus value  $Y$  of any wavelength. In Fig. 23 the points of all spectral colours are located on a 3-dimensional curve.



**Fig. 23: 3-dimensional colour values**

Fig. 23 shows the 3-dimensional colour values in the colour space ( $A$ ,  $B$ ,  $Y$ ), and the projection in the plane ( $A$ ,  $B$ ) (white curve). The 3-dimensional curve cuts the plane ( $B$ ,  $Y$ ) near 475nm (elementary blue  $B_e$ ) and 574nm (elementary yellow  $Y_e$ ). The plane ( $A$ ,  $Y$ ) is cut near 503nm (elementary green  $G_e$ ). Fig. 23 includes the linear relation between the luminous and chromatic values  $Y(\lambda)$ ,  $A(\lambda)$  and  $B(\lambda)$  and the CIE tristimulus values  $x_q(\lambda)$ ,  $y_q(\lambda)$ , and  $z_q(\lambda)$ .

There is a difference between chromatic value (valence in colour mixture) and chroma similar compared to the difference between luminous value and lightness.

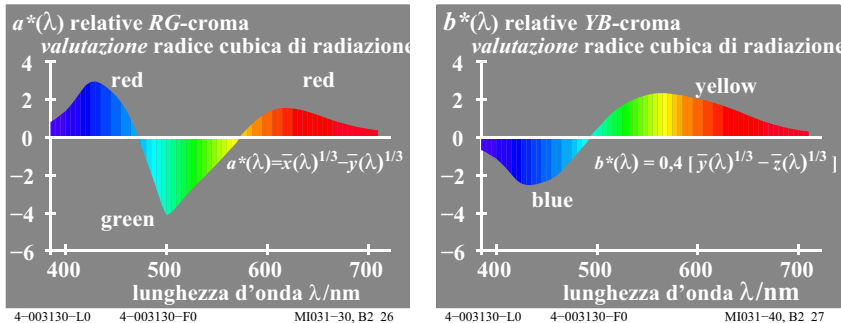


**Fig. 24: RG-chroma and YB-chroma**

Fig. 24 (*left*) shows the red-green-chroma  $a^*(\lambda)$  which describes chroma appearance of reddish and greenish spectral colours. The zero points are near 475nm and 574nm and specify the spectral elementary colours blue  $B_e$  and yellow  $Y_e$ .

Fig. 24 (*right*) shows the yellow-blue-chroma  $b^*(\lambda)$  which describes chroma appearance of yellowish and bluish spectral colours. The zero point is near 503nm and specifies the spectral elementary colour green  $G_e$ .

For the spectral colours of equal energy the lightness and the red-green-, and yellow-blue-chroma produce three numbers (a vector) for any wavelength  $\lambda$ , for example of the band width 10nm between 380nm and 720nm. In the 3-dimensional space a point is created for the coordinates red-green-chroma  $a^*$ , yellow-blue-chroma  $b^*$  and lightness  $L^*$  for any wavelength. In Fig. 25 the points of all spectral colours are located on a 3-dimensional curve.

It is useful to define the group term colorness (*German Farbheit*) which covers the terms lightness, red-green-chroma, yellow-blue-chroma, whiteness, blackness, deepness, and other visual colour attributes. Instead of the term chroma also the term chromaticness is used, for example in the NCS-colour system.

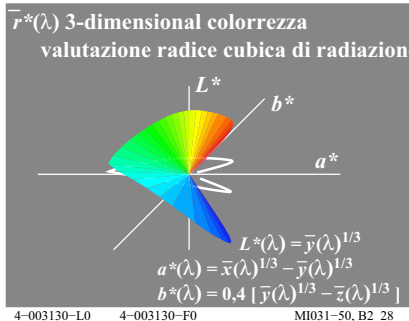
**Fig. 25: 3-dimensional colorness**

Fig. 25 shows the three colorness data  $L^*$ ,  $a^*$ ,  $b^*$  in the 3-dimensional colour space ( $a^*$ ,  $b^*$ ,  $L^*$ ), and the projection in the plane ( $a^*$ ,  $b^*$ ) (white curve). The 3-dimensional curve cuts the plane ( $b^*$ ,  $L^*$ ) near 475nm (elementary blue  $B_e$ ) and 574nm (elementary yellow  $Y_e$ ). The plane ( $a^*$ ,  $L^*$ ) is cut near 503nm (elementary green  $G_e$ ).

In Fig. 25 the projection of the 3-dimensional curve in the plane ( $a^*$ ,  $b^*$ ) is shown by a white curve. Fig. 25 includes the nonlinear relation of the spectral lightness and chroma  $L^*(\lambda)$ ,  $a^*(\lambda)$ , and  $b^*(\lambda)$  with the spectral tristimulus values  $x_q(\lambda)$ ,  $y_q(\lambda)$ , and  $z_q(\lambda)$ .

## 11 Dispositivo per miscelare i colori spettrali e riflettanza

With a spectrophotometer one can measure at each wavelength the reflection of the radiation which falls upon a surface. By comparison of the reflection of a surface colour with the reflection of the ideal white surface one normally gets a spectral reflection curve with numerical values between 0,0 and 1.0 for each wavelength.

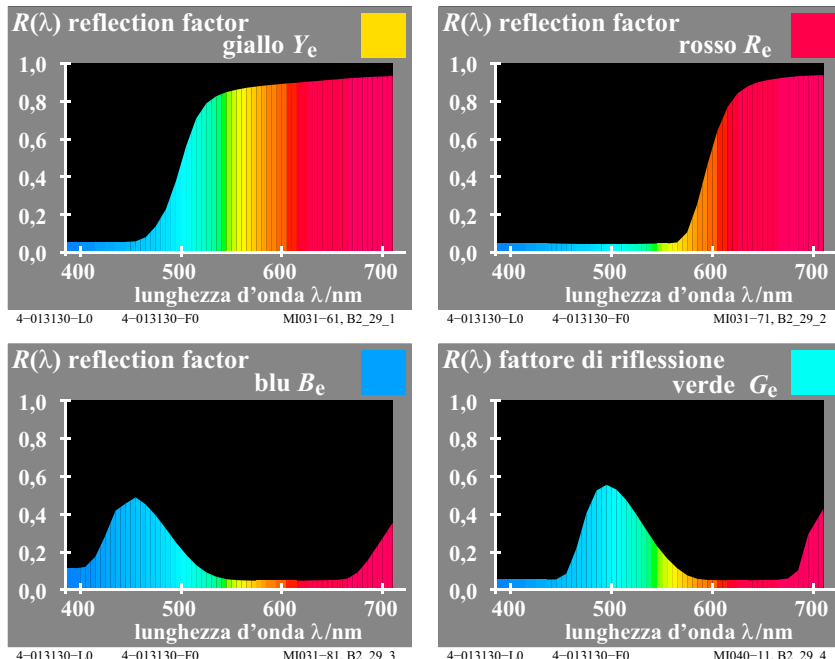


Fig. 26: Spectral reflection factor of the four elementary colours  $RYGB_e$

Fig. 26 shows spectral reflection factors which are transferred to "masks" with corresponding transmission factors. With a spectral apparatus for mixing spectral colours one can produce optically the elementary colours  $RYGB_e$ .

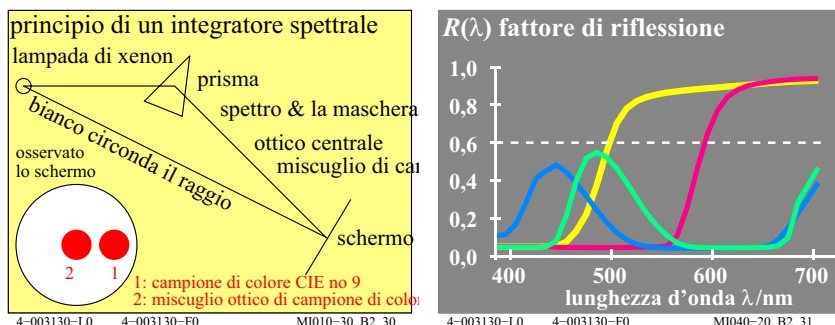


Fig. 27: Apparatus for mixing spectral colours and reflection factor as mask

Fig. 27 (*left*) shows the principle of an apparatus for mixing spectral colours. From a white xenon arc lamp two light paths are started.

The surround light path produces a white surround with the shape of a circular ring on the projection screen.

In the central-field light path the light is split by a prism into a spectrum. This spectrum is mixed optically and produces a circular white central field. The white light of the central and surround field is equal at the projection screen.

By the help of masks at the location of the spectrum some spectral colours may be partially or totally masked out. The remaining parts of the spectrum are mixed optically. Different masks will lead to different central field colours, for example to the CIE-test colour no. 9 (elementary red  $R_e$  according to CIE R1-47).

Fig. 27 (*right*) shows the masks for the elementary colours  $RYGB_e$ . The masks are produced according to the reflection factors  $R(\lambda)$  of the CIE-test colours no. 9 (red  $R_e$ ), no. 10 (yellow  $Y_e$ ), no. 11 (green  $G_e$ ) and no. 12 (blue  $B_e$ ). According to CIE 13.3 these CIE-test colours and others are used for the specification of colour rendering properties of light sources. In addition a constant reflection factor  $R(\lambda) = 0,6$  is shown which corresponds to a light grey colour.

## 12 Fluorescenza

Fluorescence changes short wave absorption to longer wave radiation. Optical brighteners use this effect. With optical brighteners laundry and paper appears whiter and paints appear more luminous. Luminous red is used as warning colour. The luminous paints or fluorescent colours produce an extension of the normal colour gamut of normal (non-fluorescent) surface colours.

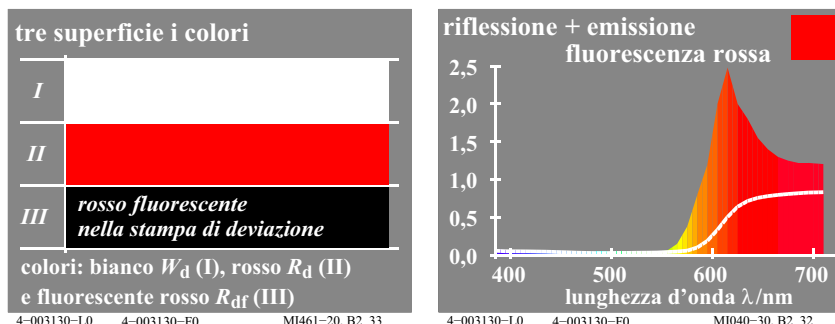


Fig. 28: Surface colours and reflection and emission of a fluorescent colour

Fig. 28 shows three surface colours white  $W_d$  (I), red  $R_d$  (II) and a fluorescent red  $R_{df}$  (III) (*left*), and the reflection and emission of a fluorescent colour red  $R_{df}$  (*right*). Fluorescent colours reflect more long wave (red appearing) light than a white diffuse reflecting sample. In Fig. 28 (*right*) the sum of the spectral emission and reflection is for the fluorescent colour red larger than 1,0 in the long wave spectral region. This surface colour appears especially luminous red. Therefore we call this colour a luminous colour.

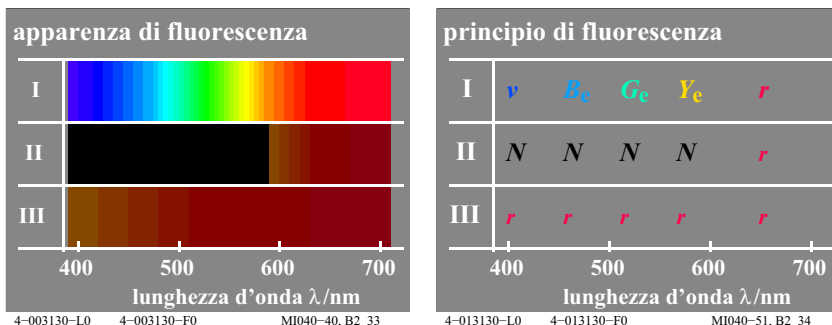


Fig. 29: Spectral appearance and principle of fluorescence

Fig. 29 shows the appearance (*left*) and the principle (*right*) of the fluorescence. The spectrum appears on an white surface (I), a normal red surface (II) and a fluorescent red surface (III) very different (*left*).

The change of the colour appearance of the spectrum can be demonstrated on different colour areas. One produces a spectrum with a continuous interference filter. The spectrum is projected on the three different colour areas I to III:

- The spectrum on a white surface (I) appears as the usual colour series violet-blue  $v$ , blue  $B_e$ , green  $G_e$ , yellow  $Y_e$ , and red  $r$  (*left*). This is indicated by letters according to the colours (*right*).
- The spectrum on a red surface (II) appears dark in the range violet-blue  $v$  to yellow  $Y_e$ , and reflects in the red region similar compared to white (*left*). The letter  $N$  (=black) indicates absorption in the range violet-blue  $v$  to yellow  $Y_e$  and the letter  $r$  reflection (*right*).
- The spectrum on a fluorescent red surface (III) appears red  $r$  in the whole spectral range between violet-blue  $v$  and red  $r$  (*left*). The letter  $r$  for the whole spectrum indicates this reflection property (*right*).

## 13 Retroriflessione

Retroreflective materials appear as particular chromatic and luminous colours under special lighting and observing conditions. The colour is here produced by the illuminant, an achromatic (white appearing) material surface with special geometric reflection properties, and a transparent colour layer as a colour filter. This colour filter has different transmission factors depending on its colouring.

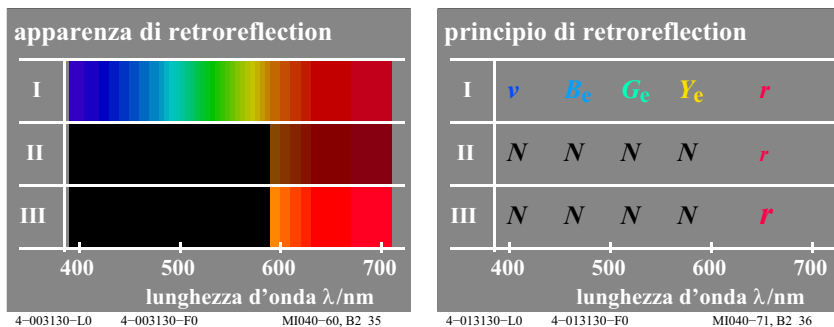


Fig. 30: Spectral appearance and principle of retroreflection

Fig. 30 shows the appearance (*left*) and the principle (*right*) of the retroreflection. The spectrum appears on an white surface (I) and the normal red surfaces (II) and a retroreflective red surface (III) very different (*left*).

The change of the colour appearance of the spectrum can be demonstrated on different colour areas. One produces a spectrum with a continuous interference filter. The spectrum is projected on the three different colour areas I to III:

- The spectrum on a white surface (I) and a normal red surface (II) is already described in Fig. 29.
- The spectrum on a retroreflective red surface (III) appears dark in the range violet-blue  $v$  to yellow  $Y_e$ , and may reflect in the red region more compared to white (*left*). The letter  $N$  (=black) indicates absorption in the range violet-blue  $v$  to yellow  $Y_e$  and the large letter  $r$  an increase of reflection (*right*). This reflection reaches a maximum when the direction of illumination and observation agree.

## 14 Miscela di colori

### 14.1 Dichromatic additive Colour Mixture

*Miescher* has called the additive mixture of two colours a *dichromatic* colour mixture. Similarly one calls a mixture of three colours a *trichromatic* colour mixture. The mixture of two compensatory colours, which may result in an achromatic colour, is according to *Miescher* (1961, 1965) called an *antichromatic* colour mixture.

Colours of any given spectral distribution can be produced by additive colour mixture with an apparatus for mixing spectral colours, compare Fig. 27 on page 26. It is even possible to obtain the *optimal colours*, representing the possible limits of surface colours. Among the optimal colours the *most chromatic* colours, for example the reddest red, are of large importance for image technology, see section 19 on page 64.

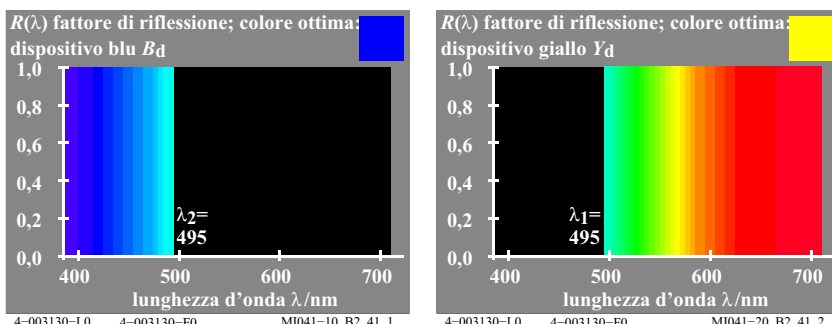


Fig. 31: Dichromatic additive colours  $B_d$ ,  $Y_d$

Fig. 31 shows the dichromatic mixture of white. White  $W$  is produced by additive mixture of any pair of *compensatory* (or complementary) optimal colours (for example blue  $B_d$  and yellow  $Y_d$ ). In the following and in reproduction processes a greenish yellow which we call the device yellow  $Y_d$  ( $Y = \text{yellow}$ ,  $d = \text{device}$ ), and a reddish blue  $B_d$  is usually used.

In Fig. 31 (*left*) the reflection curve of the optimal colour blue  $B_d$  has a sharp transition between the value 1,0 and 0,0 at 490nm. The reflection curve has the value 1,0 between 380nm and 490nm and the value 0,0 between 490nm and 720nm.

In Fig. 31 (*right*) the reflection curve of the optimal colour yellow  $Y_d$  has the value 0,0 between 380nm and 490nm with a sharp cut off at 490nm. Between 490nm and 720nm the value is 1,0.

The additive mixture of both optimal colours  $B_d$  and  $Y_d$  results in an achromatic colour with a spectral reflection curve  $R(\lambda)$  of the value 1,0 throughout, which appears white.

Fig. 31 shows two device colours yellow  $Y_d$  and blue  $B_d$  which are different compared to the elementary colours yellow  $Y_e$  and blue  $B_e$ .

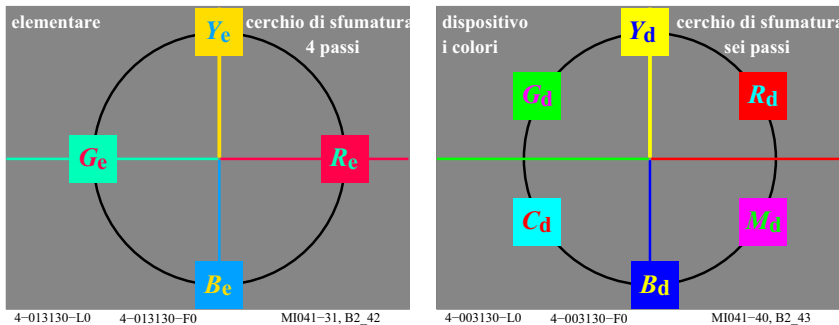


**Fig. 32: Four elementary colours  $YRGB_e$  and six device colours  $RYGCBM_d$**

Fig. 32 (*left*) shows the four elementary colours red  $R_e$ , yellow  $Y_e$ , green  $G_e$ , and blue  $B_e$  in a symmetric elementary colour circle.

Fig. 32 (*right*) shows the six chromatic colours  $RYGCBM_d$  of a 6 step hue circle, which serves as basis for the colour reproduction. According to the location in the symmetric hue circle yellow  $Y_d$  appears slightly greenish compared to yellow  $Y_e$  and blue  $B_d$  appears reddish compared to blue  $B_e$ .

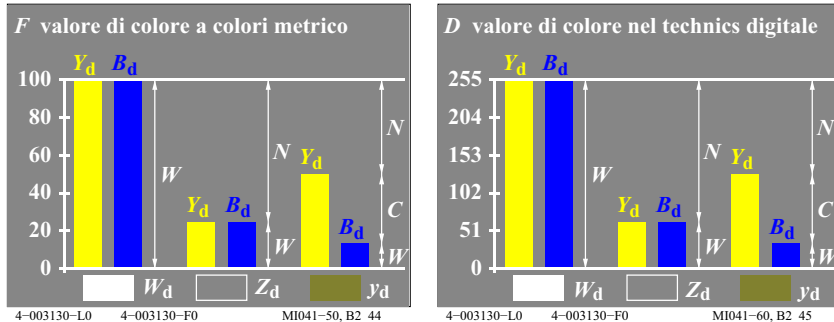


**Fig. 33: Dichromatic colour value in colorimetry and digital technic**

Fig. 33 shows the colour value  $F$  in colorimetry (*left*), and the colour values  $D$  in the digital technology (*right*). In colorimetry 100 steps and in digital technic 255 steps are used.

Fig. 33 shows mixture colours between a dominant colour yellow  $Y_d$  and the compensatory colour blue  $B_d$ : white  $W_d$ , central grey  $Z_d$ , and a yellow colour  $y_d$  (*bottom right*).

If one uses 100% of both the dominant colour  $Y_d$  and the compensatory colour blue  $B_d$ , then the achromatic mixture is the colour white  $W_d$  with the spectral reflection factor of the value 1,0 throughout. It is valid in the left part: white value  $W = 100$ , black value  $N = 0$  and chromatic value  $C = 0$ . The mixture colour  $W_d$  is shown (*bottom left*).

If one uses only 25% of both the dominant colour  $Y_d$  and the compensatory colour blue  $B_d$ , then the achromatic mixture is the colour central grey  $Z$ . With the apparatus for spectral mixtures the masks may have only two jumps between 0,0 and 0,25. It is valid in the middle part for central grey  $Z_d$ : white value  $W = 25$ , black value  $N = 75$ , and chromatic value  $C = 0$ .

If the dominant colour  $Y_d$  is larger compared to the compensatory colour blue  $B_d$ , then a chromatic colour is produced which has the hue of the dominant colour. It is valid in the right part: white value  $W = B_d = 15$ , black value  $N = 100 - Y_d = 50$ , and chromatic value  $C = Y_d - B_d = 35$ .

The image technology leads to the reproduction of equidistant colour series of the colour attributes. For example equidistant lightness series  $\Delta L^*=\text{constant}$  are described on a white surround by the square root of the colour values. For example the CIE tristimulus value  $Y$  with the values  $Y=1, 4, 9, 16, \dots, 81, 100$  produce the equal distant lightness series  $L^*=10, 20, 30, \dots, 90, 100$ .

The coordinates of the colour attributes are the colourness  $F^*$  in colorimetry or the colourness  $D^*$  in the digital technic. The group term *colourness* covers the colour attributes lightness, blackness, whiteness, deepness and others. The group term colour values covers the colour values white value, black value, chromatic value and others. There is often a nonlinear (square root) relation between both group terms, for example between lightness  $L^*$  and the tristimulus Value  $Y$  on a white surround (white paper or white monitor).

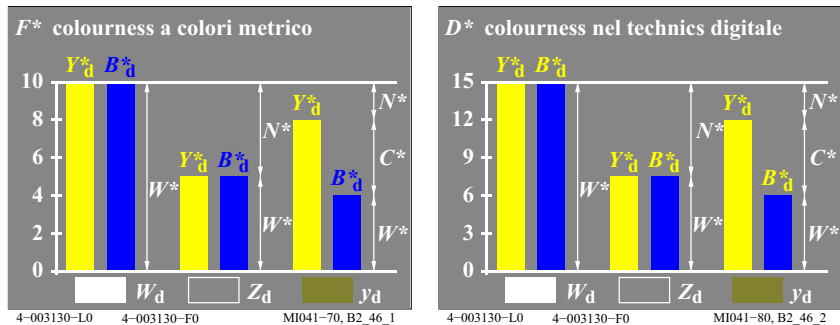
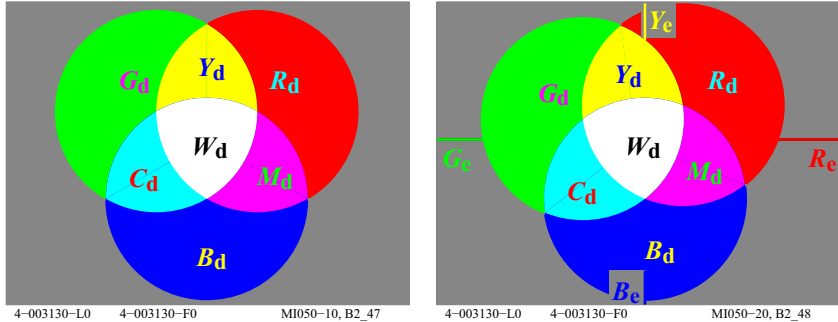


Fig. 34: Colourness in colorimetry and digital technic

Fig. 34 (left) shows the colourness  $F^* = Y_d^*$  or  $B_d^*$  between 0 and 10 used in colorimetry (left). 10 steps are used in the *Munsell*-colour system. Fig. 34 (right) shows the colourness  $D^*$  between 0 and 15 in the digital technic. 15 steps are used in the European standard CEPT for Videotext (*Btx*).

## 14.2 Trichromatic additive Colour Mixture

White  $W_d$  may be produced by additive mixture of *three* optimal colours red  $R_d$  (or orange-red  $O$ ), green  $G_d$  (or leaf-green  $L$ ) and blue  $B_d$  (or violet-blue  $V$ ). *Miescher* called this mixture with three basic colours a trichromatic mixture.



**Fig. 35: Trichromatic additive colour mixture and location of elementary colours**

Fig. 35 (*left*) shows die additive colour mixture with three basic colours red  $R_d$  (or orange-red  $O$ ), green  $G_d$  (or leaf-green  $L$ ), and blue  $B_d$  (or violet-blue  $V$ ). They mix to three dichromatic mixture colours yellow  $Y_d$ , Cyan-blue  $C_d$ , and Magenta-red  $M_d$ . White  $W_d$  is the trichromatic mixture colour with the three basic colours.

Fig. 35 (*right*) shows die location of the additive basic colours, and the dichromatic mixture colours  $CMY_d$ , and the trichromatic mixture colour  $W_d$  in relation to the four elementary colours  $RYGB_e$ . It is necessary to consider the difference between  $R_d$  and  $R_e$ , and between  $G_d$  and  $G_e$ .

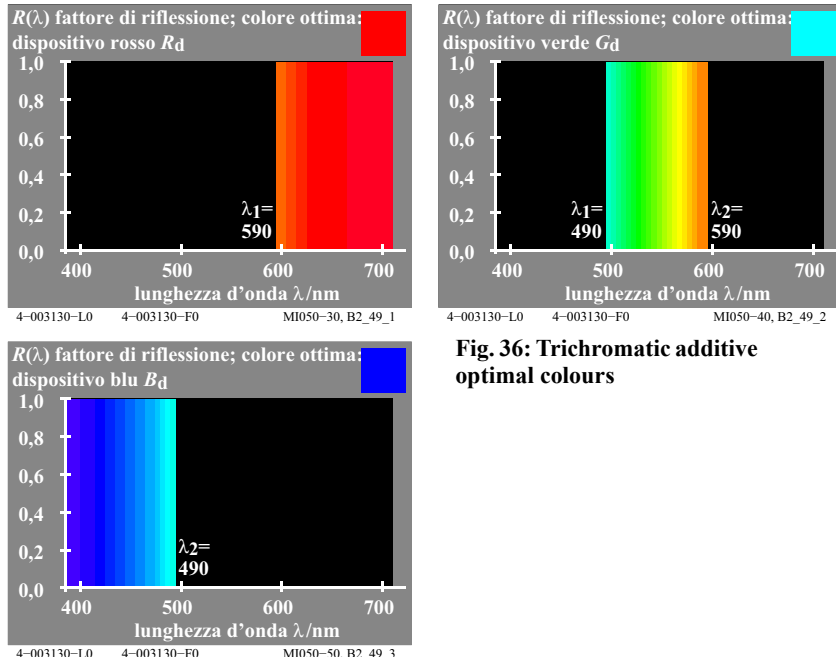
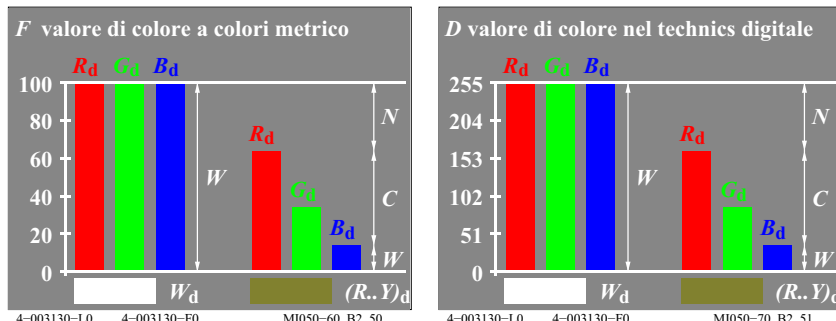


Fig. 36: Trichromatic additive optimal colours

Fig. 36 shows the three optimal colours red  $R_d$ , green  $G_d$ , and blue  $B_d$ , which mix additively to white. The additive mixture with different values of the three basic colours red  $R_d$ , green  $G_d$ , and blue  $B_d$  is of general importance.

In Fig. 36 the three colour values of the device colours  $R_d$ , green  $G_d$ , and blue  $B_d$  are ordered according to their values, in the example it is valid  $R_d > G_d > B_d$ .



**Fig. 37: Trichromatic colour values  $RGB_d$  in colorimetry and digital technic**

Fig. 37 shows the colour values  $F = R_d$ ,  $G_d$ , and  $B_d$  between 0 and 100 in colorimetry (*left*) and the colour values  $F = R_d$ ,  $G_d$ , and  $B_d$  between 0 and 255 in the digital technic (*right*).

The relation with the black value  $N$ , the white value  $W$  and the chromatic value  $C$  of colours is shown.

attributi di colore di basso e l'alto colore metrico	modo miscuglio di colore bicromatico	modo miscuglio di colore tricromatico
<i>colore basso- o valenza metrica</i>		
valore bianco $W$	(per $Y_d \geq B_d$ ) $B_d$	(per $R_d \geq G_d \geq B_d$ ) $B_d$
valore nero $N$	$100 - Y_d$	$100 - R_d$
valore cromatico $C$	$Y_d - B_d$	$R_d - B_d$
<i>alto colore- o sensazione metrica</i>		
biancore $W^*$	(per $Y_d^* \geq B_d^*$ ) $B_d^*$	(per $R_d^* \geq G_d^* \geq B_d^*$ ) $B_d^*$
oscurità $N^*$	$100 - Y_d^*$	$100 - R_d^*$
croma $C^*$	$Y_d^* - B_d^*$	$R_d^* - B_d^*$

4-003130-LO 4-003130-F0

MI480-10

**Tabelle 1-1: Mode of colour mixture, colour value and colorness in colorimetry**

Table 1-1 shows the two modes of colour mixture. The relation between the colour attributes and the colour values  $Y_d$  and  $B_d$  of the dichromatic colour mixture, and the colour values  $R_d$ ,  $G_d$ , and  $B_d$  of the trichromatic colour mixture are given.

The colour attributes of the high colour metric use the group term *colorness* (whiteness, blackness, chroma). In the table the *colorness* is specified by the \* (star), for example the whiteness  $W^* = B_d^*$ .

The abbreviations in Fig. 33 on page 32 and in Fig. 37 on page 36 and Table 1-1 mean:

Fig. 33 on page 32 for  $Y_d \geq B_d$ :

$Y_d$ dominant colour	$B_d$ compensatory colour
$W$ white	$Z$ central grey
	$y_d$ light yellow

Fig. 37 on page 36 for  $R_d \geq G_d \geq B_d$

$R_d$ red	$G_d$ green
$B_d$ blue	$(Y..R)_d$ yellow-red

In Table 1-1 the colour values of the dominant colour yellow  $Y_d$  and the compensatory colour blue  $B_d$  or the three basic colours red  $R_d$ , green  $G_d$ , and blue  $B_d$

are in a simple relation with the colour attributes: relative white value  $w$ , relative black value  $n$ , and relative chromatic value  $c$  of *Ostwald*.

It is valid, compare Fig. 33 on page 32, and Fig. 37 on page 36:

$$\begin{aligned} w \text{ relative white value} &= \text{white value} / 100 & = W / 100 \\ n \text{ relative black value} &= \text{black value} / 100 & = N / 100 \\ c \text{ relative chromatic value} &= \text{chromatic value} / 100 & = C / 100 \end{aligned}$$

The three colour values  $RGB_d$  of colorimetry or of the digital technic may be used to calculate the white value  $W$ , the black value  $N$ , and the chromatic value  $C$ . Based on the nonlinear relation between colour value and colorness the two ratios between white value / black value and whiteness / blackness are different.

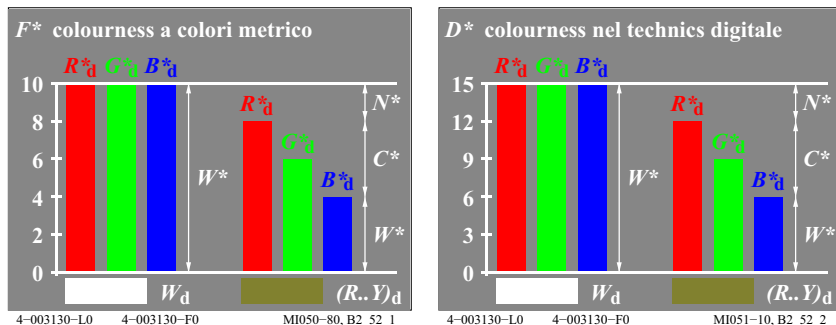


**Fig. 38: Colourness  $RGB^*_d$  in colorimetry and digital technic**

Fig. 38 shows the colourness  $R^*_d$ ,  $G^*_d$  or  $B^*_d$  between 0 and 10 in colorimetry (*left*) and between 0 and 15 in the digital technic (*right*). The relation with the blackness  $N^*$ , the whiteness  $W^*$  and the chroma  $C^*$  of colours is given.

Note: In the CIELAB system the lightness  $L^*$  and the chroma  $C^*$  varies in the range between 0 and 100 instead of 0 and 10, for example in the *Munsell*-colour system.

The most known application of the additive colour mixture is the television and the computer colour monitor. Here the display output is mixed by many raster points red  $R_d$ , green  $G_d$ , and blue  $B_d$ . The luminance of these points is changed by the television signals or the computer image software. On the standard television monitor there are at least 1.2 million luminous points. The points are small and can not be seen separately in a viewing distance of about 3m under normal viewing conditions. An additive raster colour mixture is created on the screen.

### 14.3 Trichromatic subtractive Colour Mixture

The insertion of three appropriate colour filters in the path of the *same* light source leads (in a white surround) to black if nearly all light is absorbed. Contrary to the additive colour mixture described above, filters are put one upon the other in the path of only *one* light source.

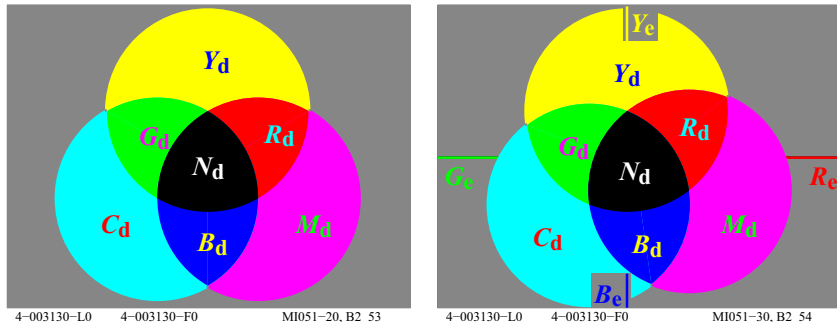


**Fig. 39: Trichromatic subtractive colour mixture, and location of elementary colours**

Fig. 39 (*left*) shows the subtractive colour mixture with the three basic colours cyan-blue  $C_d$ , magenta-red  $M_d$  and yellow  $Y_d$ . The three dichromatic mixture colours red  $R_d$ , green  $G_d$ , and blue  $B_d$  are produced. Black  $N_d$  (= noir) is the trichromatic mixture colour of the three basic colours. For subtractive colour mixture techniques *three* special filters are appropriate with spectral transmission curves similar to the optimal colours yellow  $Y_d$ , cyan-blue  $C_d$  and magenta-red  $M_d$ , see Fig. 40 on page 39.

Fig. 39 (*right*) shows the location of the subtractive basic colours  $CMY_d$ , and of the dichromatic mixture colours  $RGB_d$ , and of the trichromatic mixture colour  $N_d$ . The relative location compared to the four elementary colours  $RYGB_e$  is shown. There is an important difference between  $R_e$  and  $R_d$  or  $M_d$ . In the printing area  $M_d$  is often named *red* instead of *magenta-red*. In addition there is a difference between  $B_e$  and  $B_d$  or  $C_d$ , which is often named *blue* instead of *cyan-blue* in the printing area.

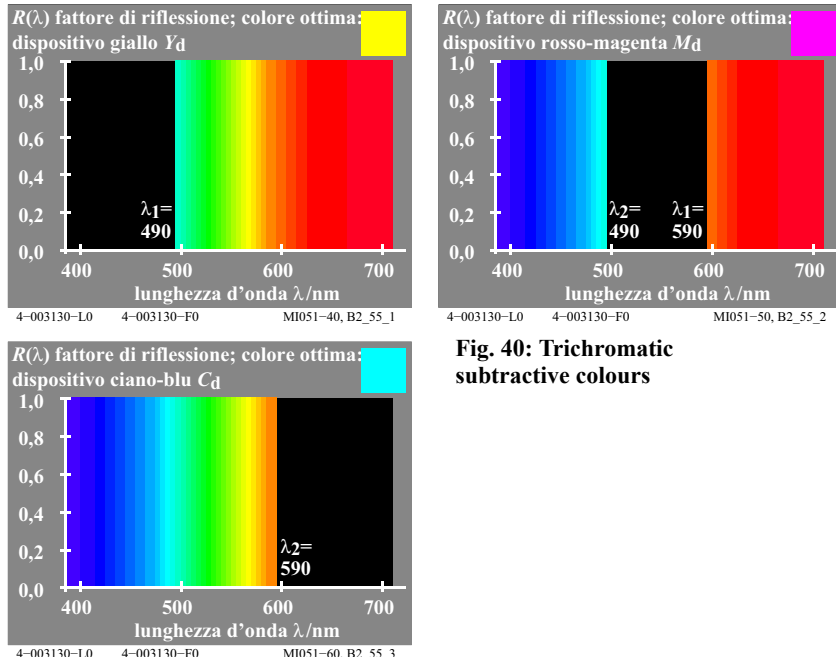


Fig. 40: Trichromatic  
subtractive colours

Fig. 40 shows die spectral reflection factors  $R(\lambda)$  (or transmissions factors  $T(\lambda)$  of filters) which are appropriate for the subtractive colour mixture: The optimal colour yellow  $Y_d$  with  $R(\lambda) = 1$  starting at the wavelength 490nm, the optimal colour magenta-red  $M_d$  with  $R(\lambda) = 1$  up to the wavelength 490nm and starting again at 590nm, and the optimal colour cyan-blue  $C_d$  with  $R(\lambda) = 1$  up to the wavelength 590nm.

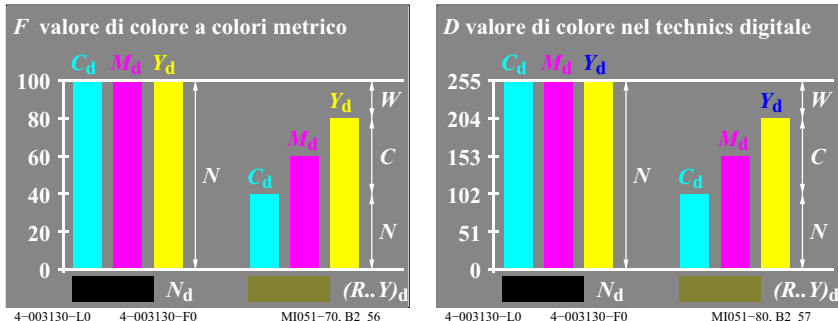


Fig. 41: Colour values  $CMY_d$  in colorimetry and digital technic

Fig. 41 shows the colour values  $F$  in the colorimetry (*left*), and the colour values  $D$  in the digital technic (*right*) for a trichromatic subtractive colour mixture.

The specification of the mixture colours based on three standard printing colours cyan-blue  $C_d$ , magenta-red  $M_d$ , and yellow  $Y_d$  is shown. If the colour value of yellow  $Y_d$  is dominant compared to the values of magenta-red  $M_d$  and cyan-blue  $C_d$ , then the mixture of  $Y_d$  and  $M_d$  leads at first to red  $R_d$ . Because of the large value of yellow  $Y_d$ , the mixed hue is a yellowish red colour  $(R..Y)_d$ .

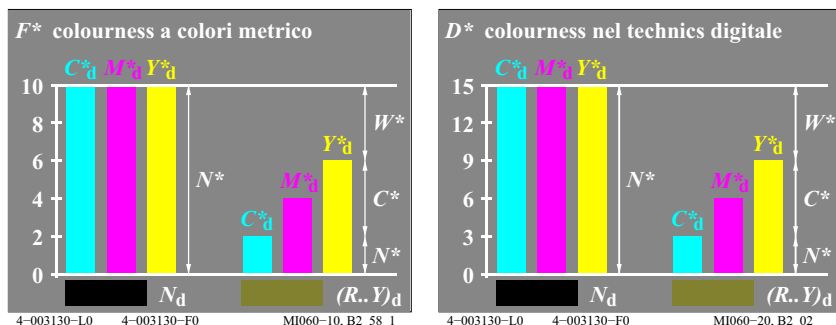


Fig. 42: Colourness  $CMY_d^*$  in colorimetry and in digital technic

Fig. 42 shows the colourness  $F^*$  in the colorimetry, and the colourness  $D^*$  in the digital technic for a trichromatic subtractive colour mixture.

The most known *technical application* of the *subtractive* colour mixture is in *colour photography*. In a colour reversal film (slide film) there are three filter layers, one after another, with colours cyan-blue  $C_d$ , magenta-red  $M_d$ , and yellow  $Y_d$ . The transmission factors of the layers are controlled by the exposure and the developing process.

In standard multicolour printing both additive and subtractive colour mixtures are involved and this kind of mixture is called an auto-typic mixture. The mixture is additive if two printing colours are printed side by side, and subtractive if the two transparent inks are printed on top of each other. One calls this type of mixture in printing a auto-typic mixture.

## 15 Radiazione spettrale

Colours with the same appearance can be created by different spectral distribution of light radiation. In modern colorimetry metameric colours can be calculated with special numerical procedures, taking the illuminance into account.

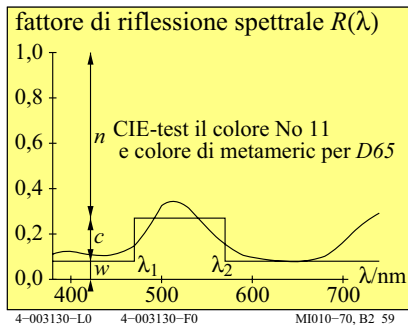


**Fig. 43: Reflection factor of metameristic colours**

Fig. 43 shows the CIE-test colour no. 11 (green) according to CIE 13.3, and a metameristic colour of rectangular reflection for the CIE standard daylight D65. Usually one tries to avoid using metameristic colours on different parts of an industrial product since such colours will only match under one illuminant. By a change of the illuminant, for example from daylight to incandescent light, *colour differences* appear, the metameristic colours no longer match.

Fig. 43 includes the *relative black value*  $n$ , the *relative chromatic value*  $c$ , and the *relative white value*  $w$ . The *Ostwald*-equation  $n + c + w = 1$  is valid.

The two compensatory wavelength limits  $\lambda_1=480\text{nm}$  and  $\lambda_2=580\text{nm}$  for D65 belong to an optimal colour with the elementary hue green  $G_e$ . This optimal colour has the maximum chromatic value  $C_{AB}$  and creates a *colour half* according to *Ostwald*.

The corresponding *linear*  $rgb_e$ -colour values are for  $n=0.73$  and  $w=0.08$ :

$$rgb_e = (w, (1-n), w) = (0.08, 0.27, 0.08)$$

The corresponding *nonlinear (visual)*  $rgb^*_e$ -colour values lead to (*for square root relation of white surround*):

$$rgb^*_e = (w^{1/2}, (1-n)^{1/2}, w^{1/2}) = (0.28, 0.52, 0.28)$$

For the reproduction of the CIE-test colour no. 11 in colour printing or on the colour display the  $rgb_{de}$ -colour values (*de = device to elementary hue*) must be calculated and may get approximately the following values:

$$rgb_{de} = (w, (1-n), w+0.20w) = (0.08, 0.27, 0.10)$$

According to Fig. 10 on page 11, and for production of the elementary colour green  $G_e$  the  $b$ -value increases by 20% ( $=3/F\%-3/15\%$ ) from 0.08 to 0.10.

For this print output all the calculations shown here are done automatically by the software. The software uses the measurement data of 729 ( $=9 \times 9 \times 9$ ) colours of the output device for the steering of the output.

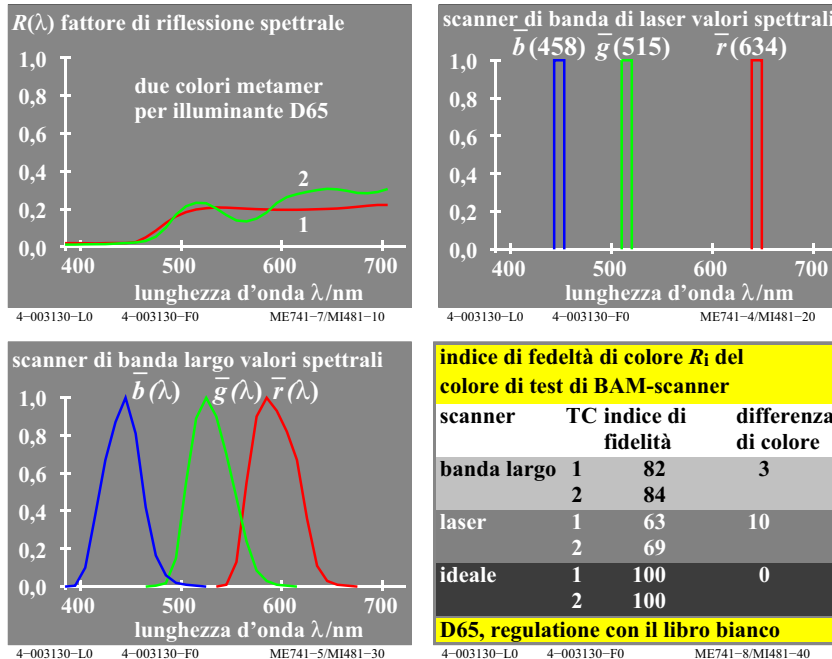


Fig. 44: Two metamer test colours, scanner values and colour rendering

Fig. 44 (*top left*) shows two metamer test colours which are scanned by a laser scanner and a broad band scanner. The scanner values are usually normalized for the white paper to  $r=g=b=1$ .

Depending on the type of scanner the two colours no. 1 and 2 in Fig. 44 (*top left*) produce usually two different *rgb* data sets. However, the two colours appear equal for the CIE- illuminant D65 and they have equal CIE-XYZ data.

The *rgb*-scan values are usually interpreted in the *sRGB*-colour space according to IEC 61966-2-1, and are then transformed to CIE-XYZ data and to colour differences  $\Delta E^*$ . For the ideal scanner, which has the broad band sensitivities of the CIE tristimulus values, the *rgb* values are equal. Maxima and minima of the spectral reflection curves, and the *real* spectral sensitivities of the scanner type, for example a laser or wide band scanner, determine the differences of the *rgb* scanner values. In Fig. 44 (*bottom right*) the colour differences  $\Delta E^*$  are in the range 0 to 10.

In the ideal case the colour rendering index  $R_i$  according to CIE 13.3 has the value 100. It decreases according to the formula  $R_i = 100 - 4,6 \Delta E^*$ . For exam-

ple  $R_i = 86 (=100 - 3*4,6)$  for the colour difference  $\Delta E^*=3$  in Fig. 44 (*bottom right*).

In offset print and with colour printers the achromatic colours may be printed only with the achromatic colour black  $N_d$  or only with the three chromatic colours cyan-blue  $C_d$ , magenta-red  $M_d$ , and yellow  $Y_d$ , especially in images. The achromatic colours, which are printed by the black ink  $N_d$ , have approximately a constant reflection curve. The achromatic colours, which are printed by  $CMY_d$ , have usually up to three maxima and minima, compare Fig. 44 (*top left*).

Test and metameric colours for the CIE standard illuminants D65 and A, and the CIE-illuminants D50 and P40 are printed as test charts no. 1 to 3 in the annex with the format A4 landscape. The spectral reflection factors of the samples of three test charts are available. The *rgb* data are given and the many CIE data for six CIE illuminants D65, D50, P40, A, C, and E have been calculated. The colour samples are based on the 16-step colour circle of the *Relative Elementary colour system RECS*, compare DIN 33872-1 to -6.

CIE R1-47 defines the elementary hue angles for the CIE standard illuminant D65. Elementary yellow  $Y_e$  and blue  $B_e$  have the hue angles 92 and 272 degree. However, for CIE standard illuminant A the elementary hue angles may shift from 92 and 272 degree to 82 and 262 degree in CIELAB (for D65 and A). The exact values are unknown. Therefore the elementary hues under D65 appear not any more as elementary hues under the CIE standard illuminant A. For example the elementary blue  $B_e$  under the CIE standard illuminant D65 appears reddish under the CIE standard illuminant A. Similar the elementary yellow  $Y_e$  under the CIE standard illuminant D65 appears greenish under the CIE standard illuminant A. In future the CIE may define the change of the elementary hue angles for the different CIE illuminants.

If in offset print or with colour printers the achromatic colours are only printed with the three colorants  $CMY$  instead of *only N*, then this needs 3 times higher material resources. If achromatic colours are *only* printed with  $CMY$  then the price may increase by a factor 6. The price for the three chromatic inks  $CMY$  is usually twice compared to the achromatic ink  $N$ . In addition for the  $CMY$  print there are up to three maxima and minima of the reflection curves which may produce colour differences  $\Delta E^*=10$  for equal (metameric) colours, see Fig. 44 (*bottom right*).

In the annex, the test charts no. 2 and 3 (*PI2311L* and *PI3311L*) use the above two print technologies for the print of achromatic colours. The offset print of the test charts no. 2 and 3 has produced metameric achromatic colours for the four different CIE illuminants D65, D50, P40 and A. In addition there are metameric colours for a 8 step colour circle with half the maximum CIELAB chroma  $C_{ab}^*$  compared to the maximum chroma of offset print.

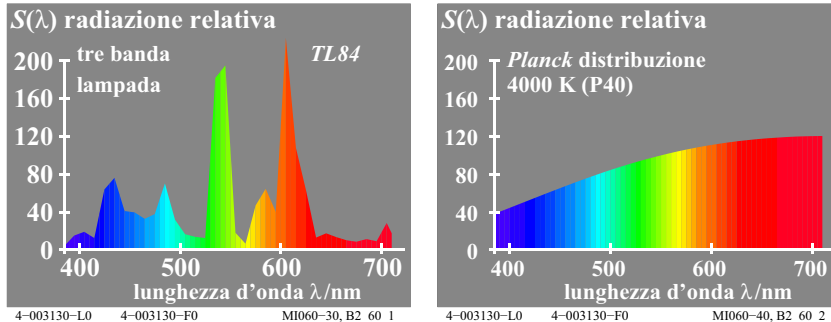


**Fig. 45: Relative spectral distribution of the radiation**

Fig. 45 shows the relative spectral distribution of the radiation  $S(\lambda)$  of a three band fluorescent lamp of high luminous efficiency (energy saving lamp), and a (hypothetical) light source of the colour temperature 4000K according to the radiation law of *Planck*. Both illuminants appear equal white, although they have different spectral distributions.

Alternative illumination of chromatic test colours under these metamerical lamps leads to differences in the colour appearance of the test colours. One speaks of this as *differences in the colour rendering properties*, compare CIE 13.3. The two *metamerical* colours in Fig. 43 on page 41, which appear equal for daylight D65, appear *different* under the two illuminants TL84 and 4000K in Fig. 45.

The test chart no. 1 to 3 in the annex allow both a *visual evaluation* and a *colorimetric specification* of the *colour rendering properties* of LED lamps and of the *colour reproduction properties* in the field of information technology. The test charts are based on the *Relative Elementary colour system RECS*, compare DIN 33872-1 to -6.

## 16 Contrasto

Contrast, already known to *Leonardo da Vinci* and described in detail by *Goethe* (1749-1832), is one of the *most important principles of expression* in fine art, arts and crafts, and industrial design. Contrast is conditioned by the mutual influence of different parts of the visual field.

## 16.1 Achromatic contrast

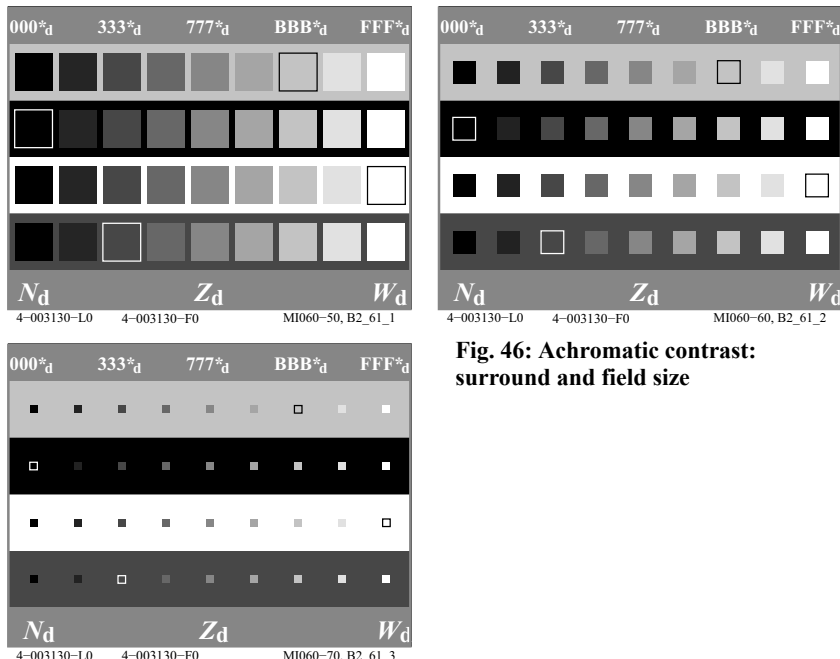


**Fig. 46: Achromatic contrast:  
surround and field size**

The perceived lightness of a central field in a light surround shifts in the opposite sense. For example the lightness of different steps of four *physically identical* grey series changes, depending on the surround luminance. Without a lighter reference field there is no grey or black.

Fig. 46 shows four achromatic grey series between black  $N_d$  and white  $W_d$  viewed against four surrounds, different in lightness. The  $rgb^*_d$  code (with a star) shall indicate, that on a medium grey surround the nine-step grey series is equally spaced, and has the CIELAB lightness  $L^* = 15, 25, 35, \dots, 95$ . In a white surround the samples appear *darker* and in a black surround *lighter* compared to a medium grey surround ( $Z_d$  = central grey, here shown as rectangle at top and bottom).

According to Miescher (1961) an equally spaced scale with 100 steps on a white, medium grey and a black surround obey the following equations for the CIE tristimulus value  $Y$ :

- white surround:  $L^*_W = 100 ( Y_W / 100 )^{1/2}$

According to this formula for a medium grey step with  $L^*_W = 50$  the CIE tristimulus value is  $Y_W = 25$ .

- medium grey surround:  $L^*_Z = 100 ( Y_Z / 100 )^{1/2,4}$

According to this formula for a medium grey step with  $L^*_Z = 50$  the CIE tristimulus value is  $Y_Z = 19$ .

- black surround:  $L^*_N = 100 ( Y_N / 100 )^{1/3,0}$

According to this formula for a medium grey step with  $L^*_N = 50$  the CIE tristimulus value is  $Y_N = 12,5$ .

On a medium grey surround the medium grey step with  $Y_Z = 19$  in the original has the lightness  $L^*_Z = 50$ . According to the above formulas  $Y_W = 19$  has on a white surround the lightness  $L^*_W = 44$ , and  $Y_N = 19$  has on a black surround the lightness  $L^*_N = 58$ .

The formulae given for the ranking of the greys on different surrounds provides only a first step in describing contrast by taking the surround into account. The absolute luminance also influences this ranking.

With increasing luminance, the discrimination of individual grey steps increases. White appears more and more white and black more and more black with increasing luminance. This means that the sensory colour difference between white and black also increases. If the illuminance of the grey series is increased from 500 lux to 5000 lux, then the discrimination increases by approximately 20%. This effect seems small compared to the change of the illuminance by the factor 10 (1000%).

Fig. 46 includes three separate figures with different field size of the central fields compared to the surround. The largest contrast influence by the surround occur by a central field with a viewing size of about one degree ( $1^\circ$ ), and if the field size of the surround is at least 10 times larger ( $>10^\circ$ ).

## 16.2 Chromatic contrast

The colour of a chromatic surround shifts all the colour attributes of the central field in the opposite direction.

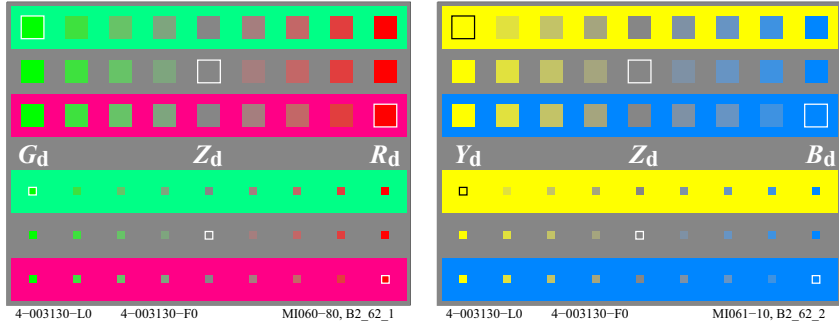


**Fig. 47: Chromatic contrast: surround and field size**

Fig. 47 shows three physically identical chroma series with equally spaced steps viewed against a medium grey surround  $Z_d$  and two surrounds red  $R_d$  and green  $G_d$ . In Fig. 47 the red samples appear on a green surround redder compared to a red surround. The green samples appear on a red surround greener compared to a green surround. In addition the grey samples  $Z_d$  appear in red and green surround not achromatic, but are influenced in *opposite directions*.

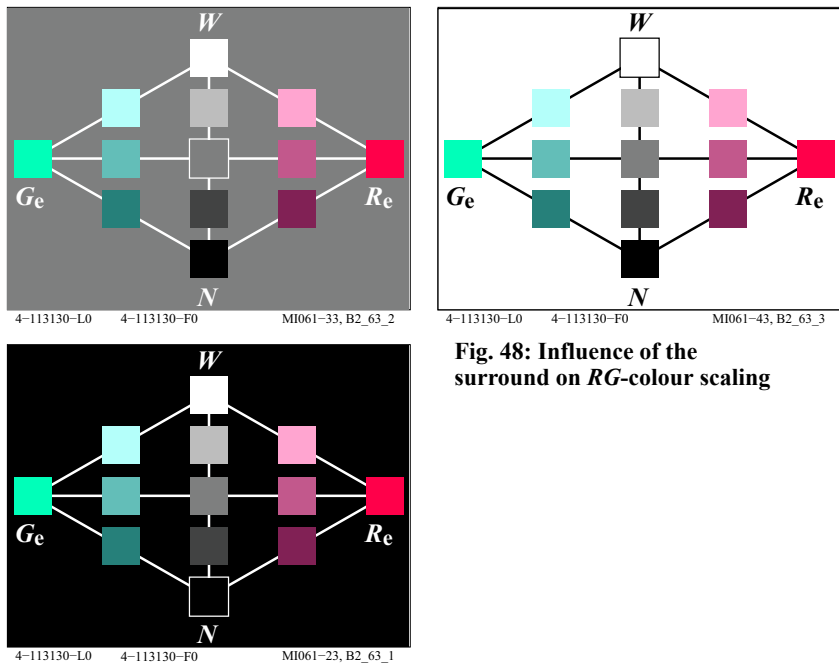
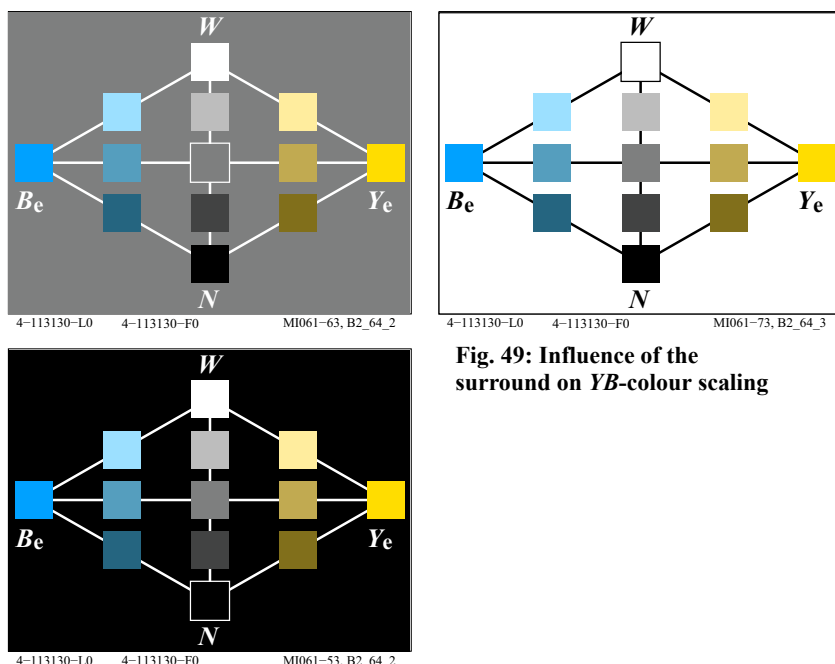


**Fig. 48: Influence of the surround on RG-colour scaling**

Fig. 48 shows a further important property of the achromatic and chromatic contrast in a hue plane red-green.

The colour multiplicity and the colour gamut appear on a medium grey surround larger compared to a white and black surround. On a black surround many colours appear luminous, and the important component “blackish” is missing. On a white background many colours appear “blackish” and the important attribute “luminous” is missing. On a medium grey background both colour attributes “blackish” and “luminous” are present with an appropriate part compared to the natural viewing.

Fig. 48 shows that all red colours have a better agreement in hue with the elementary red hue  $R_e$  compared to Fig. 7 on page 10. In Fig. 48 a 3-dimensional linearization has been used, to calculate (from the undefined  $rgb$ -input data in the file) the intended  $rgb_{de}$ -coordinates (*Index de* = device to elementary hue). The  $rgb_{de}$ -coordinates produce for all red colours the CIELAB-hue  $h_{ab}=26$  in the output, which is defined in CIE R1-47 for the elementary hue red  $R_e$ .



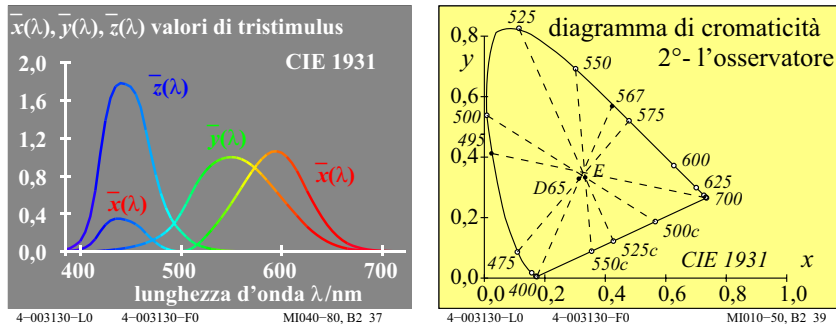
**Fig. 49: Influence of the surround on YB-colour scaling**

Fig. 49 shows the colour multiplicity and the colour gamut in a hue plane yellow-blue. Similar as for the hue plane red-green, again on a medium grey back-

ground the two colour attributes “blackish” and “luminous” are present with an appropriate part compared to the natural viewing.

The appearance change of colours by the surround colours depends on physiological processes in the eye. Up to now there are only first steps to describe these processes, compare also the section 18 on page 56.

## 17 Specificazione standard del colore e misurazione standard del colore



**Fig. 50: CIE tristimulus values and CIE chromaticity diagram for 2° observer**

Fig. 50 shows the three CIE spectral tristimulus values  $x_q(\lambda)$ ,  $y_q(\lambda)$ , and  $z_q(\lambda)$  for CIE illuminant E (equal energy radiation) between 380nm and 720nm. In Fig. 50 the curves show the colour values of the spectral colours. There are three tristimulus functions which may be specified roughly by three colours blue  $z_q(\lambda)$ , green  $y_q(\lambda)$ , and red  $x_q(\lambda)$ .

For the spectral colours the CIE has defined the spectral chromaticity

$$\begin{aligned}x(\lambda) &= x_q(\lambda) / [ x_q(\lambda) + y_q(\lambda) + z_q(\lambda) ] \\y(\lambda) &= y_q(\lambda) / [ x_q(\lambda) + y_q(\lambda) + z_q(\lambda) ] \\z(\lambda) &= z_q(\lambda) / [ x_q(\lambda) + y_q(\lambda) + z_q(\lambda) ] = 1 - x(\lambda) - y(\lambda)\end{aligned}$$

The spectral tristimulus values, the physical spectral radiation, and the spectral reflection of samples allow to calculate the CIE tristimulus values  $X$ ,  $Y$  and  $Z$  and the CIE standard chromaticities  $x$ ,  $y$  and  $z$ .

$$\begin{aligned}x &= X / (X + Y + Z) \\y &= Y / (X + Y + Z) \\z &= Z / (X + Y + Z) = 1 - x - y\end{aligned}$$

Examples of these calculations for the three additive optimal colours are given by *K. Richter* (1996), pages 276-277, for download see (288 pages, 2,8 MB) <http://130.149.60.45/~farbmektrik/BUA4BF.PDF>

In Fig. 50 the CIE spectral chromaticities define the border of the CIE chromaticity diagram. Together with the so called purple line a closed area is defined. The purple line is created by the connection of the chromaticities of the short and long wave spectral colours, approximately  $\lambda = 400\text{nm}$  and  $\lambda = 700\text{nm}$ .

All colours, for example surface colour, spectral, and optimal colours, have chromaticities within or at the edge of the chromaticity diagram.

The chromaticities  $x$  and  $y$  and the CIE tristimulus value  $Y$ , which is normalized to the value 100 for a reference white, specify a colour as well as the CIE tristimulus values  $X$ ,  $Y$ , and  $Z$ . The numerical values of the CIE tristimulus values  $X$ ,  $Y$ , and  $Z$  are between 0 and 100 according to CIE 15 (“Colorimetry”) for the CIE illuminant E. The chromaticity coordinates are always smaller than 1.0. The  $x$  and  $y$  coordinates specify chromaticity points on a rectangular  $(x, y)$  diagram.

In the  $(x, y)$  chromaticity diagram there is a whole colour series with different CIE tristimulus values  $Y$  ( $0 \leq Y \leq 100$ ) that belong to each chromaticity point. Therefore colours with a constant chromaticity point in the region “yellow” of the chromaticity diagram can appear either approximately black (for example with  $Y=4$ ) or as a chromatic light yellow (with  $Y=90$ ). Both the chromaticity and the tristimulus value  $Y$  are required to define a colour stimulus.

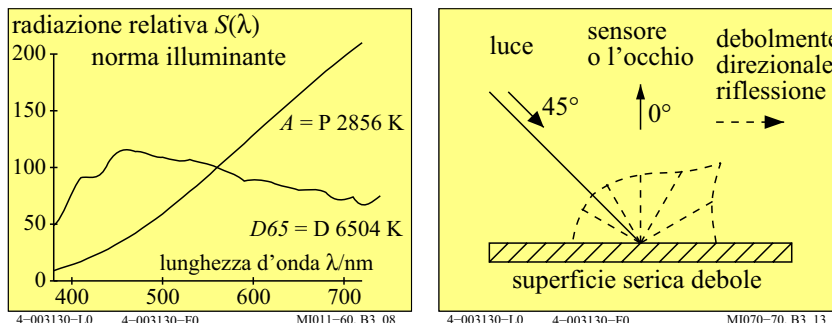


**Fig. 51: Radiation of illuminants D65 and A, and CIE-measurement geometry**

The standard tristimulus values are dependent on the illuminant, for example the CIE standard illuminants D65 or A, see Fig. 51 (left). The illumination angle of the sample surface is usually  $45^\circ$ . The viewing or measuring angle is usually  $0^\circ$ , see Fig. 51 (right). The silky weak surface of the standard offset

print produces usually a diffuse reflection in all directions. However, there is some more reflection in the mirror or gloss direction -45°. Therefore black colours appear blacker under 0° compared to -45°. The CIE tristimulus value is Y=2,5 for the angle 0° and approximately Y=5 for the angle -45°.

valenza di color metrici: (dati: relazione lineare a CIE 1931)		
termini di colore lineare	nome ed il rapporto a CIE tristimulus o la cromaticità valutano	note
valori di tristimulus	X, Y, Z	
valore cromatico	diagramma di lineare cromatico (A, B) $\begin{aligned} A &= [X / Y - X_n / Y_n] Y = [a - a_n] Y \\ &= [x / y - x_n / y_n] Y \\ \\ giallo-blu &B = -0,4 [Z/Y - Z_n/Y_n] Y = [b - b_n] Y \\ &= -0,4 [z / y - z_n / y_n] Y \\ \\ radiale &C_{AB} = [A^2 + B^2]^{1/2} \end{aligned}$	$n=D65$ (circonda)
cromaticita	diagramma di cromaticità lineare (a, b) $\begin{aligned} a &= X / Y = x / y \\ giallo-blu &b = -0,4 [Z / Y] = -0,4 [z / y] \\ radiale &c_{ab} = [(a - a_n)^2 + (b - b_n)^2]^{1/2} \end{aligned}$	paragona eccitazione lineare di cono $L/(L+M)=P/(P+D)$ $S/(L+M)=T/(P+D)$

4-003130-L0

4-003130-F0

MI480-70

**Tabla 2:** Colour coordinates of low colour metric or colour valence metric

Table 2 shows the coordinates of the low colour metric or the colour valence metric. All these coordinates are *linear* transformations of the CIE tristimulus values X, Y, Z or the CIE chromaticities x, y and the tristimulus value Y. The main coordinates are the chromatic values A, B, and C and the chromaticities a, b, and  $c_{ab}$ . The chromatic values are dependent on the chromaticities of the surround (index n). Usually the chromaticity x = 0,3127 and y=0,3390 of the CIE standard illuminant D65 is used.

The CIE-receptor sensitivities of the human colour vision  $l_q(\lambda)$ ,  $m_q(\lambda)$ , and  $s_q(\lambda)$  according to CIE 170-1 are linear functions of the CIE spectral tristimulus values  $x_q(\lambda)$ ,  $y_q(\lambda)$ , and  $z_q(\lambda)$ . The luminous efficiency  $y_q(\lambda)$  is approximately the sum of  $l_q(\lambda)$  and  $m_q(\lambda)$ . Section 18 on page 56 shows the CIE-receptor sensitivities.

In Table 2 the chromaticity  $a$  (red or green content) is roughly equal to the ratio  $L/(L+M)$  and the chromaticity  $b$  (blue or yellow content) is equal to the ratio  $S/(L+M)$ . In the literature instead of the letters  $L$ ,  $M$ ,  $S$  the letters  $P$ ,  $D$ ,  $T$  are used, according to the three colour vision deficiencies  $P=Protanop$ ,  $D=Deuteranop$ , and  $T=Tritanop$ .

Anomalies of colour vision, either of the colour receptors in the retina or in the neural signal transmission, result in partially or totally defective colour vision. Defective colour vision occurs in 8% of men, but only 0,5% of woman (ratio 16:1). Most of these people confuse red and green colours. They appear grey or greyish for these persons.

Persons with colour vision deficiencies shall not take some professions, which depend on normal colour vision, for example pilots, bus or taxi drivers, and print technicians. Only very less people confuse the colours yellow and blue. Even less people perceive all colours as achromatic (white, grey, and black). For tests of defective colour vision there are test charts, for example those of *Ishihara* (1953) in which digits or symbols are used. Observers with normal and defective colour vision see different digits or symbols on these test charts. The anomaloscope of *Nagel* according to DIN 6160 allows the determination the degree of the colour vision deficiency.

più alto colore metrici ( dati: relazione non lineare a CIE 1931 dati)		
atribuisce non lineare	nome ed il rapporto con tristimulus o la cromaticità valutano	note
leggerezza	$L^* = 116 \left( \frac{Y}{100} \right)^{1/3} - 16 \quad (Y > 0,8)$ approssimazione: $L^* = 100 \left( \frac{Y}{100} \right)^{1/2,4} \quad (Y > 0)$	CIELAB 1976
croma	trasforma non lineare dei cromatici $A, B$	
rosso-verde	$a^* = 500 \left[ \left( \frac{X}{X_n} \right)^{1/3} - \left( \frac{Y}{Y_n} \right)^{1/3} \right]$ $= 500 \left( a' - a'_n \right) Y^{1/3}$	CIELAB 1976
giallo-blu	$b^* = 200 \left[ \left( \frac{Y}{Y_n} \right)^{1/3} - \left( \frac{Z}{Z_n} \right)^{1/3} \right]$ $= 500 \left( b' - b'_n \right) Y^{1/3}$	CIELAB 1976
radiale	$C^*_{ab} = [a^*{}^2 + b^*{}^2]^{1/2}$	$n=D65$ (circonda)
cromaticità	trasforma non lineare di cromaticità $x/y, z/y$	paragona log
rosso-verde	$a' = \left( \frac{1}{X_n} \right)^{1/3} \left( \frac{x}{y} \right)^{1/3}$ $= 0,2191 \left( \frac{x}{y} \right)^{1/3} \text{ per D65}$	cono eccitazione log[L / (L+M)]
giallo-blu	$b' = -0,4 \left( \frac{1}{Z_n} \right)^{1/3} \left( \frac{z}{y} \right)^{1/3}$ $= -0,08376 \left( \frac{z}{y} \right)^{1/3} \text{ per D65}$	= log[P / (P+D)] log[S / (L+M)]
radiale	$c'_{ab} = [ (a' - a'_n)^2 + (b' - b'_n)^2 ]^{1/2}$	= log[T / (P+D)]

4-003130-L0 4-003130-F0

MI481-70

**Tabla 3: Colour coordinates of high colour metric or sensation colour metric**

Table 3 shows the coordinates of the high color metric or sensation colour metric. The lightness  $L^*$ , the chroma coordinates  $a^*$ ,  $b^*$ , and  $C^*_{ab}$ , and the chromaticities  $a'$ ,  $b'$ , and  $c'_{ab}$  are the most important coordinates of the high or sensation colour metric. In Table 4 the nonlinear chromaticities  $a'$  and  $b'$  serve as alternate to calculate the chroma coordinates  $a^*$ ,  $b^*$ , and  $C^*_{ab}$  of the CIELAB-colour space. The chromaticity  $(a', b')$  for CIELAB is not defined in CIE 15 and ISO 11664-4. The *nonlinear* chromaticity  $(a', b')$  seems roughly similar compared to the *linear* chromaticity  $(u', v')$  of CIELUV in CIE 15.

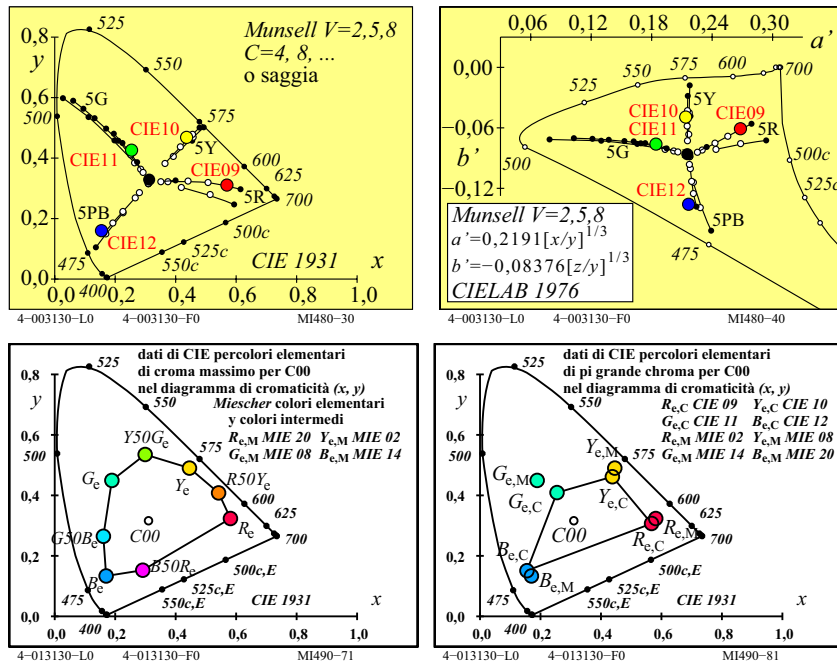


Fig. 52: Munsell, Miescher, and CIE colours in ( $x, y$ ) and ( $a', b'$ )

Fig. 52 shows the four elementary hues  $RYGB_e$  and in addition the *Miescher*-intermediate hues  $R50Y_e$ ,  $Y50G_e$ ,  $G50B_e$ , and  $B50R_e$  (bottom left). The colours of the real (o) and the extrapolated (•) four Munsell hues 5R, 5Y, 5G, and 5PB of Value 2, 5, and 8 are shown (top left and right). In the chromaticity diagram ( $a', b'$ ) the location is more on straight lines compared to ( $x, y$ ). The chroma of the four elementary colours of the *Miescher*-hue circle is larger compared to the four CIE-test colours no. 9 to 12 according to CIE 13.3 (bottom right). The *Miescher*-hue circle has been produced by 11 appropriate colour inks. In addition the chroma is larger compared to the hue circle of the *Relative Elementary Colour System RECS*. This hue circle is produced by the three colours  $CMY_d$  of standard offset print, compare Fig. 59 on page 66 (bottom left and right).

The chromaticity diagram ( $a', b'$ ) is defined in Table 4. It has a large extension to the chromaticity of the wavelength  $\lambda=400nm$ . For the application in the information technology this is not a problem, because these colours do usually not exist in both offset printing and on colour monitors. All real colours are located within the region of Fig. 52 (top right).

Fig. 52 shows die elementary colours of *Miescher* in the chromaticity diagram ( $x, y$ ). The colour samples are not located on a circle around the chromaticity of the CIE illuminant C, which is also used in the *Munsell*-colour system. The chromaticity differences of the CIE illuminants C and D65 are small. Die elementary colours yellow  $Y_e$  and blue  $B_e$ , and the achromatic point D65 are approximately on a line. Therefore one can mix additively the colours  $Y_e$  and  $B_e$  in an appropriate mixture ratio to the achromatic colour D65. The elementary colours red  $R_e$  and green  $G_e$  are *not* located together with D65 on a line. Therefore  $R_e$  and  $G_e$  mix additively to yellowish-green, yellowish or yellowish-red colours and never to the achromatic colour D65.

Table 2 on page 51 shows colour attributes of the low and high colour metric. It is assumed, that the complementary device colours yellow  $Y_d$  and blue  $B_d$  mix additively to white. Then one can only mix achromatic, yellow or blue hues. If the yellow value is larger compared to the blue value ( $Y_d > B_d$ ), then the colour values white, black and the chromatic values are calculated according to Table 2 on page 51.

The dichromatic and trichromatic mixture is of large importance for the colour information technology. In the information technology for example on a colour monitor, or with a colour projector, or in multicolour printing all colours are reproduced by three basic device colours  $RGB_d$  or  $CMY_d$ . The additive colour mixture on a monitor, and a data projector produces with two basic colours and the third colour a dichromatic mixture, for example

$$\begin{aligned} W_d &= R_d + (G_d + B_d) = R_d + C_d \\ W_d &= G_d + (B_d + R_d) = G_d + M_d \\ W_d &= B_d + (R_d + G_d) = B_d + Y_d \end{aligned}$$

In the colour information technology usually a large colour gamut in the reproduction is intended. For this the colours with the maximum chromatic value  $C_{AB}$  and approximately of the largest chroma  $C^*_{ab}$  are produced by complementary optimal colours with compensatory wavelength limits  $\lambda_d$  and  $\lambda_e$ . Then the dichromatic mixture will lead to white. Colorimetric solutions for a large colour gamut in the output are given in section 19.

## 18 Proprietà speciali della visioni a colori

The properties of colour vision depend on the properties of the three receptors *LMS* or *PDT* for the daylight vision.

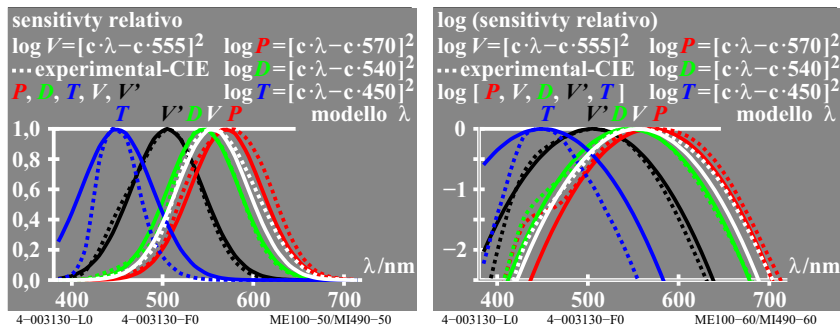


**Fig. 53: Relative receptor sensitivities *PDT* (or *LMS*),  $V(\lambda)$ , and  $V'(\lambda)$**

Fig. 53 shows the receptor sensitivities *PDT* (according to the colour vision deficiencies *P*=Protanop, *D*= Deutanop, and *T*=Tritanop or *LMS* according to CIE 170-1). The maximum sensitivities are near the wavelength 570, 540, and 450nm.

The long wave receptor (*L* or *P*) has the maximum sensitivity *not* in the region red, but in the yellow-green region. The wavelength  $\lambda_m = 570\text{nm}$  of the maximal sensitivity is smaller compared to the dominant wavelength  $\lambda_d = 575\text{nm}$  of elementary yellow  $Y_e$ . If a logarithmic vertical axis is used, then a parable with approximately an equal shape for all receptors is appropriate. In this case the sum and the differences have special properties:

$$\begin{aligned} \log V(\lambda) &= \log P(\lambda) + \log D(\lambda) \quad (\text{new maximum } 555\text{nm with } 570 \text{ and } 540\text{nm}) \\ \log P(\lambda) &= \log V(\lambda) - \log D(\lambda) \quad (\text{known maximum } 570\text{nm with } 555 \text{ and } 540\text{nm}) \\ \log R(\lambda) &= \log P(\lambda) - \log D(\lambda) \quad (\text{new maximum } 600\text{nm with } 570 \text{ and } 540\text{nm}) \end{aligned}$$

Again in the last line a parable shape is created, and in addition the missing red sensitivity  $R(\lambda)$  with a maximum at 600nm is defined.

The luminous sensitivity  $V(\lambda)$  has a large importance for the colour vision.  $V(\lambda)$  serves as basic for the definition of the luminance. According to CIE 15 Colorimetry  $V(\lambda)$  is calculated linearly by the Grassmann-law, for example by:

$$V(\lambda) = P(\lambda) + D(\lambda)$$

The calculation according to the above logarithmic formulas leads to

$$V_{\log}(\lambda) = 10^{[\log P(\lambda) + \log D(\lambda)]}$$

The difference between  $V(\lambda)$  and  $V_{\log}(\lambda)$  is about 1% for the two wavelength 400 and 700nm compared to the maximum near 555nm, see *K. Richter* (1996). The colour threshold is also near 1%. Therefore for many applications both calculation methods are approximately equal. The spectral luminous sensitivity  $V(\lambda)$  is of special importance for the lighting technology. The following ratios calculated with  $V(\lambda)$  have special importance for the colour field, for example

$$A(\lambda) = R(\lambda) / V(\lambda) \text{ spectral chromaticity red-green}$$

$$B(\lambda) = -T(\lambda) / V(\lambda) \text{ spectral chromaticity yellow-blue}$$

In applications these ratios correspond to the ratios  $X/Y$  and  $Z/Y$ . In Table 2 on page 51 these ratios (together with a weighting factor) are called the red-green and the yellow-blue chromaticities  $a$  and  $b$ . Both define the chromaticity diagram  $(a, b)$ . For the use of the chromaticity diagram  $(a, b)$  instead of the chromaticity diagram  $(x, y)$  in applications, and for the description of colour thresholds, see *K. Richter* (1996).

Further properties of colour vision can be described with physiological colour signals in the retina of monkeys. *A. Valberg* (2005) has described many physiological signals as function of chromaticity and luminance of both central and surround fields.

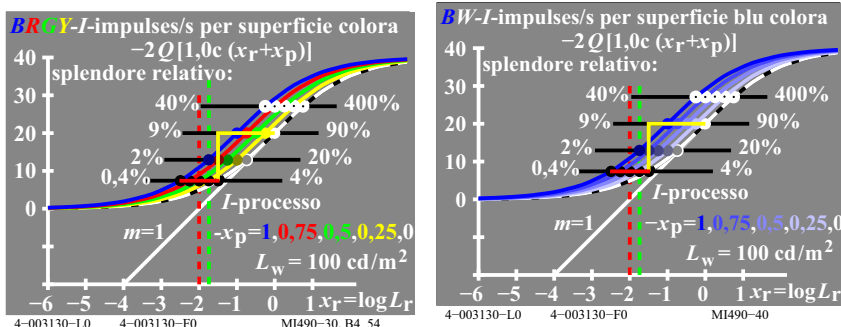


**Fig. 54: Colour signals of chromatic and blue colours**

Fig. 54 shows in principle the measured colour signals of central field colours with increasing luminance in a white surround. Both scales are logarithmic. The surround (white background  $w$ ) luminance is  $100 \text{ cd}/\text{m}^2$ . For the office the illuminance 500 lux is recommended. This corresponds to the luminance  $142 \text{ cd}/\text{m}^2$  for the white standard offset paper. This luminance is in the range of daylight vision between about  $1 \text{ cd}/\text{m}^2$  and  $10000 \text{ cd}/\text{m}^2$ .

In Fig. 54 the  $I$ -Signals ( $I$ =Increment) for achromatic and chromatic colours follow an S-shape curve which saturates at 0.9% and 9000% compared to the white surround with the value 90%. The curve for chromatic colours (left) are

shifted compared to the achromatic colours to the left. The curves for chromatic blue colours (*right*) shift with the chromaticity difference to D65 in the chromaticity diagram (*a*, *b*) to the left. For all chromatic colours equal signals are therefore created for a lower luminance  $L$  compared to the surround luminance  $L_w=100 \text{ cd/m}^2$  ( $w = \text{white background}$ ).

According to *Ostwald* (1920) optimal colours of maximum chroma are defined by a “colour half”, which has compensatory wavelength limits. The tristimulus value  $Y$  and the chromatic value  $C_{ab}$  can be calculated according to Table 2 on page 51. The tristimulus value  $Y$  and the chromatic value  $C_{ab}$  are related linearly. The ratio  $C_{ab}/Y$  may serve to describe the shift to the left in Fig. 54 on page 57.

The slope of the S-shape signal curve is largest in the middle. Therefore here the largest luminance discrimination  $L / \Delta L$  is expected. The threshold for achromatic and chromatic colours is expected at a luminance, which is at maximum by a factor 36 smaller compared to the white surround. The number 36 may be calculated by the ratio of the tristimulus values  $Y_w=90$  and  $Y_n=2,5$  of white  $W$  and black  $N$ .

Probably the luminances of the largest luminance discriminability  $L / \Delta L$  are similar to the luminances of the  $G_0$  colours of *Evans* (1967). The  $G_0$  colours appear in a white surround neither blackish nor luminous. According to *Evans* the tristimulus value  $Y_s$  at the colour threshold ( $s=\text{threshold}$ ) is for all colours by the factor 30 smaller compared to the tristimulus value of the  $G_0$  colours.

A CIE report of the committee CIE 1-83 *Validity of Formulae for Predicting Small Colour Differences* (Chairman *K. Richter*, DE) with a description of colour thresholds may be produced during 2014. A CIE report CIE R1-57 *Border between blackish and luminous colours* (Reporter *T. Seim*, NO) is planned during 2013.

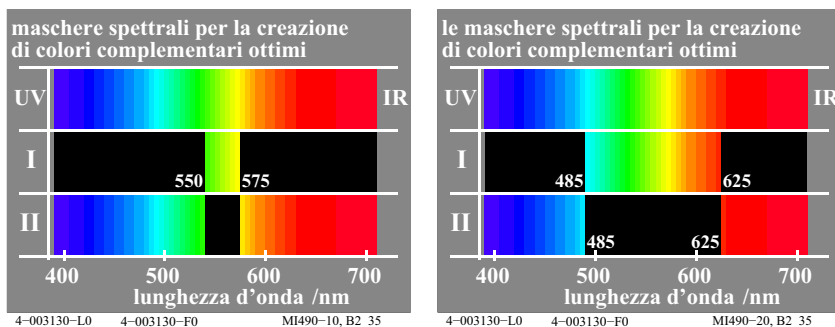


Fig. 55: Complementary optimal colours of different band width

Fig. 55 shows complementary optimal colours with different band width (*left and right*). Such complementary optimal colours are created as edge spectra of white-black and black-white, if one observes the edges of different size with a prism. Already *Goethe* (1830) has observed, that there is equal colour discrimination in the *positive* and *negative* spectrum for neighbouring locations within the continuous complementary colour series.

*T. Holmark and A. Valberg* (1971) have mixed the spectral colours of a *positive* and *negative* slit with an apparatus for mixing spectral colours. The *negative* and *positive* slit produces very different optimal colours, for example yellow and blue (*left*) or cyan and red (*right*). For the appearance of a colour difference (threshold) the shift of the slit was approximately equal for the complementary optimal colours.

An improved colour metric for the description of colour thresholds needs therefore equal and anti symmetric coordinates. The chromatic values  $A$  and  $B$  of Table 2 on page 51 have these property. The chroma coordinates  $a^*$  and  $b^*$  of the CIELAB space have *not* this property. A colorimetry for colour thresholds, which shall consider the results, is planned in 2014 in a CIE report of the Committee CIE 1-83.

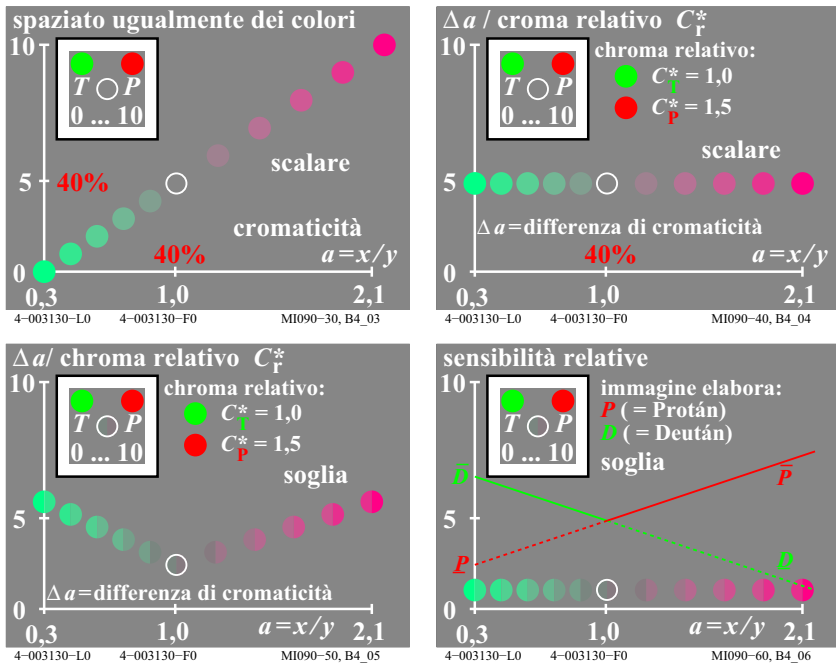


Fig. 56: colour scaling and colour thresholds of the colour series  $T - D65 - P$

Fig. 56 shows in principle some experiments and results about colour scaling and colour thresholds as function of the chromaticity  $a = x/y$ . The colour scaling and the colour thresholds are shown for colours of equal luminance  $L$ , in this case with the constant tristimulus value  $Y=18$ .

Fig. 56 (*top left*) shows a colour series between a very chromatic turquoise colour  $T$  via grey (D65 daylight) up to a very chromatic purple-red  $P$ . This colour series is approximately equally spaced. The experimental situation is shown in Fig. 57 (*top left*). In a white surround there is a quadratic grey surround. In this grey surround two "end-colours" were presented, here turquoise  $T$  and purple-red. In the lower field it was possible to produce colours of equal luminance between the two end-colours  $T$  and  $P$ .

The observer gets a fixed scale between the steps 0, 5 and 10 for  $T$ , D65 and  $P$ . By a random process within the experiments digits between 0 and 10 were produced. For 1 the observer shall produce a chromatic turquoise, for 7 a medium chromatic purple, for 5 the achromatic grey of the chromaticity D65. The goal of the production of a visual equidistant colour scale both between  $T$  and D65 and between D65 and  $P$  was explained explicitly to the observer.

Fig. 56 (*top right*) shows the results of the experiments in  $T - P$  direction. The difference  $\Delta a$  between two neighbouring colour steps (divided by the relative chroma, which was 1 for  $T - D65$ , and 1,5 for  $D65 - P$ ) as function of the coordinate  $a = x / y$  shows a straight line. Equal chromaticity differences  $\Delta a$  (divided by 1 and 1,5) correspond to equal chroma differences. There is a simple description of equal chroma differences by equal differences of a coordinate of the low colour metric (here  $a = x / y$ ).

In addition the visible colour thresholds, this are just noticeable colour differences, has been determined along the same colour series  $T - D65 - P$ . At first we assumed, that the chromaticity difference  $\Delta a$  for the threshold may be smaller, for example by a constant factor 30. However, the results are different.

Fig. 56 (*bottom left*) shows the experimental situation. In a white surround there was a grey quadratic surround. In this grey surround two "end-colours" were shown, here turquoise  $T$  and purple-red  $P$ . In the lower circular field all colours between the two end-colours could be produced. In two half circle equal amounts of  $T$  or  $P$  could be added. In general for a colour threshold about 1% of the two end-colour was necessary to recognize a colour difference.

Fig. 56 (*bottom left*) shows the chromaticity difference  $\Delta a$  for colour thresholds as function of the coordinate  $a = x / y$  of the low colour metric. The differences  $\Delta a$  for colour thresholds change in the range 1 to 3. The difference  $\Delta a$  is smallest for grey (D65), and increase linearly towards  $T$  and  $P$ . At grey about 30 thresholds correspond to a chroma step. At purple-red  $P$  and turquoise  $T$  10 thresholds correspond to a chroma step.

The BAM-research results of *K. Richter* (1985) are in agreement with other results, for example of *Inamura and Yaguchi* (2011). In principle two different kinds of metric are necessary to describe for example the *MacAdam*-ellipses (at threshold) and the colour order systems which apply the colour scaling.

Fig. 56 (*bottom right*) shows the *relative sensitivities* of two colour vision processes in red-green direction. In each section an other colour vision process determines the recognition of colour thresholds. According to this model the chromaticity difference  $\Delta a$  is small for achromatic colours and large for chromatic colours. According to Fig. 56 (*bottom left*) the experimental results are opposite. The colour vision model with the colour signals as function of luminance and chromaticity can explain this property.

Fig. 54 on page 57 shows the colour signals of blue colours with an increasing chromaticity difference  $\Delta b$  compared to the achromatic series (*right*). The *largest luminance discrimination*  $L / \Delta L$  is reached on a *horizontal* line and for *decreasing* luminance of blue colours compared to the achromatic white. This is described by the *largest slope* of all the signals on a *horizontal* line (slope change of the signals). The *luminance discrimination*  $L / \Delta L$  on a *vertical* line decreases for this blue colours of *equal* luminance, because the slope of the signal curve decreases. If one in addition assumes a linear relation between  $\Delta L$  and  $\Delta b$  on a *vertical* line, then  $\Delta b$  *decreases* for blue colours of *equal luminance* according to Fig. 54 on page 57.

Fig. 56 (*bottom right*) seem to show that the *relative sensitivities* increase with the chromaticity difference. This is not true and may be described as follows. The luminance of the black threshold is by a factor 1:36 lower compared to white luminance. According to *Evans* (1974) the luminance of the chromatic threshold is usually lower compared to the black luminance. This result is in agreement with Fig. 56. However with increasing chromaticity difference, for colours of equal luminance the signal slope decreases and therefore the chromatic threshold decreases which seems opposite to Fig. 56 (*bottom right*).

The research results require at least a colour metric for colour thresholds and a colour metric for scaling, and if possible with transitions. In applications the colour thresholds are important for the determination of small colour differences. The equal spacing of larger colour differences is important for the spacing of colour rendering properties. Colour samples in colour order systems have usually colour differences around 30 colour thresholds (or  $\Delta E^*_{ab} = 10$ ). An example is the colour order system *RAL-Design* (1993), which is based on CIELAB and has sample differences of  $\Delta E^*_{ab} = 10$  in any hue plane, and for 36 hues.

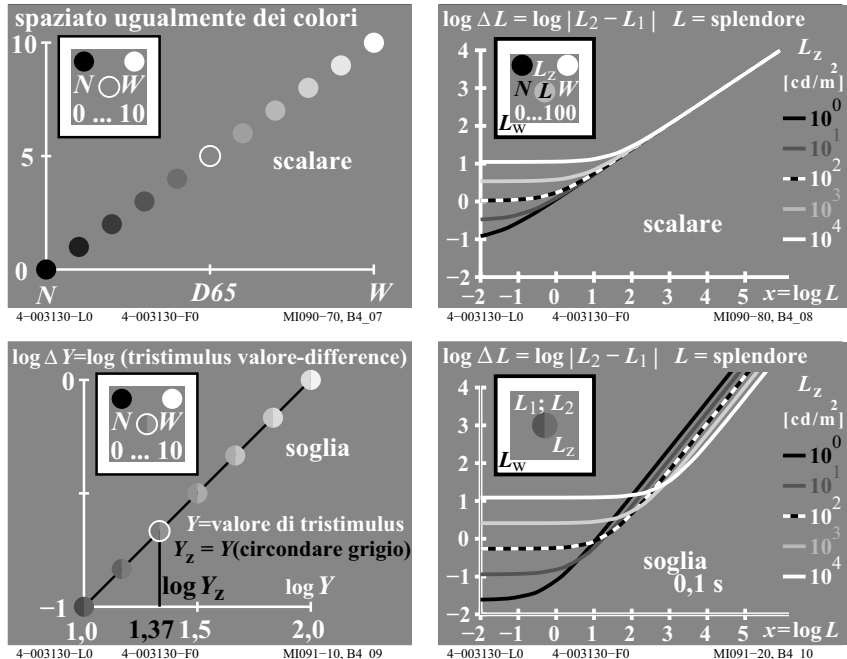


Fig. 57: Luminance scaling and thresholds of lightness series  $N - Z - W$

Fig. 57 shows in principle experiments and results of colour scaling and colour thresholds as function of the luminance  $L$ . Instead of the luminance  $L$  one can also use the tristimulus value  $Y$ , which represents a relative luminance and is always normalized to 100 for white. The formula

$$Y = 100 \frac{L}{L_W}$$

uses the central field luminance  $L$  and the surround field luminance  $L_W$  (outer white frame in the experimental situation, see Fig. 57).

Fig. 57 (top left) shows the equally spaced colour (lightness) scaling for a central field luminance series in the two regions  $N - D65$  and  $D65 - W$ .

Fig. 57 (top right) shows the measured central field luminance differences  $\Delta L$  as function of the central field luminance  $L$ . A  $\log$  scale is used on both axis. As a parameter the surround luminance is given. The black-white curve is valid for the surround field luminance  $L_z = 100 \text{ cd/m}^2$  of the grey surround u. The luminance  $L_z = 100 \text{ cd/m}^2$  corresponds to a medium illuminance of 1500 lux ( $= 5 \cdot \pi$

•100 lux). The factor five is used for a medium grey with the reflection factor 0,2.

Fig. 57 (*bottom left*) shows the results of colour thresholds along the grey series. For the central field and only a part of the grey scale the tristimulus value difference  $\Delta Y$  (proportional  $\Delta L$ ) is a function of the tristimulus value  $Y$ . The threshold  $\Delta Y$  is constant and 1% of the central field tristimulus value  $Y$ . The constant slope near the value 1 (or 0,9) is based on the law of *Weber-Fechner*  $\Delta Y / Y = \text{constant}$  or  $\Delta L / L = \text{constant}$ .

Fig. 57 (*bottom right*) shows in addition the results for very dark and very light colours for a luminance range of six *log* units (in Fig. 57 (*bottom left*) only one unit is shown). The parameter surround-field luminance describes especially the large change of the black threshold with the surround-field luminance. For small central-field luminances  $L$  a constant black threshold  $\Delta L_s$  ( $s=\text{threshold}$ ) is reached. Luminance differences smaller  $\Delta L_s$  are not visible.

A comparison of Fig. 57 (*top and bottom right*) shows, that the luminance differences  $\Delta L_{\text{scaling}}$  for equally spaced grey series and  $\Delta L_{\text{thresholds}}$  for luminance thresholds are not proportional along the same gray scales. The different slopes (about 0,9 and 0,45) are the basis for this statement. One may explain the differences along the grey scale by two visual processes in white-black direction, see *K. Richter* (1996).

Also in Fig. 56 on page 59 for colours of equal luminance along the colour series *T - D65 - P* two different slopes are necessary for the chromaticity differences  $\Delta a_{\text{scaling}}$  for scaling and  $\Delta a_{\text{threshold}}$  for thresholds.

A colour vision model for the description of both scaling and thresholds results and the transitions is missing up to now.

## 19 Colori elementari e tecnologia dell'informazione a colori

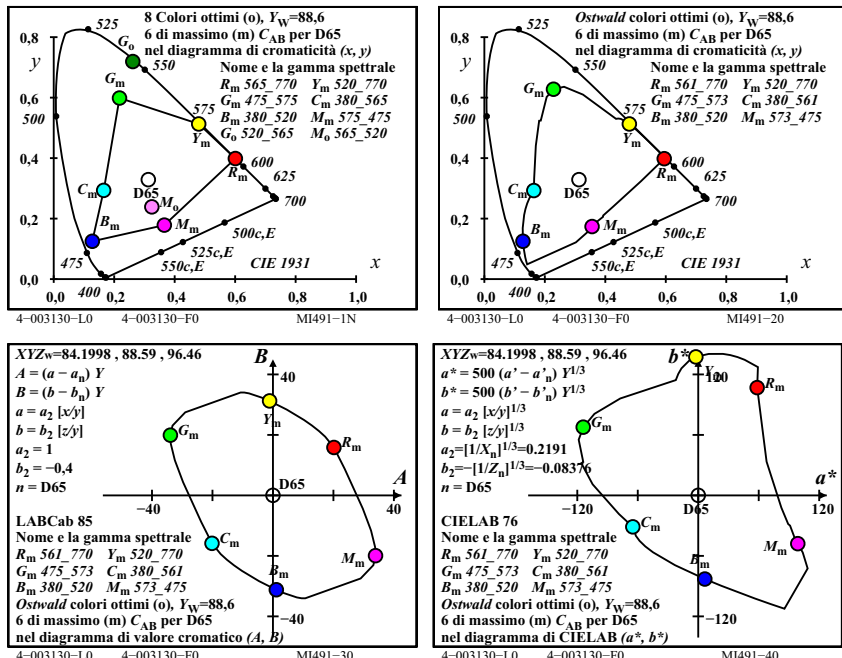


Fig. 58: Three complementary and all optimal colours of maximum chroma

Fig. 58 shows three optimal colour pairs  $R_m-C_m$ ,  $Y_m-B_m$ , and  $G_m-M_m$ . The two colours of each pair are complementary, mix to white and are called dichromatic. The chromatic values  $A$  and  $B$  defined in Table 2 on page 51 are shown in Fig. 58 (*bottom left*). The chromatic value  $C_{ab}$  is *equal* for the dichromatic optimal colours.

For all optimal colours approximately instead of a triangle in the standard chromaticity diagram ( $x, y$ ) now an ellipses is produced in the chromatic value diagram ( $A, B$ ).

The anti symmetry in the chromatic value diagram ( $A, B$ ) is a requirement for an efficient description of the *equal* threshold for complementary optimal colours. For this experimental result by *Holtsmark and Valberg* (1969), compare Fig. 55 on page 58.

Dichromatic optimal colours, for example  $R_m$  and  $C_m$ , include for red and cyan-blue the complementary spectral ranges 565nm to 770nm and 380 to 565nm, compare the description in Fig. 58 (*top left*). For example the wavelength limits  $\lambda_1=380\text{nm}$  and  $\lambda_2=565\text{nm}$  are located with D65 approximately on a line.

The colour cyan-blue  $C_m$  of the spectral range 380nm to 565nm (“colour half”) has the largest chromatic value  $C_{ab}$ . For example an additional spectral colour red with  $\lambda_r=600\text{nm}$  mix to a more whitish cyan-blue  $C_m$ , and the chromatic value  $C_{ab}$  decreases.

Fig. 58 (*top left*) shows in addition two optimal colours  $G_o$  and  $M_o$ , which produce a triangle in the standard chromaticity diagram ( $x, y$ ) together with  $RYCB_m$ . The spectral range 495 to 565nm of the colour  $G_o$  is smaller compared to the range 475 to 575nm (with compensatory wavelength limits) of the colour  $G_m$ . Green  $G_o$  is therefore darker compared to  $G_m$ . In the standard chromaticity diagram ( $x, y$ ) the chromaticity difference between  $G_o$  and D65 is larger as the one between  $G_m$  and D65. However, for the chromatic value it is opposite and it is valid  $C_{ab,Go} < C_{ab,Gm}$ .

The *area* of the basic and mixture colours in any *chromaticity diagram* is therefore *not* appropriate to specify the colour gamut. However, the colour area in a chromaticity diagram is often used to specify the colour gamut in many IEC and ISO standards. A more appropriate specification uses the chromatic value or chroma area.

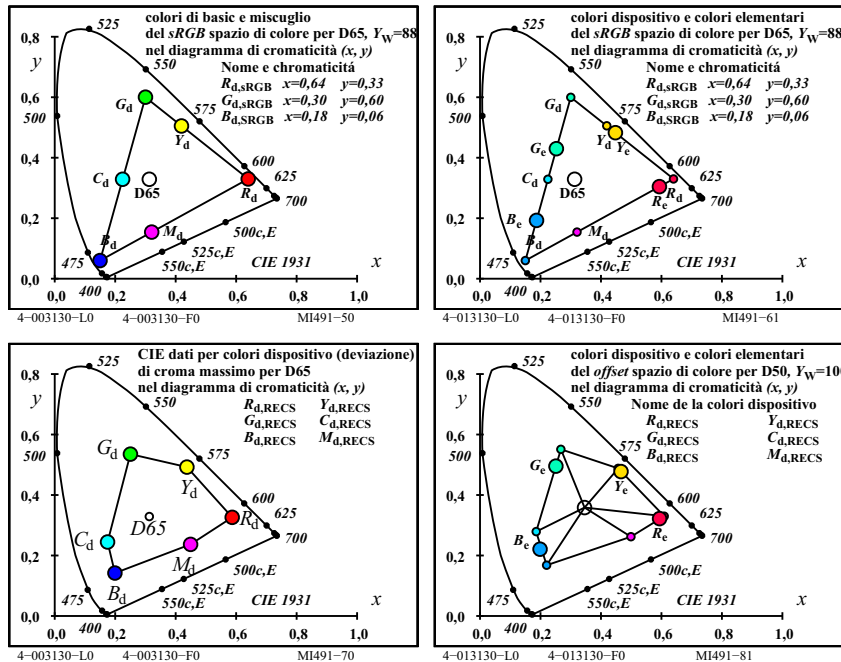
Experimental results of *Miescher and Weisenhorn* (1961) with optimal colours in a white surround have shown, that the dichromatic optimal colours which have all the largest chromatic value, have at the same time the largest chroma. However, in may cases the band width was a little smaller compared to the *colour half* with compensatory wavelength limits.

Fig. 58 (*top right*) shows all dichromatic optimal colours as continuous curve in the standard chromaticity diagram ( $x, y$ ) (*top right*), the chromatic value diagram ( $A, B$ ) (*bottom left*) and the CIELAB-chroma diagram ( $a^*, b^*$ ) (*bottom right*). These complementary optimal colours have all the maximum chromatic value  $C_{ab}$  (*bottom left*). The calculated wavelength limits (*top right*) for D65 differ slightly compared to the approximation for the three CIE illuminants D65, E, and C (*top left*).

The CIELAB-colour system is mainly based on colour scaling of the *Munsell*-colour order system and requires *nonlinear* coordinates.

For the description of colour thresholds for example the colour vision models of *Guth* (1972) require only *linear* coordinates.

All dichromatic optimal colours have the same chromatic value  $C_{ab}$ . In CIELAB for dichromatic optimal colours the chroma is in the red-yellow region about twice compared to the complementary region cyan-blue. Therefore the CIELAB-definition of chroma  $C^*_{ab}$  may be wrong by a factor 2.



**Fig. 59: Device- and elementary colours of the colour spaces sRGB and RECS (Offset)**

Fig. 59 shows the device colours of a sRGB standard display, and of the *Relative Elementary Colour System RECS* (standard offset) (*top and bottom left*). The device independent elementary hues  $RYGB_e$  according to CIE R1-47 with the CIELAB-hue angles  $h_{ab} = 26, 92, 162,$  and  $272$  degree (larger balls) may be mixed from six device colours  $RYGCBM_d$  ( $d=\text{device}$ ) (*top and bottom right*).

In the *Relative Elementary Colour System RECS* with about 2000 colours a 16-step hue circle with the four elementary hues  $RYGB_e$  as anchor hues is printed, see *RECS*. In each of the four sectors there are three intermediate hues. For the 16 hues there are 5- and 16-step colour series in standard offset printing on standard offset paper.

## 20 Output dei Colori elementari indipendente dal dispositivo per la riproduzione del colore

For the elementary colours the report CIE R1-47 defines the hue angles  $h_{ab,e} = 26, 92, 162$  and  $272$  which allows a device-independent hue output on any colour device. Fig. 59 on page 66 shows the solution for the *sRGB*-colour space (standard display) and the *RECS*-colour space (standard offset). For the visual  $rgb^*_e$  data  $(1,0,0)_e, (1,1,0)_e, (0,1,0)_e, (0,0,1)_e$  the device colours of maximum chroma  $C^*_{ab,d}$  with the hue angles  $h_{ab,e} = 26, 92, 162$ , and  $272$  are produced. This leads to device specific values for lightness  $L^*_d$  and chroma  $C^*_{ab,d}$ .

As a future next step, and in addition to the definition of the CIELAB-elementary hue angles, the definition of a special lightness  $L^*_e$  and a special chroma  $C^*_{ab,e}$  for the elementary colours is appropriate. A first definition may be included in 2013 in the report CIE R1-57 “Border between blackish and luminous colours” (*Reporter T. Seim, Norway*).

For the illuminant D65 the dichromatic optimal colours (index o and e) with the largest chromatic value  $C_{ab,oe}$ , and the CIELAB elementary hue angles  $h_{ab,oe} = 26, 92, 162$ , and  $272$  may be located at the border “neither blackish nor luminous”. These colours have the following *device-independent* lightness  $L^*_{oe}$  and chroma  $C^*_{ab,oe}$ .

colour	$rgb^*_{oe}$	$nce^*_{oe}$	$L^*_{oe}$	$C^*_{ab,oe}$	$h_{ab,oe}$	$x_{oe}$	$y_{oe}$	$Y_{oe}$
$R_e$	1 0 0	0 1 0,00	75	65	26	0,57	0,33	48
$Y_e$	1 1 0	0 1 0,25	89	136	92	0,47	0,51	73
$G_e$	0 1 0	0, 1 0,50	79	120	162	0,19	0,52	55
$B_e$	0 0 1	0 1 0,75	60	69	272	0,17	0,19	25

CIE TR1-57 shows that the here calculated optimal colours are located approximately on the visual border between “neither blackish nor luminous”. The *fluorescent red* colour printed in Fig. 28 on page 27 and which appears luminous is above this border.

With displays and special software one perhaps may reach the *natural* colour data  $LCh^*_{oe}$  of CIELAB for the standard display luminance  $142\text{cd/m}^2$ . This luminance is required for the standard illuminance 500 lux in offices, and the white paper of offset printing with the standard reflection factor  $R(\lambda) = 0.886$ .

For surface colours (with no fluorescence and retroreflection) it seems impossible to reach the CIELAB values for green  $G_e$  and blue  $B_e$ . The shape of the

reflection factors of these surface colours is too different compared to the reflection factor of the intended optimal colours, compare Fig. 26 on page 26.

## 21 Riproduzione del colore affine

In colour image technology the colour gamut is limited in any hue plane approximately by the triangle white - most chromatic colour - black. Both for displays and printing there is approximately an additive mixture at the border of this triangle. Solutions for the reproduction of both the border and within the triangle are most important.

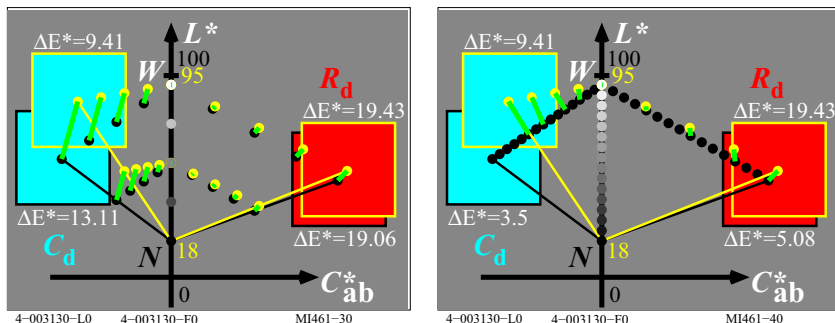


Fig. 60: Affine colour reproduction and minimum colour difference  $\Delta E^*_{ab}$

Fig. 60 shows the affine colour reproduction (*left*) and a reproduction with the smallest colour difference  $\Delta E^*_{ab}$  (*right*) between monitor colours (yellow balls) and standard printing colours (black balls).

Fig. 60 (*left*) shows that for the hue cyan-blue 20% of the monitor colours and 30% of the printing colours are outside the common reproduction area. The affine colour reproduction uses the whole colour gamut of both devices.

Fig. 60 (*right*) shows the present solution of most colour management methods. The goal is the smallest colour difference  $\Delta E^*_{ab}$ . In this case 30% of the cyan-blue printing area is not used. The ICC-colour management standard allows company specific solutions and therefore a wide variety of outputs may be produced for example by test charts according to DIN 33872-1 to -6, see  
<http://www.ps.bam.de/33872E>

For a filled out DIN-form of output questions see (*look for many others nearby*)  
<http://130.149.60.45/~farbmetri/LE95>

Any user can ask the device manufacturer for solutions in agreement with DIN 33872-1 to -6 or other international standards, for example ISO/IEC 15775.

This paper may have shown that both the *device-independent hue* reproduction and the *affine* reproduction are possible. One possible next step the *device-independent colour* reproduction may be based on CIE data of Fig. 58 on page 64 for optimal colours of maximum chromatic value and section 21.

## 22 Riferimenti

### *Standards and similar publication*

CIE 13.3:1995, Method of measuring and specifying colour rendering of light sources.

CIE 15: 2004, Colorimetry, 3rd edition.

CIE 170-1:2006, Fundamental chromaticity diagram with physiological axes

CIE R1-47:2009, Hue angles of elementary colours, see <http://div1.cie.co.at/>  
ISO 11664-4:2008(E)/CIE S 014-4/E:2007: Joint ISO/CIE Standard: Colorimetry — Part 4: CIE 1976  $L^*a^*b^*$  Colour Space

DIN 33872-1 to -6 (2010), Information technology - Office machines - Method of specifying relative colour reproduction with YES/NO criteria, see <http://www.ps.bam.de/33872E>

ISO/IEC TR 24705 (2005) Information technology - Office machines - Method of specifying relative colour reproduction with YES/NO criteria

### *Author publications*

Evans, R. M. and S. B. Swenholz (1967), Chromatic Strength of Colors; Dominant Wavelength and Purity, J. opt. Soc. Amer. 57, S. 1319-1324

Holtsmark, T. and Valberg, A. (1969), Colour discrimination and hue, Nature, Volume 224, October 25, S. 366-367.

Miescher, K. (1948), Neuermittlung der Urfarben und deren Bedeutung für die Farbordnung, Helv. Physiol. Acta 6, C12-C13

Miescher, K., Richter, K. und Valberg, A. (1982), Farbe und Farbsehen, Beschreibung von Experimenten fuer die Farbenlehre, Farbe + Design, no. 23/24

Newhall, S.M., D. Nickerson and D.B. Judd (1943), Final report of the O.S.A. subcommittee on the spacing of the Munsell colors. J. opt. Soc. Amer. 33, S. 385-418

Richter, K. (1979), BAM-Forschungsbericht Nr. 61, Beschreibung von Problemen der höheren Farbmetrik mit Hilfe des Gegenfarbsystems, 99 Seiten, ISSN 0172-7613

Richter, K. (1980), Cube root colour spaces and chromatic adaptation, Color Research and Application 5, no. 1, pages 25-43

Richter, K. (1985), BAM-Forschungsbericht Nr. 115, Farbempfindungsmerkmal Elementarbunton und Buntheitsabstände als Funktion von Farbart und Leuchtdichte von In- und Umfeld, 118 Seiten, ISBN 3-88314-420-7

Richter, K. (1996), Computergrafik und Farbmetrik - Farbsysteme, *PostScript* und geräteunabhängige CIE-Farben, VDE-Verlag, 288 pages with about 500 colour figures and many additional references, see <http://www.ps.bam.de/buche>

Richter, K (2011) ISO-CIE trend for the description of colour threshold data by new coordinates based on the device independent elementary colour coordinates of the report CIE R1-47:2009, see  
[http://130.149.60.45/~farbmefrik/CIE\\_ISO\\_10.PDF](http://130.149.60.45/~farbmefrik/CIE_ISO_10.PDF)  
Valberg, A. (2005), Light, Vision, Color, Wiley, ISBN 0470 849037, 462 pages.

## 23 Ringraziamenti

La Fondazione per il sostegno alla scienza colore Karl Miescher ha sostenuto il costo della stampa a colori di questa opera “Colore e visione a colori” in tedesco e in inglese, e della pubblicazione in internet delle versioni in altre lingue.

Dal 2000 i professori H. Kaase e S. Voelker hanno continuamente sostenuto le esposizioni “Farbe und Farbssehen” al “Das Sekretariat des Fachgebiets Lichttechnik der TU” di Berlino.

### ***Note sulla storia dell'esposizione “Colore e Visione Colore”***

Negli anni 1963-1964 K. Richter, sotto la guida del Dr. Karl Miescher, ha sviluppato l'esposizione “Colore e Visione a colori” presso il Laboratorio “Metrica del colore” presso l'Istituto di Fisica Università di Basilea / Svizzera. La mostra sul colore è stata esposta per sei mesi “Expo 64 Nazionale Svizzero” a Losanna / CH. Dopo l'Expo 64, la mostra sul colore è stata esposta per 30 anni alla scuola superiore Mathematisch Naturwissenschaftliches-Gymnasium di Basilea. Nel 2000 la mostra è stata ricostruita col sostegno finanziario della Fondazione Karl Miescher-presso l'Università di Berlino of Technology. A Berlino K. Richter ha continuamente ampliato la mostra con alcuni nuovi sviluppi nel settore della tecnologia dell'informazione a colori. Dal 2000 molti studenti e persone interessati al colore hanno visitato la mostra.

### ***Note sulle edizioni precedenti esull'edizione 2012***

Nel 1964 la prima edizione dell'esposizione nazionale svizzera Expo 64 a Losanna, in tedesco, francese e italiano, fu senza figure a colori.

La terza edizione del 1982, dopo la seconda edizione del 1978, fu con 50 figure a colori fu pubblicata a colori in tedesco sulla rivista "Farbe + Design". Inoltre, una edizione speciale fu stampata in tedesco e in inglese. Coautore di questa edizione è stato il Prof. Dr. Arne Valberg, Trondheim / Norvegia.

La quarta edizione del 2012 fu con 135 figure a colori, le quali mostrano anche i nuovi sviluppi nel settore delle tecnologie dell'informazione a colore. Ci sono la versione per la stampa offset, per il monitor e la stampante e internet nelle lingue tedesco e inglese. Le ulteriori versioni Internet sono destinati alle lingue francese, spagnolo e italiano.

Per il download delle ultime edizioni internet e per ordinare le versioni a stampa offset vedere <http://130.149.60.45/~farbmefrik/color>

### ***Scopo e applicazione della edizione speciale del 2012***

Le stampe speciali servono a fini didattici e come introduzione nel campo della scienza del colore. Campi di applicazione differenti di colore sono collegati senza conoscenze di base sul colore, ma con un po 'di conoscenze tecniche, ad esempio

- Basi di Visual e le proprietà di misurazione del colore
- Colore visione e metriche
- *Relativi colori elementari RECS Colour System* nella tecnologia dell'informazione colore.

Per ulteriori studi un libro a colori (solo in tedesco) è consigliato con il titolo *computer grafica e colorimetria - sistemi a colori, PostScript, e dispositivi colori indipendenti CIE*. Questo libro è stato curato dal VDE-Verlag nel 1996 ed è la descrizione di circa 500 figure a colori in tedesco e inglese. Le figure a colori possono essere utilizzati separatamente per scopi didattici. I file PDF di questo libro e le figure a colori sono disponibili come download gratuito, vedere <http://130.149.60.45/~farbmetrik/buche.html>

La segreteria del dipartimento di Illuminotecnica presso l'Università di Berlino di tecnologia potrebbe organizzare guide su richiesta presso del colore mostra e visione a colori, vedere <http://www.li.tu-berlin.de>

Copyright of the fourth edition of Colour and Colour Vision  
Prof. Dr. Klaus Richter Walterhoferstrasse 44, D-14165 Berlin, Germany  
Internet: <http://130.149.60.45/~farbmetrik/>  
Fax: +49 30 84509039  
email: klaus.richter@me.com

## 24 Test charts and technical remarks

The following text version in Italian is old. A new version is only available in English and this version is presented after the old version in Italian.

### *Le due copertine, fronte e retro, presentano due cartelle di colori*

*PI7311B:*

Cerchio delle tinte elementari con 16 e 8 colori elementari spaziati secondo CIE R1-47 e DIN 33872-1 6

*PI9311B:*

Scale di colori relative alla tinta rossa Re con 5 e 8 colori spaziati secondo i testi CIE R1-47 e DIN 33872-4

### *Sei cartelle test annesse*

*PII311L:*

Cartella test 1 per la resa del colore con 54 colori del sistema dei colori RECS.

*PI2311L:*

Cartella test 2 per la resa del colore con colori metamericci per l'illuminante D65 e per l'illuminante D50.

*PI3311L:*

Cartella test 3 per la resa del colore con colori metamericci per l'illuminante A e per l'illuminante P4000.

*PI4300L:*

1080 colori per la misurazione e la gestione dell'output, "start output"

*PI4310L:*

1080 colori per la misurazione con linearizzazione 3D del colore in output nel dispositivo per la riproduzione del colore.

*RI9810L:*

Cartella test dei colori acromatici secondo ISO/IEC 15775, ISO/IEC 24705 e ISO 9241-306, Annesso D.

*RI9711L:*

Cartella test dei colori cromatici con una immagine ISO/IEC secondo ISO/IEC 15775, ISO/IEC 24705, e ISO 9241-306, Annesso proposto E.

### **Osservazioni tecniche sul tavolo il coperchio posteriore interno:**

Per un cerchio 48 passo tinta della tabella è riportato nella colonna 2 dei dati di input RGB ei colori CIELAB dei dati di misura *LabCh*\*. Nella colonna 3 i dati sono interpolati per il prossimo numero, anche di un angolo di tinta CIELAB-*h<sub>ab</sub>* ( $0 < i < 360$ ). Il sistema *sRGB* (s = standard) si riferisce al-dati *rgb* (1,0,0), (1,1,0), (0,1,0), (0,1,1), (0,0,1, e (1,0,1) per gli angoli 30, 90, 150, 210, 270, e 330. simili secondo CIE R1-47 gli angoli di 26, 92, 162, 217, 272, e 329 sono relative al gli angoli del sistema di colore elementare. Inoltre per entrambi i sistemi CIELAB dati vengono interpolati come funzione dell'angolo di tinta i.

per ogni insieme rgbdata (eccetto  $r = g = b$ ) è valido secondo DIN 33.872-1  
 $i = 360 \text{ atan} \{[r \sin(30) + g \sin(150) - b \sin(270)] / [r \cos(30) + g \cos(150)]\}$   
L'indice i produce da due tabelle con i dell'angolo compreso tra 0 e 360 gradi  
sia il CIELAB-dati *LabCh\**, ed i relativi dati rgb per il colore o il dispositivo  
elementare sistema di stampa a colori.

In applicazione delle intese CIELAB colori dati sono calcolati per ogni angolo  
di tinta  $i$  dalla CIELAB dati *LabCh\** di colori con il massimo croma  $C^*_{ab}$ , e del  
bianco e nero  $WN$ . Per produrre un colore previsto il  $rgb_{dd}$  dati (da periferica a  
periferica uscita) e  $rgb_{de}$  (dispositivo di output elementare) utilizzare un 3D  
linearizzazione in CIELAB-spazio colore.

We hop that we can translate the following new English version into Italian  
soon.

### **Names of the test charts with 7 characters,**

Examples: *PE40S0S, PG7011S, PI7311L, PF4611P, PG7911P*

The first character describes a large file folder (here *P*). The second describes  
the language (E=English, G=German, F=French, S=Spanish, I=Italian).

The following two numbers include the range 00 to 99. The last number 0  
produces the output of an sRGB display. The last numbers 3 or 6 define an out-  
put in offset print on the paper *L* with the two separations *CYMK* and *CYMO*.  
The last number 9 defines a printer output on the paper *A* (=APCO) with the  
separation *CYMK*.

The following two letters *S0* define a start output (*S0*) with mixed *rgb* and *cmyk*  
data in the file. Or the two numbers *00* or *01* define an *rgb* transfer for the out-  
put of device colours (*00*) or elementary colours (*01*). Or the two numbers *10*  
and *11* define an *rgb-3D* linearisation for the output of device colours (*10*) or  
elementary colours (*11*).

The last letter *S, L, or P* defines the output of an *sRGB* display (*S*), or in offset  
print on paper *L* (*L*), or of a printer on the paper *A* (*P*).

### **Test chart on the front cover**

*PI7011S, PI7311L, PI7911P:*

16 and 8 step elementary hue circle with the elementary colours according to  
CIE R1-47 and DIN 33872-1 to 6

### **Test charts in the annex**

1. Output *S* without separation and *L* and *P* with the separation *CYMK*

*PI1011S, PI1311L, PI1911P:*

Test chart 1 for colour rendering with 54 colours of the RECS-colour system.

*PI40SOS, PI4000S, PI4001S, PI4010S, PI4011S*

*PI43S0L, PI4300L, PI4301L, PI4310L, PI4311L*

*PI49S0P, PI4900P, PI4901P, PI4910P, PI4911P:*

1080 colours for colour measurement and for the steering of the output.

*TI7011S, TI7311L, TI7911P:*

Achromatic test chart according to ISO/IEC 15775, ISO/IEC TR 24705 and ISO 9241-306, Annex D.

*TI8011S, TI8311S, TI8911S:*

Chromatic test chart with an ISO/IEC image according to ISO/IEC 15775, ISO/IEC TR24705 and ISO 9241-306, annex E.

2. Outputs *L* and *P* with the separation CMY0

*PI46S0L, PI4600L, PI4601L, PI4610L, PI4611L*

*PI46S0P, PI4600P, PI4601P, PI4610P, PI4611P:*

1080 colours for colour measurement and for the steering of the output

3. Outputs *L* and *P* with the two separations CMYK and CMY0

*PI2311L, PI2311P:*

Test chart 2 for colour rendering with metameric colours for D65 and D50.

*PI3311L, PI3311P:*

Test chart 3 for colour rendering with metameric colours for A and P4000,

### Test charts on the inner back cover

*PI91S0S, PI91S0L, PI91S0P:*

Table with CIE data of a 48 step colour circle.

*PI9011S, PI9311L, PI9911L:*

5 and 16 step colour series for the elementary colour rot  $R_e$  according to DIN 33872-4.

### Technical remarks about the table at the inner back cover:

For a 48 step hue circle the table shows in column 2 the *rgb* input data and CIE-LAB-colour measurement data *LabCh*\*. In column 3 the data are interpolated for the next even number of a CIELAB-hue angle  $h_{ab}$  ( $0 < i = h_{ab} < 360$ ). The *rgb<sub>s</sub>*-system (*s*=standard) relates the *rgb<sub>s</sub>*-data  $(1\ 0\ 0)_s$ ,  $(1\ 1\ 0)_s$ ,  $(0\ 1\ 0)_s$ ,  $(0\ 1\ 1)_s$ ,  $(0\ 0\ 1)_s$ , and  $(1\ 0\ 1)_s$  to the hue angles 30, 90, 150, 210, 270, and 330 degrees. Similar according to CIE R1-47 the *rgb<sub>e</sub>*-system (*e*=elementary) relates the

$rgb_e$ -data  $(1\ 0\ 0)_e, (1\ 1\ 0)_e, (0\ 1\ 0)_e, (0\ 1\ 1)_e, (0\ 0\ 1)_e$ , and  $(1\ 0\ 1)_e$  to the hue angles 26, 92, 162, 217, 272, and 329 degrees.

In addition for example for the sRGB system the output of the file

<http://130.149.60.45/~farbmetrik/RE69/RE69L0NP.PDF>

produces the CIELAB data as function of the hue angle  $i$  ( $0 \leq i \leq 360$ ). For any  $rgb$ -data set (except  $r=g=b$ ) it is valid according to DIN 33872-1:

$$i = 360 \arctan \{ [r \sin(30) + g \sin(150) - b \sin(270)] / [r \cos(30) + g \cos(150)] \}$$

The index  $i$  produces tables with the angle  $i$  between 0 and 360 degree, and the CIELAB-data  $LabCh^*$ , and the related  $rgb$  data for the device colour or the elementary colour output system.

In applications the intended CIELAB-colour data are calculated for any hue angle  $i$  from the CIELAB data  $LabCh^*$  of colours with maximum chroma  $C_{ab}^*$ , and of white  $W$  and black  $N$ . To produce an intended colour the data  $rgb_{dd}$  (device to device output) and  $rgb_{de}$  (device to elementary output) use a 3D-linearization in the CIELAB-colour space.

For more information on output linearization of displays, offset print and printers see a so called “white report” for a draft standard document on output linearization

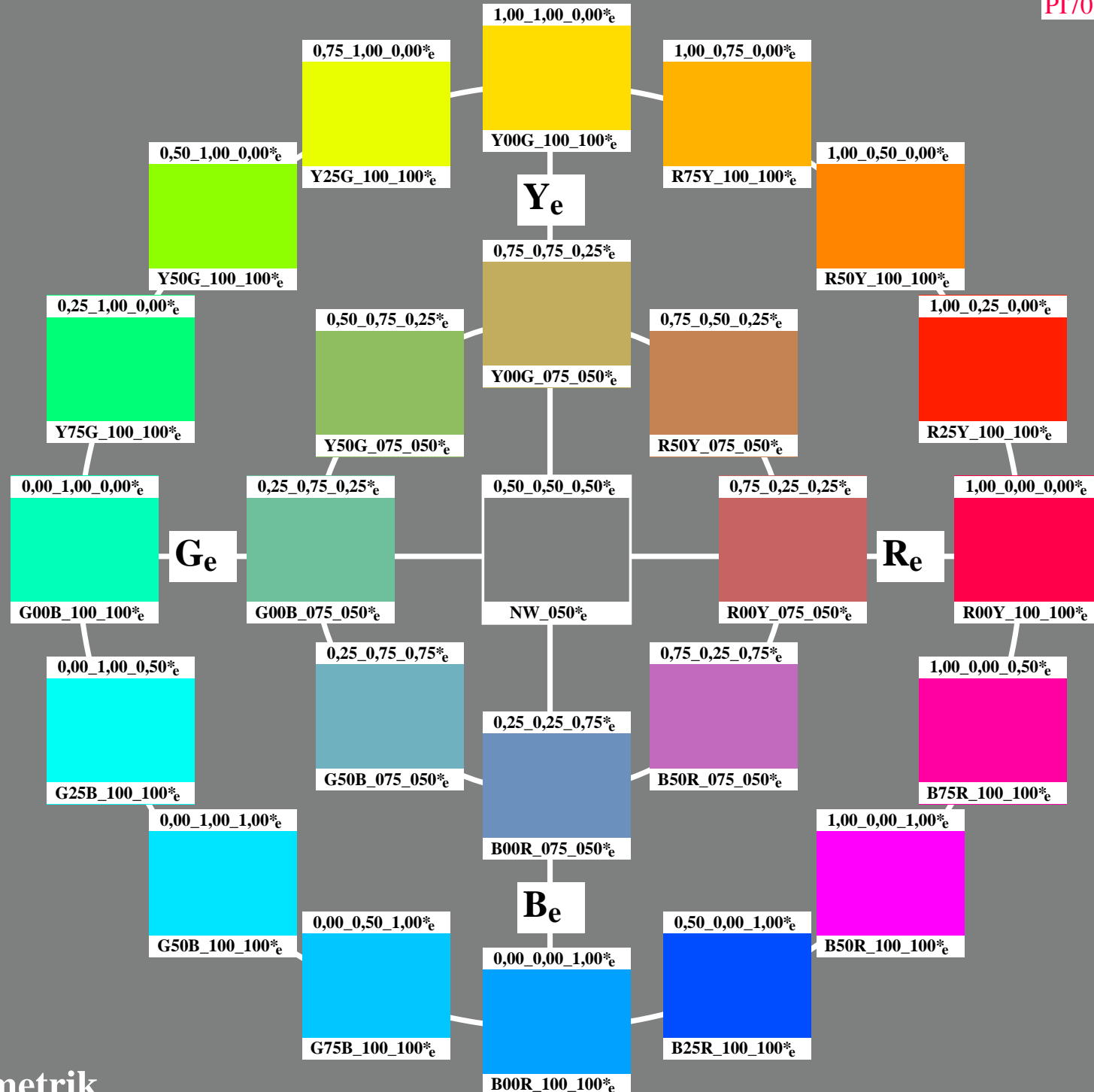
<http://130.149.60.45/~farbmetrik/outlin>

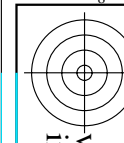
The reportership report CIE R8-09:2015 is an extended summary of this report on output linearization, and includes many examples for applications.

# Colore e Visione a Colori

Colori Elementari nella Tecnologia dell'Informazione

PI7011S



c  
M  
Y  
o  
L  
v

vedere dei file simili: <http://130.149.60.45/~farbmetrik/PI10/PI10L0FP.PDF/PS>  
 informazioni tecniche: <http://www.ps.bam.de> o <http://130.149.60.45/~farbmetrik>

TUB iscrizione: 20130201-PI10/PI10L0FP.PDF/PS  
 la domanda per la misura di stampa di display, nessuna separazione

TUB materiale: code=rha4ta

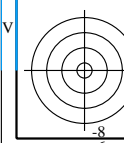
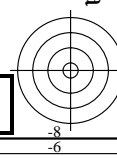
-8  
-6

grafico TUB-PI10; riproduzione di colore; *sRGB*  
 54 colori di norma, 3D=1, de=1,  $sRGB^{*de}$   
 immettere:  $rgb/cmky \rightarrow rgb^{*de}$   
 uscita: 3D-linearizzazione a  $rgb^{*de}$

-8  
-6

PI40S05

v  
L  
o  
Y  
M  
C  
-8  
http://130.149.60.45/~farbmetrik/PI40/PI40L0NP.PDF/.PS; cominciare l'uscita  
N: nessun 3D-linearizzazione (OL) nel file (F) o PS-startup (S), pagina 1/2

TUB iscrizione: 20130201-PI40/PI40L0NP.PDF/.PS  
la domanda per la misura di stampa di display

TUB materiale: code=rha4ta

vedere dei file simili: http://130.149.60.45/~farbmetrik/PI40/PI40L0NP.PDF/.PS  
informazioni tecniche: http://www.ps.bam.de o http://130.149.60.45/~farbmetrik

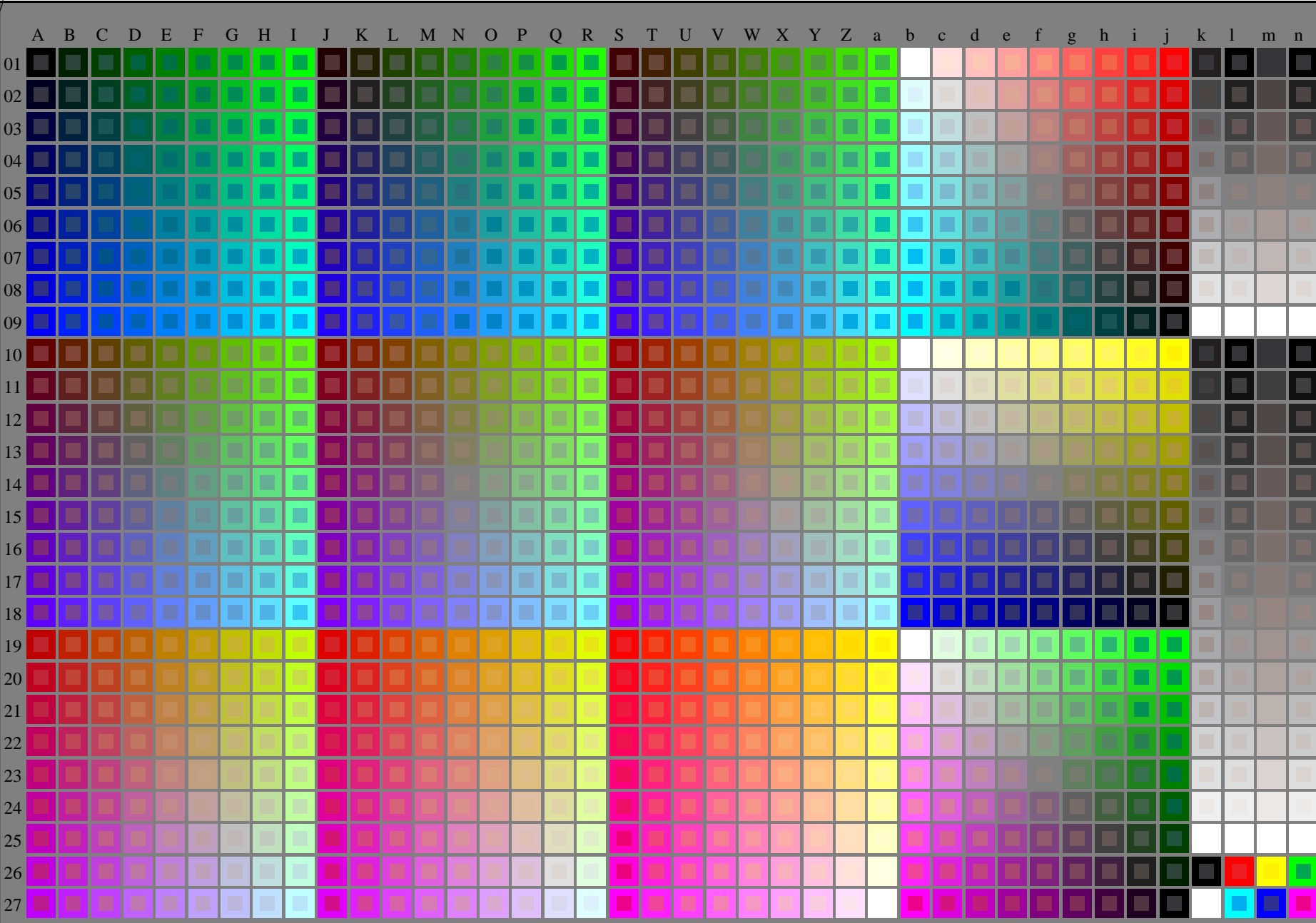


grafico TUB-PI40; grafico per il test  
1080 colori di norma; tecnologia di immagine

immettere:  $rgb/cmkyk \rightarrow rgb/cmkyk$   
uscita: nessun cambiamento

-8  
4-003030-L0  
C  
M  
Y  
O  
L  
V  
-6

PI400-7N

Test chart G with 40x27=1080 colours; digital equidistant 9 or 16 step colour scales; Colour data in column (A-n):  $rgb + cmy0$  (A-j + k26\_n27), 000n (k), w (l), mnn0 (m), www (n); 3D = 0

-8  
-6

PI400S

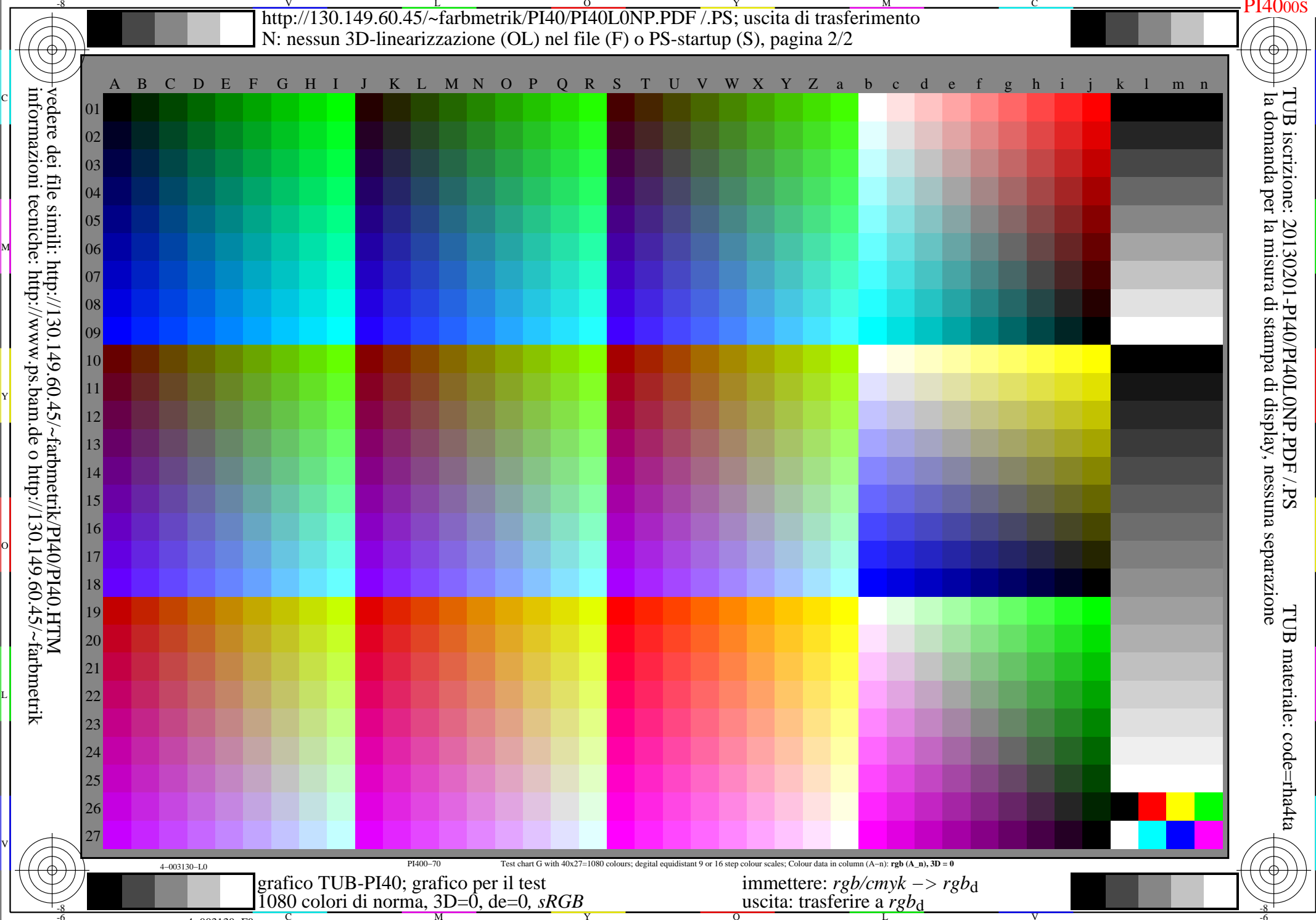
http://130.149.60.45/~farbmetrik/PI40/PI40L0NP.PDF/.PS; uscita di trasferimento

N: nessun 3D-linearizzazione (OL) nel file (F) o PS-startup (S), pagina 2/2

TUB iscrizione: 20130201-PI40/PI40L0NP.PDF/.PS  
la domanda per la misura di stampa di display, nessuna separazione

TUB materiale: code=rha4ta

vedere dei file simili: <http://130.149.60.45/~farbmetrik/PI40/PI40.HTML>  
informazioni tecniche: <http://www.ps.bam.de> o <http://130.149.60.45/~farbmetrik>

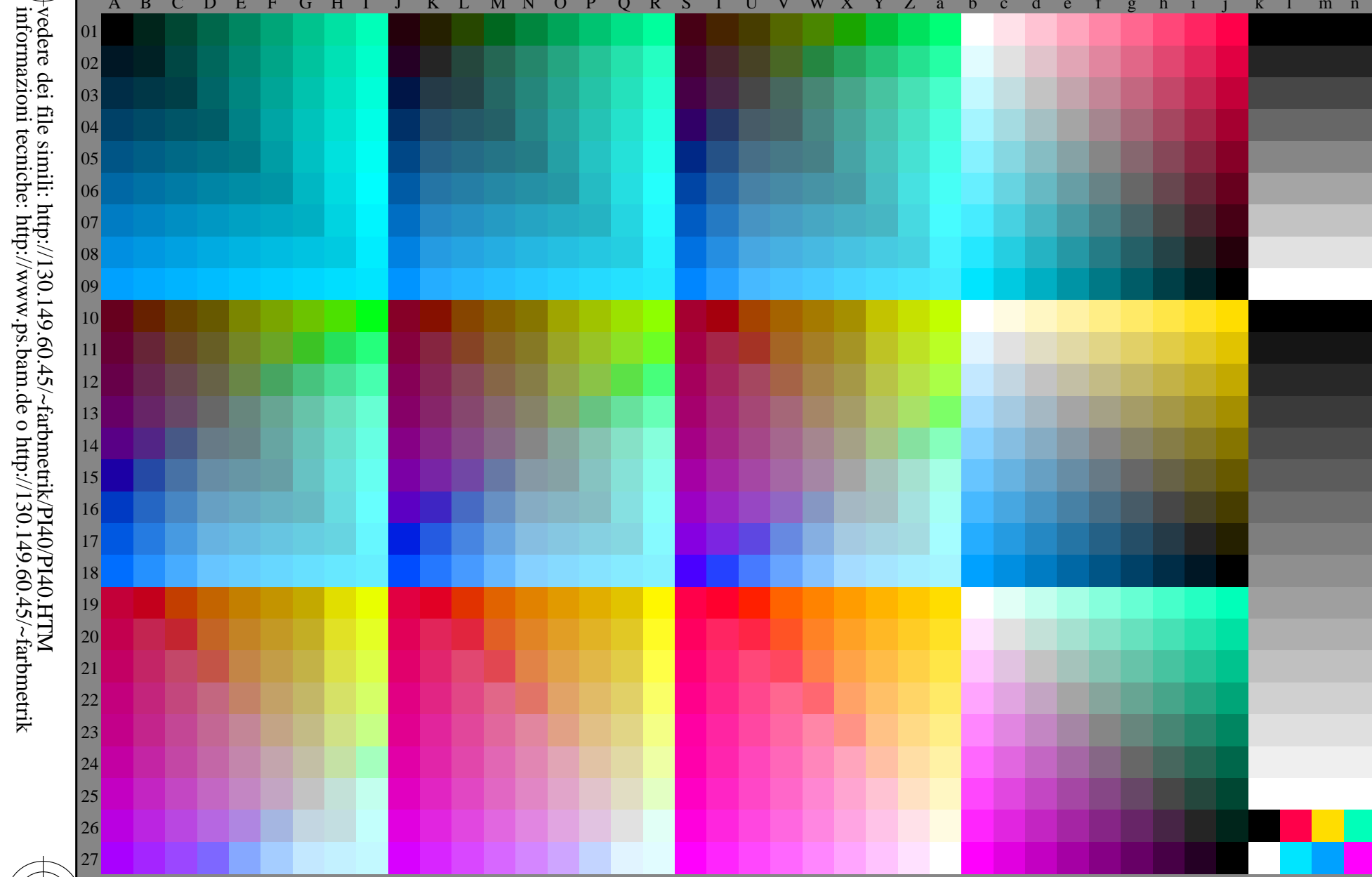


PI4001S

v  
L  
o  
Y  
M  
C  
-8  
http://130.149.60.45/~farbmetrik/PI40/PI40L0NP.PDF/.PS; uscita di trasferimento  
N: nessun 3D-linearizzazione (OL) nel file (F) o PS-startup (S), pagina 2/2

TUB iscrizione: 20130201-PI40/PI40L0NP.PDF/.PS  
la domanda per la misura di stampa di display, nessuna separazione

TUB materiale: code=rha4ta



vedere dei file simili: <http://130.149.60.45/~farbmetrik/PI40/PI40.HTML>  
informazioni tecniche: <http://www.ps.bam.de> o <http://130.149.60.45/~farbmetrik>

PI400-71

Test chart G with 40x27=1080 colours; digital equidistant 9 or 16 step colour scales; Colour data in column (A-n): rgb (A-n), 3D = 0

grafico TUB-PI40; grafico per il test  
1080 colori di norma, 3D=0, de=1, sRGB

immettere:  $rgb/cmky \rightarrow rgbe$   
uscita: trasferire a  $rgbe$

-8  
4-013130-L0 C M Y O L V  
-6  
4-013130-F0

PI4010S

v  
L  
o  
Y  
M  
C  
-8  
-6  
4-103130-L0  
grafico TUB-PI40; grafico per il test  
1080 colori di norma, 3D=1, de=0, sRGB\*

TUB iscrizione: 20130201-PI40/PI40L0FP.PDF /PS  
la domanda per la misura di stampa di display, nessuna separazione

TUB materiale: code=rha4ta

C

M

Y

O

V

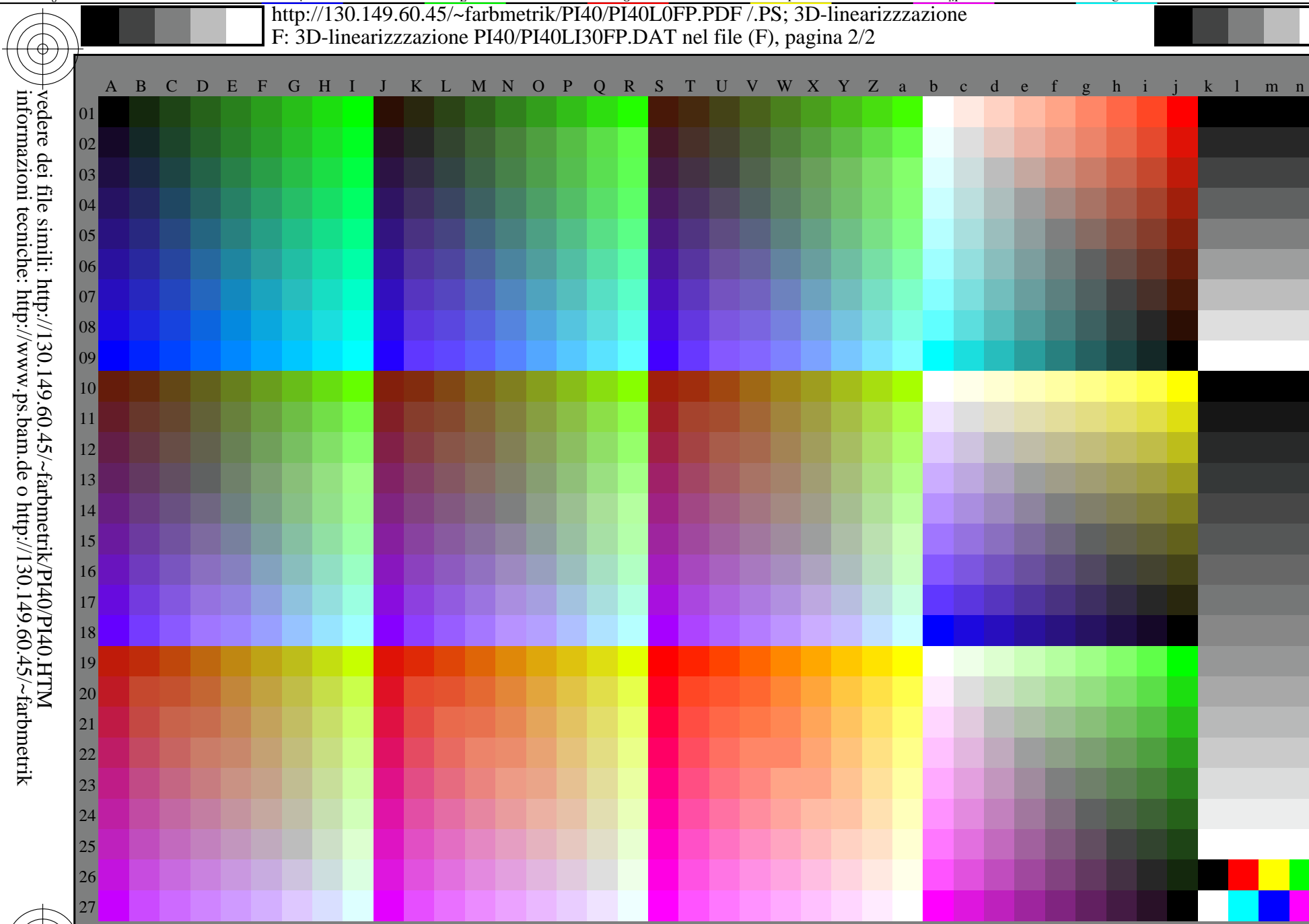
L

o

-8

-6

immettere:  $rgb/cmky -> rgbd$   
uscita: 3D-linearizzazione a  $rgb^*dd$



vedere dei file simili: <http://130.149.60.45/~farbmetrik/PI40/PI40L0FP.PDF /PS>  
informazioni tecniche: <http://www.ps.bam.de> o <http://130.149.60.45/~farbmetrik/PI40/PI40.HTML>

PI400-72

Test chart G with 40x27=1080 colours; digital equidistant 9 or 16 step colour scales; Colour data in column (A-n): rgb (A\_n), 3D = 1

4-103130-F0

C  
M  
Y  
O  
L  
V  
-8  
-6

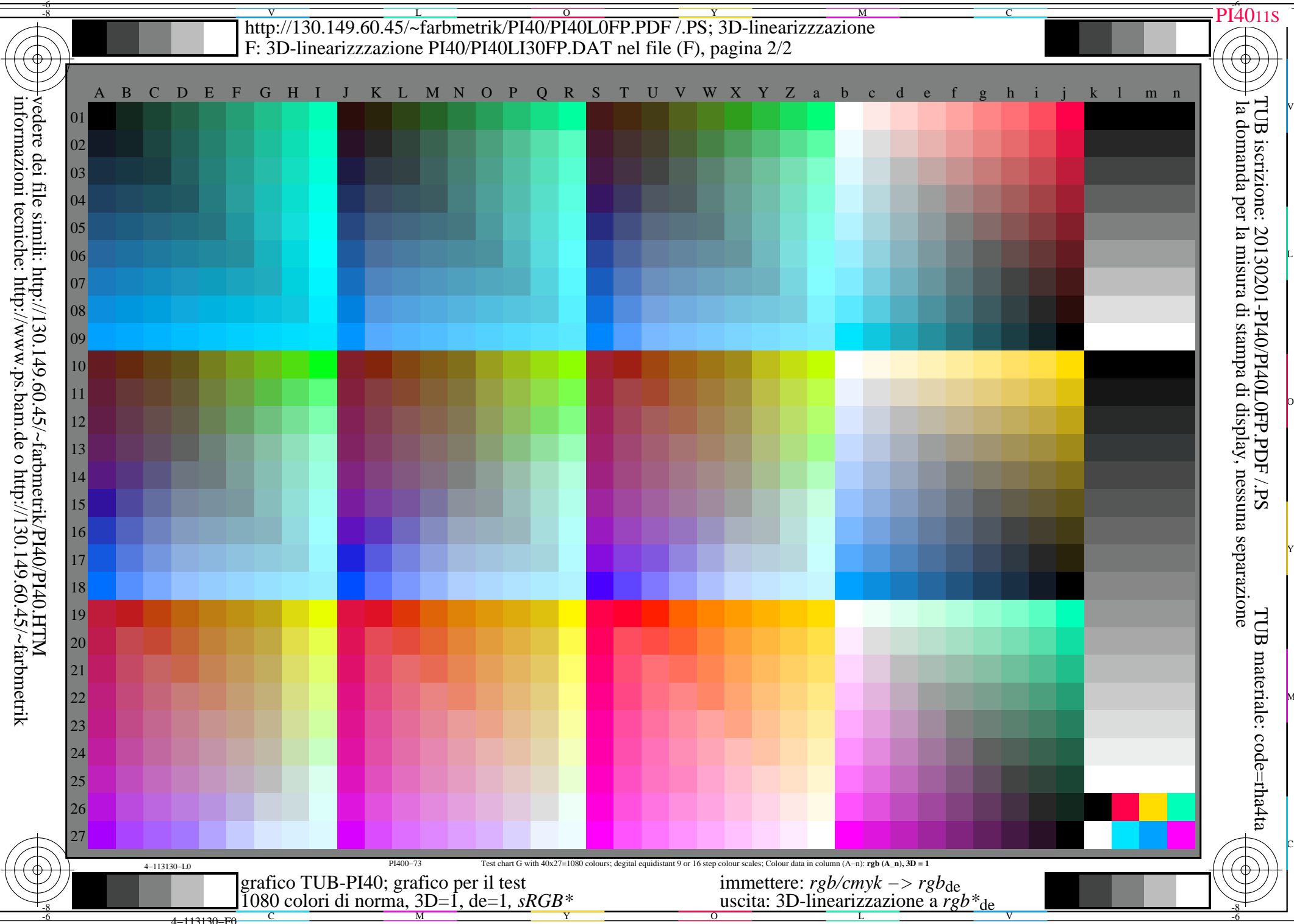
C  
M  
Y  
O  
L  
V  
-8  
-6

PI4011S

http://130.149.60.45/~farbmetrik/PI40/PI40L0FP.PDF /PS; 3D-linearizzazzione  
F: 3D-linearizzazione PI40/PI40LI30FP.DAT nel file (F), pagina 2/2

TUB iscrizione: 20130201-PI40/PI40L0FP.PDF /PS  
la domanda per la misura di stampa di display, nessuna separazione

TUB materiale: code=rha4ta





TI8011S

TUB iscrizione: 20150701-TI80/TI80L0FP.PDF /PS  
la domanda per la misura di stampa di display, nessuna separazione

TUB materiale: code=rha4ta

